

UNCLASSIFIED



AD NUMBER

AD-816 663

NEW LIMITATION CHANGE

TO

DISTRIBUTION STATEMENT: A

Approved for Public Release; Distribution Unlimited.

LIMITATION CODE: 1

FROM

DISTRIBUTION STATEMENT: B

LIMITATION CODE: 3

AUTHORITY

Cmdr, Air Force Materials Lab, USAF Systems Cmd, May 26, 1972

19990805007

THIS PAGE IS UNCLASSIFIED

AFML-TR-67-144

**HYDROTHERMAL GROWTH OF ZINC OXIDE CRYSTALS**

**TECHNICAL REPORT AFML-TR-67-144**

**JUNE 1967**

**AD816663**

**Directorate of Laboratories  
Air Force Materials Laboratory  
Air Force Systems Command  
Wright-Patterson Air Force Base, Ohio**

This document is subject to special export controls and each transmittal to foreign governments or foreign nationals may be made only with prior approval of the Manufacturing Technology Division, AFML, WPAFB, Ohio 45433.

Reproduced From  
Best Available Copy



**HYDROTHERMAL GROWTH OF ZINC OXIDE CRYSTALS**

**Roch R. Monchamp, Richard C. Puttbach, J.W. Nielsen**

**This document is subject to special export controls and each transmittal to foreign governments or foreign nationals may be made only with prior approval of the Manufacturing Technology Division, Air Force Materials Laboratory, Wright-Patterson AFB, Ohio 45433.**

## FOREWORD

This Final Technical Report covers all work performed under Contracts AF33(657)-8795 and AF33(615)-2228 from 1 June 1962 to 31 December 1966. The manuscript was released by the authors in May 1967, for publication as an AFML Technical Report.

These contracts with Airtron, a division of Litton Industries, Morris Plains, New Jersey, were initiated under Manufacturing Methods Project 7-988, "The Hydrothermal Growth of Zinc Oxide Crystals". It was accomplished under the technical direction of Mr. Robert C. Bratt of the Electronics Branch (MATE), Manufacturing Technology Division, Air Force Materials Laboratory, Wright-Patterson Air Force Base, Ohio.

Closely related efforts are covered under MDP No. 8-132, "The Hydrothermal Growth of Large Ruby Single Crystals".

Dr. Roch R. Monchamp, Manager, Crystal Growth Research and Development, of Airtron's Solid State Laboratory, was the Project Director. Others who cooperated in the research and in the preparation of the report were: Dr. J. W. Nielsen, Manager, Solid State Laboratory, and Richard C. Putzbach, Project Engineer. This report has been given Airtron's report number R11-534.

This project has been accomplished as a part of the Air Force Manufacturing Methods Program, the primary objective of which is to develop, on a timely basis, manufacturing processes, techniques and equipment for use in economical production of USAF materials and components. The program encompasses the following technical areas.

Design of pilot line for ZnO crystals by the molten salt technique, the hydrothermal growth of large ZnO crystals, the hydrothermal growth of doped ZnO crystals.

Suggestions concerning additional Manufacturing Methods development required on this or other subjects will be appreciated.

This technical report has been reviewed and is approved.



CHARLES H. NELSON  
Assistant Chief  
Manufacturing Technology Division

## ABSTRACT

A pilot line for the production of large high quality ZnO single crystals was established and many large crystals were produced. The pilot line can be divided into two units, 1) a molten salt line for the production of seed plates to be used in 2) the hydrothermal crystal growth pilot line. The design and construction of both lines were successfully completed and functioned as planned.

The molten salt crystal growth effort was not as successful as had been anticipated. Large area, high quality crystals could not be made reproducibly by this technique. The most apparent reasons for the failure to do so rests in thermal gradient control during the growth cycle and/or the presence or absence of impurities in the melt.

Although these problems were not completely resolved, the molten salt pilot line did yield sufficient plates for the initial portion of the hydrothermal crystal growth program.

Once growth conditions and procedures were established in the hydrothermal pilot line, the hydrothermally grown crystals were sectioned and used as seeds for subsequent runs. The area of the crystals were increased by continued growth until large high quality crystals weighing more than 150 grams could be grown on such seeds within reasonable operating times.

One problem arose which had not been encountered in previous hydrothermal systems. It was found that the silver liner or can was corrosively attacked during the course of the growth cycle. The silver which was dissolved in the fluid in the nutrient chamber would also be deposited in the crystals in the growth chamber. This problem was solved by adding a reducing agent (metallic zinc) to the reactants. The cause of the corrosion apparently is due to the presence of oxygen dissolved in the solvent and as air entrapped in closure of the can. The reason this phenomenon had not been observed in other small systems using noble metal liners is that no other similar system has been scaled-up to the ZnO size. The solution of this problem for the ZnO case will undoubtedly be of value to other large hydrothermal crystal growth systems.

In addition to the growth of the large crystals many smaller crystals were grown which were doped with copper to give resistivities in the  $10^2$  -  $10^4 \Omega$  cm range. This is the range most desirable for acoustical amplifier devices.

Other doping studies indicate a wide variation of resistivities within the virgin crystal, and from crystal to crystal within a run. After heat treatment, however, the variation of resistivity is reduced to an order of magnitude or less. It was also observed that impurities not detected by spectrographic analysis may be as important in determining the resultant resistivity as deliberate doping additions and growth conditions.

Abstract (Continued)

During the course of these contracts many samples of hydrothermally grown ZnO were given to scientists and engineers in government, industrial and university laboratories for measurement of the fundamental properties of ZnO and for device design and development.

This abstract is subject to special export controls and each transmittal to foreign governments or foreign nationals may be made with prior approval of the Manufacturing Technology Division, Air Force Materials Laboratory, Wright-Patterson AFB, Ohio 45433.

TABLE OF CONTENTS

	<u>Page</u>
1.0 INTRODUCTION	1
1.1 Applications	1
1.2 Properties	2
1.3 Growth Method	3
2.0 PILOT LINE	6
2.1 Molten Salt	6
2.1.1 Floor Layout and Equipment	6
2.1.2 The Ten Inch Furnace	6
2.1.3 The Three Inch Furnace	17
2.1.4 Materials and Purity	21
2.1.5 Weighing and Loading Procedures	21
2.1.6 Seed Crystal Growth Conditions	23
2.1.7 Unloading Operation	23
2.1.8 Crystal Separation and Cleaning	24
2.2 Hydrothermal	25
2.2.1 Laboratory Facility	25
2.2.2 Hydrothermal Crystal Growth Autoclaves	26
2.2.3 Silver Cans	32
2.2.4 Large Can Technique	32
2.2.5 Hydrothermal Furnaces	37
2.2.6 Temperature Control	39
2.2.7 Pressure Measurement	41
2.2.8 Equipment Developed During Contract	42
2.2.8.1 Autoclave Opener	43
2.2.8.2 Can Extractor	43
2.2.8.3 Seal Area Lapping Tool and Polish- ing Tool	43
2.2.9 Operating Procedure	48
2.2.9.1 Preparation of Large Crystal Growth Autoclaves	48
2.2.9.1.1 Seal Ring	48
2.2.9.1.2 Cover	48
2.2.9.1.3 Autoclave Seal Area	52

TABLE OF CONTENTS (Continued)

	<u>Page</u>
2.2.10 Nutrient Preparation	52
2.2.11 Solution Preparation	52
2.2.12 Seed Preparation	52
2.2.13 Preparation of Silver Can Loading of Autoclaves	53
2.2.14 Warm-Up	54
2.2.15 Shut-Down	54
<b>3.0 CRYSTAL GROWTH</b>	<b>55</b>
<b>3.1 Molten Salt</b>	<b>55</b>
3.1.1 Background for Program	55
3.1.2 Crystal Growth Experiments	55
3.1.3 Controlled Nucleation and Crystal Growth	58
3.1.3.1 Vertical Gradient Method	58
3.1.3.2 Lateral Gradient Method	72
<b>3.2 Hydrothermal</b>	<b>76</b>
3.2.1 Low Pressure Crystal Growth	76
3.2.2 Hydrothermal Seed Development	91
3.2.3 High Pressure Crystal Growth	96
3.2.4 Silver Corrosion	122
<b>4.0 DOPING AND ELECTRICAL PROPERTIES</b>	<b>127</b>
<b>4.1 Resistivity Measurement Technique</b>	<b>127</b>
<b>4.2 Doping</b>	<b>127</b>
4.2.1 Lithium	127
4.2.2 Copper Doping	133
4.2.3 Indium Doping	135
<b>4.3 Run Uniformity and Crystal Uniformity</b>	<b>136</b>
<b>5.0 CONCLUSIONS</b>	<b>142</b>
<b>6.0 RECOMMENDATIONS FOR FUTURE WORK</b>	<b>144</b>
<b>7.0 REFERENCES</b>	<b>145</b>

LIST OF ILLUSTRATIONS

	<u>Page</u>
Figure 1 - Hydrothermal System	5
Figure 2 - Floor Plan - Hydrothermal Laboratory	7
Figure 3 - 10 Inch I.D. Furnace	8
Figure 4 - Inside Cross Section 10 Inch I.D. Furnace	9
Figure 5 - Typical Plug and Pedestal	10
Figure 6 - Slip Ring Device	12
Figure 7 - Elevator and Crucible Rotating Mechanisms	13
Figure 8 - Grasping Arm	15
Figure 9 - Globar Hook-Up	16
Figure 10 - Furnace Control Schematic	18
Figure 11 - Three Inch Furnace Position Dimensions	19
Figure 12 - Photo of Molten Salt Furnaces in Hydrothermal Pilot Line	22
Figure 13 - Pit Area, Furnaces and Autoclaves	27
Figure 14 - Reactor Details	29
Figure 15 - Engineering Drawing of Autoclave with Newly Designed Bott	31
Figure 16 - Large Can Assembly	33
Figure 17 - Engineering Drawing of Silver Can Parts	34
Figure 18 - Schematic for P-T Behavior of Water	36
Figure 19 - Furnaces Used to Heat Autoclaves	38
Figure 20 - Electric Range Element	40
Figure 21 - Schematic of the Control System and Furnace	41
Figure 22 - Main Nut Opener	44

LIST OF ILLUSTRATIONS (Continued)

	<u>Page</u>
Figure 23 - Can Extractor	45
Figure 24 - Seal Area Lapping Tool	46
Figure 25 - Polishing Tool	47
Figure 26 - Expanding Mandrel	49
Figure 27 - Seal Ring Caliper	50
Figure 28 - Seal Ring	51
Figure 29 - Photograph of Large ZnO Crystal Prior to Cleaning	56
Figure 30 - ZnO Crystals Grown from PbF <sub>2</sub>	57
Figure 31 - Cross Section of Molten Salt Crucible	71
Figure 32 - Diagram of Lindberg Furnace	7
Figure 33 - 3" Furnace Showing Thermocouple Positions for Measuring Lateral Gradient	78
Figure 34 - Hydrothermally Grown ZnO Crystals	82
Figure 35 - Hydrothermally Grown ZnO Crystals	85
Figure 36 - High Quality Crystal from Run No. 51 with Seed and c <sup>-</sup> Side Removed	86
Figure 37 - Crystals from the Seed Development Runs Showing Basal Area Increase	94
Figure 38 - Schematic Drawing of Electrical Twinning of ZnO	95
Figure 39 - NaOH Etch Pattern on (0001) Surface	97
Figure 40 - NaOH Etch Pattern on (000 $\bar{1}$ ) Surface	97
Figure 41 - Photomicrograph of ZnO Electrical Twinning After Etching	98
Figure 42 - Growth Rate vs $\Delta T$ Neglecting Li <sup>+</sup> Concentration Difference	102

LIST OF ILLUSTRATIONS (Continued)

	<u>Page</u>
Figure 43 - High Quality Crystals from Run No. 76	123
Figure 44 - Resistivity Measurement Circuit Diagram	128
Figure 45 - Crystal from Run No. 67 Showing Spontaneous Nucleation and Lateral Growth	137
Figure 46 - Crystal from Run No. 67 with Spontaneous Nucleation Removed	137
Figure 47 - Resistivity Map Crystal No 84-3	139

LIST OF TABLES

		<u>Page</u>
TABLE I	Typical Molten Salt Composition for ZnO Crystal Growth	33
TABLE II	Molten Salt Crystal Growth Runs	59
TABLE III	Molten Salt Crystal Growth Runs	60
TABLE IV	Molten Salt Crystal Growth Runs	65
TABLE V	Molten Salt Crystal Growth Runs	73
TABLE VI	Crystal Growth Operational Data	80
TABLE VII	Crystal Growth Operational Data	83
TABLE VIII	Seed and Crystal Data for Run No. 44	87
TABLE IX	Seed and Crystal Data for Run Nos. 46 - 54	89
TABLE X	Summary of Data for Basal Area Increase	93
TABLE XI	Crystal Growth Operational Data	99
TABLE XII	Summary of Selected High Pressure Crystal Growth Data	103
TABLE XIII	Seed and Crystal Data for Run Nos. 58 - 85	104
TABLE XIV	Spectrographic Analysis for Hydrothermally Grown ZnO	124
TABLE XV	Resistivity Measurements	129
TABLE XVI	Resistivity Measurements	130
TABLE XVII	Acoustic Velocity Measurements of Copper Doped ZnO	134
TABLE XVIII	Resistivity Change on Subsequent Heat Treatments	138
TABLE XIX	Results of Spectrographic Analysis of ZnO	141

## 1.0 INTRODUCTION

The discovery by Hutson<sup>1</sup> that zinc oxide has a piezoelectric coupling coefficient of 0.4, or four times that of quartz, stimulated much interest in this material, and work is underway in many laboratories to use crystals of zinc oxide both to improve existing devices and build new ones. The existing device which will be improved by using zinc oxide is the ultrasonic delay line.

### 1.1 Applications

At present, ultrasonic delay lines for applications requiring long delays, of the order of milliseconds or a little less, use either crystalline quartz, or barium titanate ceramic transducers. The r-f signal is impressed upon a driving transducer which resonates and sends a sound wave through a delay medium; usually fused silica, until, perhaps after several reflections, the sound wave strikes a receiving piezoelectric transducer which changes the signal back to r-f. Both quartz and barium titanate ceramics have serious shortcomings when long delays at high frequencies are desired.

Crystalline quartz is limited in the length of delay time that it can achieve. The piezoelectric coupling coefficient,  $k$ , is only 0.1. The power of a transducer depends on the square of this coefficient and the length of delay which can be achieved depends strongly on the power available since attenuation of ultrasonic waves in silica is severe. With  $k = 0.1$ , quartz is limited to short delay applications. On the other hand, quartz can be lapped into very precise and very thin plates. Since the resonant frequency of a transducer is inversely proportional to its thickness, quartz can be used at high frequencies, around 100 Mc. This is for the fundamental mode. Higher modes can be set up, but, again because of the low  $k$ , the efficiency of higher mode transducers is very low.

In the case of barium titanate ceramics, the problem is not with delay time but the upper frequency at which the delay lines can operate. Barium titanate ceramics have coupling coefficients of 0.35 and higher. With these high coefficients, delay times of 6000 microseconds have been achieved. However, the dielectric constant of these ceramics is about 500. Thus, as the transducers are made thinner for higher frequency operation, the capacitance becomes very high, and the impedance match between transducers, which is necessary for operation of the device, becomes impossible to achieve. This limits the upper frequency for delay lines having barium titanate transducers to 15 Mc.

Zinc oxide solves the problems of quartz and barium titanate simultaneously. It has a coupling coefficient of 0.4 and a dielectric constant much nearer that of quartz than of  $\text{BaTiO}_3$ . Its dielectric constant is between 9 and 12, depending on frequency. It can also be ground and lapped to close tolerances like quartz. Thus, it appears that delay lines having 3-6000  $\mu$  sec. delays at frequencies over 100 Mc are possible. Indeed, with the higher  $k$ , it is at least possible that

## Introduction (Continued)

in some applications higher modes could be used in spite of the higher losses. This would raise the frequency of operation much higher.

A second very promising use of ZnO is in the very new ultrasonic amplifier reported by Hutson, McFee and White.<sup>2,3</sup> In this device a quartz transducer sends a shear wave through a fused silica buffer which is in contact with a piezoelectric semiconductor. (Hutson, et al used cadmium sulfide since that was the only material available in suitable single crystal form.) The semiconductor is in contact with another buffer and a receiving transducer. It was found that when a light of certain intensity was used to excite the proper carrier concentration in CdS, a drift field pulse was applied to the CdS in the direction of the shear wave propagation, a gain was observed in the ultrasonic signal. Gains of 18 db at 15 Mc/sec and 38 db at 45 Mc/sec were reported for a 7mm sample of CdS.

A.R. Hutson<sup>4</sup> has suggested that ZnO would be superior to CdS as the semiconducting transducer because of its high coupling coefficient. It could also serve as the driving transducer.

Two specific applications for ZnO have been discussed. There are no doubt many others. Probably quartz and ceramic piezoelectric can be replaced with ZnO to great advantage in other devices. But in all applications large, sound, single crystals of ZnO will be required.

This report contains a description of the development of the manufacturing methods, techniques and equipment required for the hydrothermal production of high quality, large single crystals of zinc oxide.

### 1.2 Properties

Zinc oxide in the pure state is a clear water white oxide having the wurtzite structure (hexagonal.) As normally prepared it is an n-type semiconductor. Resistivities are observed as low as 5 ohm cm in newly grown crystals. This resistivity can be raised or lowered by various treatments with zinc, hydrogen or oxygen. This fact, coupled with the high energy gap (estimated at 3.3 ev), originally led to the hope that zinc oxide would be suitable for semiconductor devices applications.

The use of ZnO in semiconductor devices has been curtailed because to date no one has succeeded in making it p-type. Thus p-n junctions cannot be made. In an effort to make p-type material, Lander<sup>5</sup> studied the behavior of various ions in the zinc oxide lattice. He discovered that  $Li^+$  will act as an acceptor in ZnO and will compensate the n-type conductivity so that the material will become insulating, although it will not become p-type. This work, ~~plus~~ the growth of larger crystals, led directly to Hutson's discovery of the large piezoelectric effect in ZnO. It is the compensated ZnO which exhibits a large effect.

### Introduction (Continued)

The mechanical Q of zinc oxide is not as high as quartz but is far higher than titanate ceramics. Charlton<sup>6</sup> has measured values varying from  $10^5$  to over  $10^6$ , depending on composition, on crystals grown at Airtron. Charlton has also found that the temperature stability of the resonant frequency of a zinc oxide (0001) disk oscillating in the compressional mode is only a little poorer than a similar quartz resonator. Since no other type of oscillator has been made of zinc oxide because of a lack of suitable crystals, it is not known if certain cuts will possess the high temperature stability observed in some quartz oscillators. The temperature stability of ZnO appears to be less than that of some titanate ceramics.<sup>6</sup> This would not be serious in two-transducer devices or in those where extreme temperature stability was unnecessary.

### 1.3 Growth Method

Zinc oxide is known for its high vapor pressure and its rapid sublimation. It has not been observed, to our knowledge, in the molten state. The vapor phase has proved very difficult as a growth medium for ZnO in that it is not possible to grow large crystals reproducibly.

It appeared at the time of the beginning of this work that a combination of molten salt (for seeds)<sup>7</sup> and hydrothermal<sup>8</sup> techniques should yield large crystals reproducibly for the first time.

The growth of ZnO from the vapor phase yields crystals which are of a needle type habit. The ratio of axis length to diameter is about 50 to 1 in these crystals normally, although more truncated crystals are sometimes obtained. The largest diameters are about 5mm. The needle form is due to differences in growth rates between the <0001> direction and those perpendicular to it. While possibly suitable for some acoustical amplifier uses, the small size of such crystals make them unsuitable for large area transducer type devices.

On the other hand the molten salt crystals grow with exactly opposite differences in rates. The lateral growth rates are about 50 times greater than the <0001> growth thus yield large area flat plates which are ideally suited for hydrothermal seed crystals. It has been found that in the hydrothermal system nearly more equal growth rates are obtained in the lateral and <0001> directions.

In order to produce ZnO seed plate crystals by the molten salt technique a platinum can is charged with about 20 mole percent ZnO and  $PbF_2$  powders. The can and contents are then heated to  $1150^\circ C$  and held at that temperature for 2 hours. The melt is cooled to  $1050^\circ C$  at a rate of  $3-5^\circ C/hour$  after which the can is withdrawn and the flux poured off from the crystals.

### Introduction (Continued)

Normally, crystal growth from aqueous solution is carried out at atmospheric pressure and temperatures close to room temperature. The hydrothermal technique is one which allows crystallization to be carried out under a wide range of temperatures and pressures. The higher pressures and temperatures employed in this method provide a means of obtaining solubilities and nucleating conditions for crystals which would be difficult to grow using other techniques.

In operation, an aqueous solution is held at a high temperature and pressure in order to dissolve the source material (nutrient) in one part of the system, transport the dissolved nutrient to another part of the system and deposit it onto a seed crystal epitaxially. The process is carried out in vertically mounted, sealed autoclaves along which a temperature difference ( $\Delta T$ ) is imposed between the top and bottom. The nutrient is usually placed in the bottom, hotter portion of the autoclave chamber while the properly oriented single crystal seeds are suspended in the upper, cooler region as in Figure 1.

The aqueous solvent in the region of the nutrient becomes saturated with nutrient which is then transported by thermal convection to the cooler portion of the autoclave. In this region, the solution is supersaturated with respect to the seed crystals and, therefore, deposits the solute on the seeds. The now cooler and depleted solvent returns to the nutrient region by convection where, not now being saturated, it may again dissolve the nutrient material. Obviously, the process is continuous and stops only when the nutrient supply is exhausted.

More detailed descriptions of the hydrothermal process and equipment can be found in review articles by Laudise and Nielsen,<sup>9</sup> and Laudise.<sup>10</sup> These articles, particularly that of Laudise and Nielsen, also emphasize the hydrothermal process for quartz work.

While we were in the process of setting up the pilot line, Laudise, Kolb and Caporaso,<sup>8</sup> published their first paper concerning the hydrothermal growth of zinc oxide crystals. They used small silver-lined Morey type vessels and so all the data they presented was not easily translated to the larger vessel of the pilot line. Their solvent, its concentration, temperature range data, etc., did provide an excellent starting place. In fact, other than working at higher pressures, the growth parameters currently used are not too different from the original data of Laudise et al.

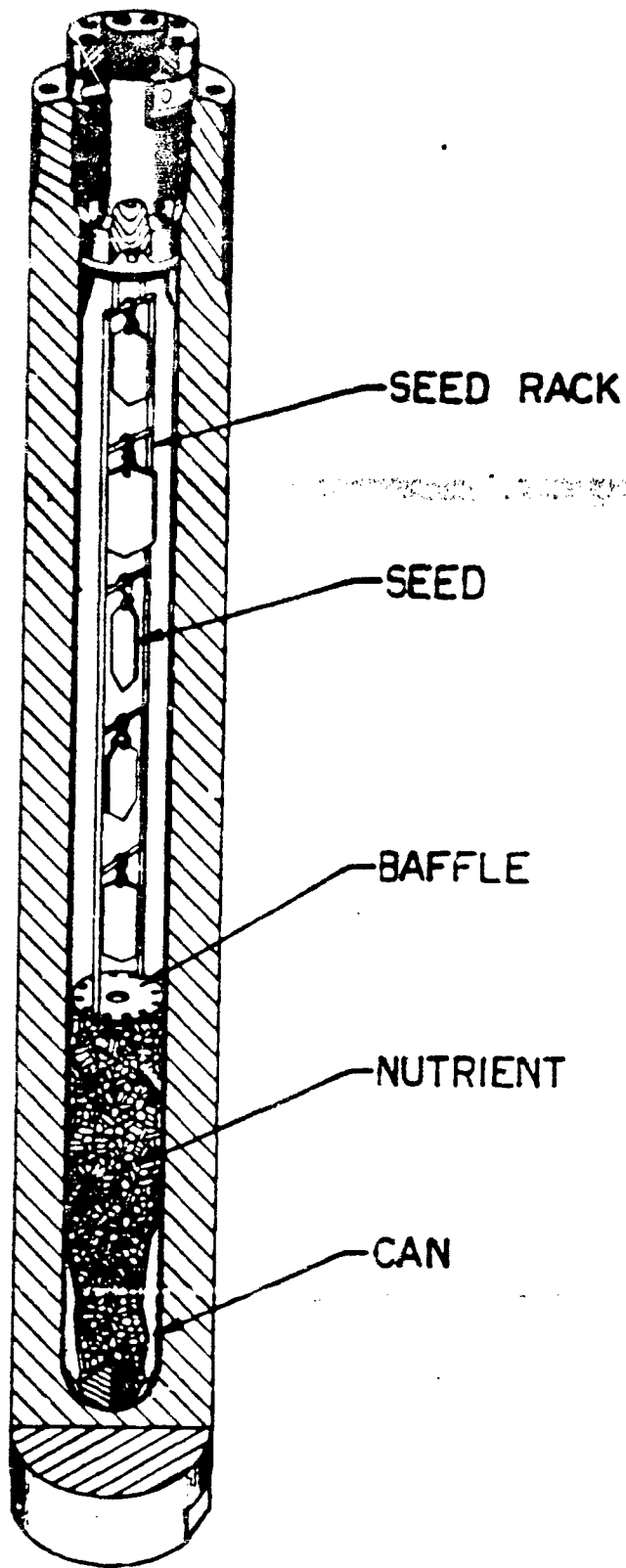


Figure 1 - Hydrothermal System

## 2.0 PILOT LINE

### 2.1 Molten Salt

#### 2.1.1 Floor Layout and Equipment

The floor plan for the ZnO crystal growth pilot line is shown in Figure 2. The figure shows the location of our three inch molten salt furnaces, the 10 inch furnace, the hydrothermal pit and general work areas. The molten salt crystal growth was mostly performed in the ten inch and three inch furnaces described in the following section.

#### 2.1.2 The Ten Inch Furnace

The metal shell of a vertical 10 inch I.D. American Electric<sup>+</sup> globar furnace was used to house a ceramic interior, see Figure 3. The bottom of the metal shell was welded; however, the top was only bolted down as was, therefore, easily removed. Thus, the furnace interior could be inserted from the top. The furnace interior, shown in Figure 4, and fabricated by Research and Development Co.<sup>†</sup> was made in two pieces. The dotted line in Figure 4 shows the individual sections (the alumina core is one piece). The furnace consists of the following:

1. A cast alumina core and cast furnace lining.
2. A.P. Green's<sup>Δ</sup> type Sair-set bonding cement.
3. High temperature firebrick, type K-30 and medium temperature insulating brick, type K-20, both supplied by Babcock and Wilcox.<sup>++</sup>

The high purity cast alumina core and alumina lining are necessary to withstand the  $PbF_2$  vapors at elevated temperatures. The pedestal and plug are also cast from high purity alumina and are supplied by Research and Development Co.<sup>††</sup> A typical 10 inch furnace pedestal and plug are shown in Figure 5. Positioning of the pedestal was varied during the course of the work as indicated in Tables II and III of Section 3.1.2.

Using normal furnace loading, the inner furnace parts had to be changed every 6 to 9 months. The tearing down and rebuilding usually took one technician about one week to accomplish after the

-----  
+ American Electric Furnace Co., Boston, Massachusetts.

+ Research and Development Co., New Market, New Jersey.

Δ A.P. Green Firebrick Co., Pennsylvania.

++ Babcock and Wilcox, New York 17, New York.

-- Research and Development Co., New Market, New Jersey.

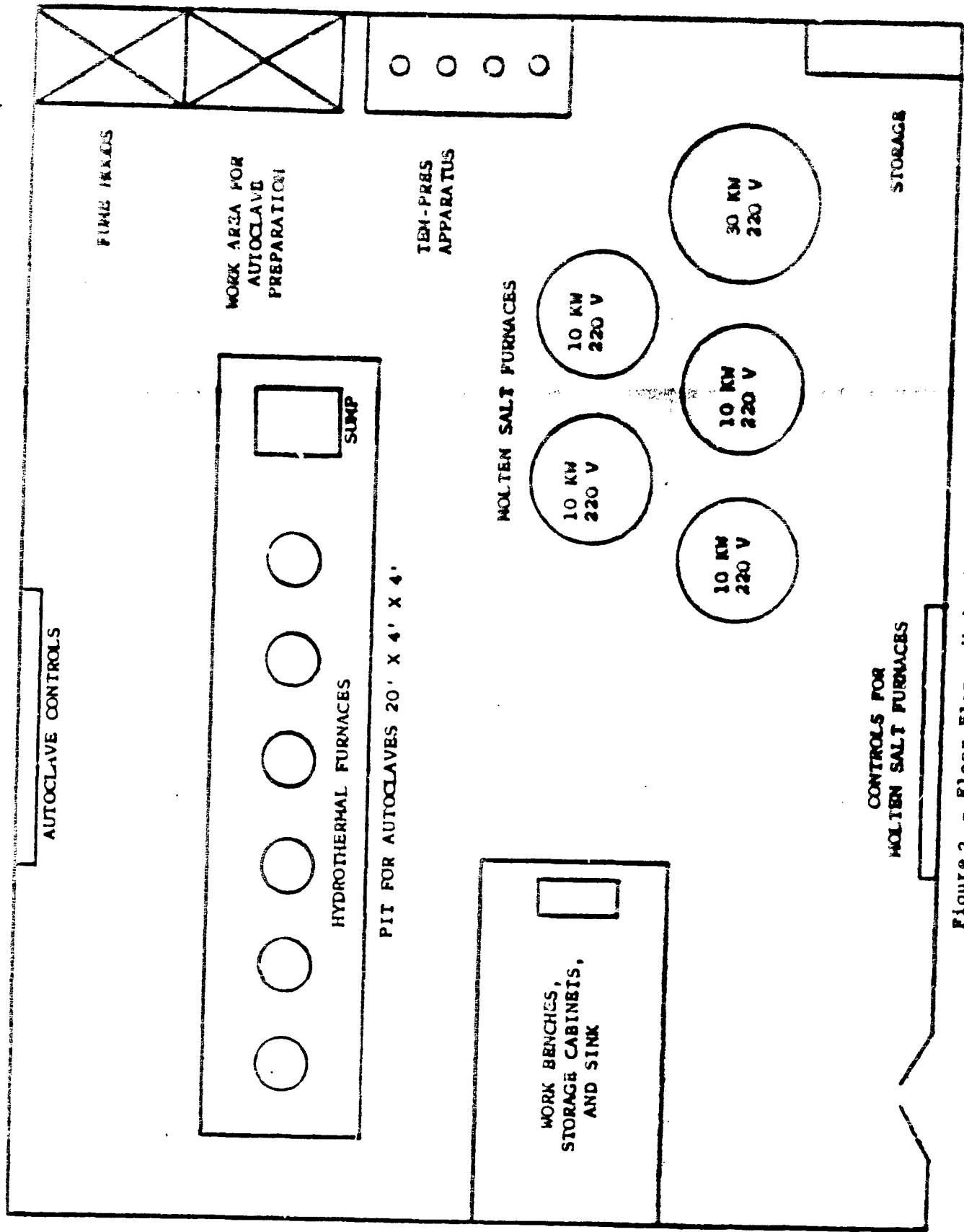


Figure 2 - Floor Plan - Hydrothermal Laboratory

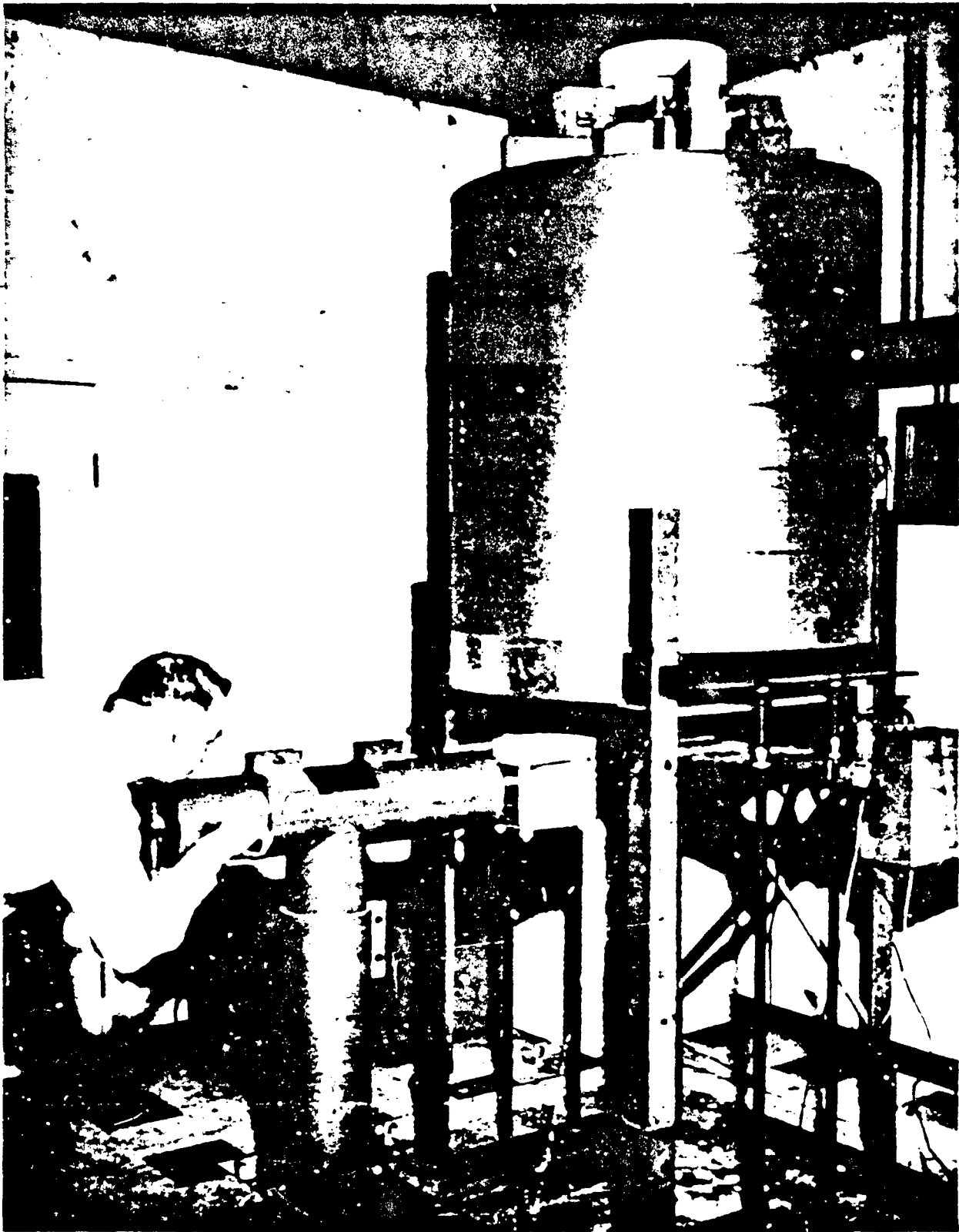


Figure 3 - 10 Inch I.D. Furnace

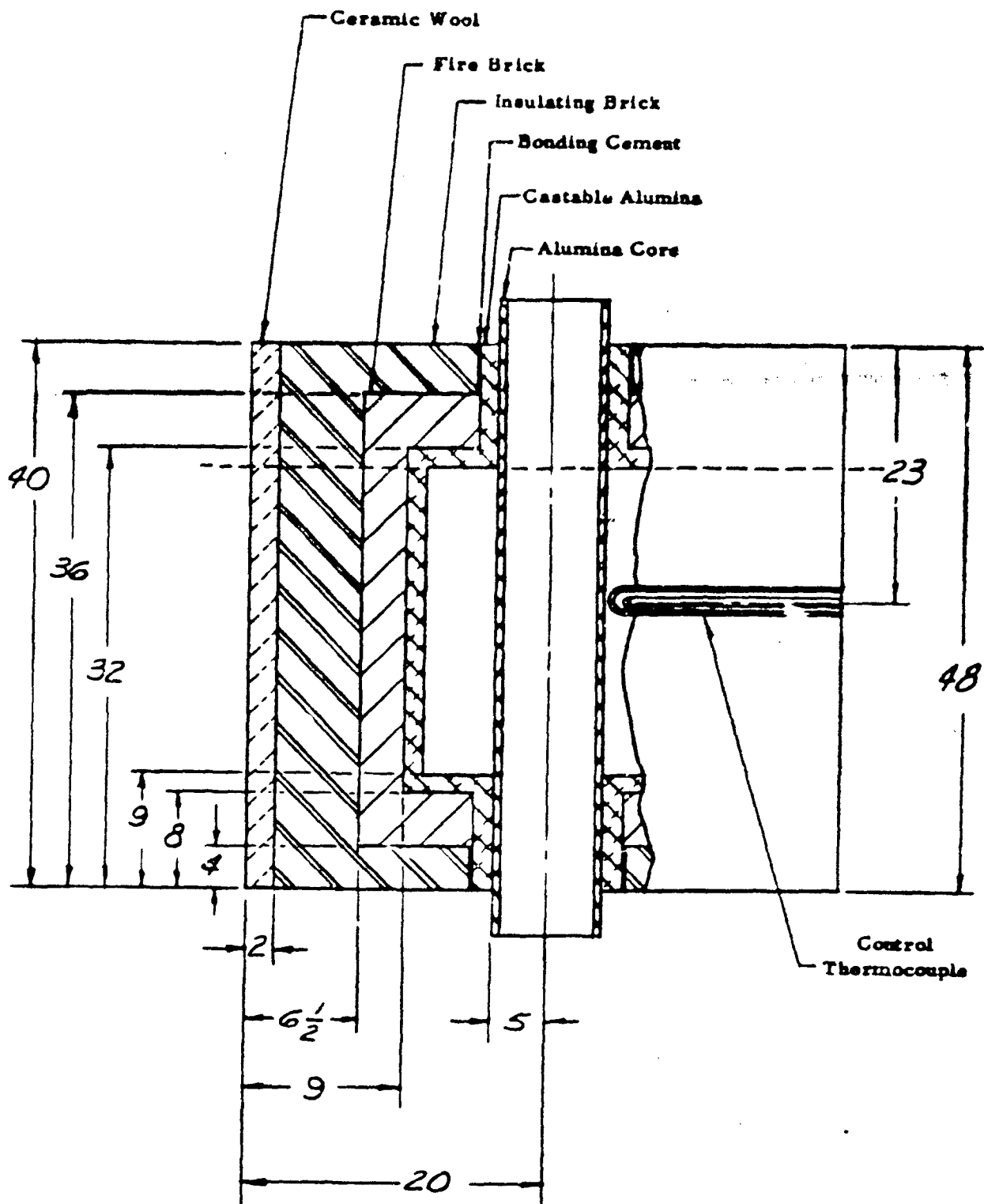
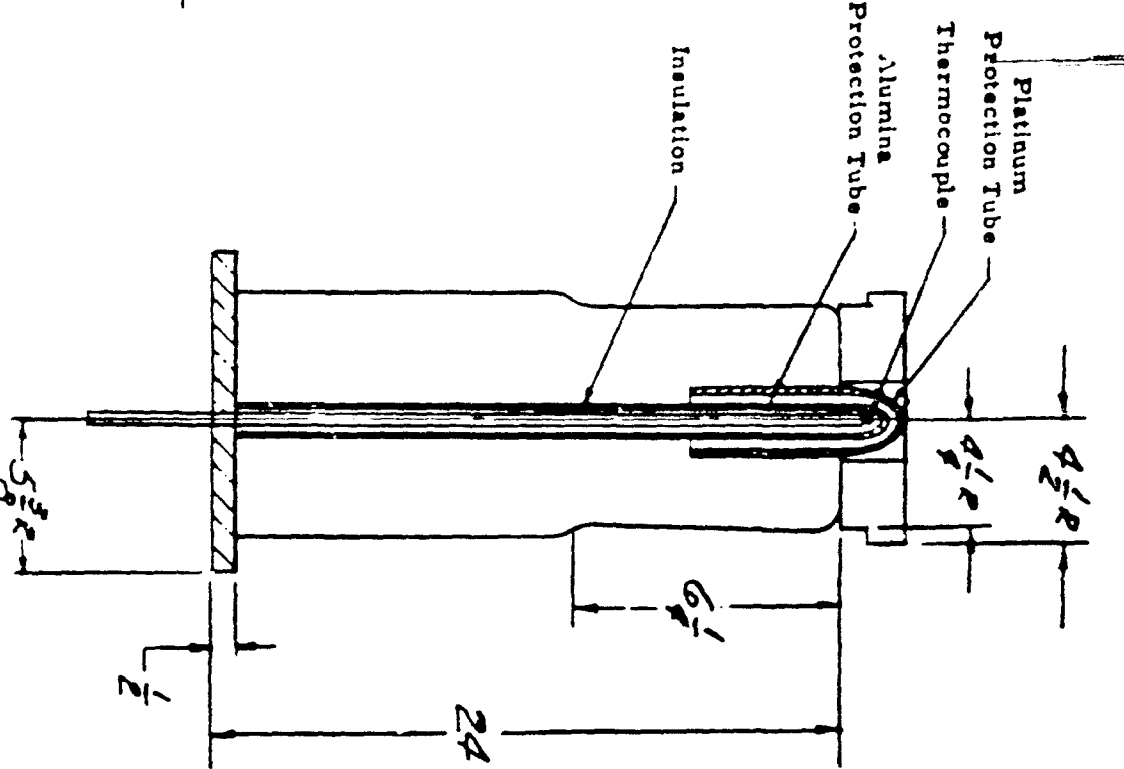
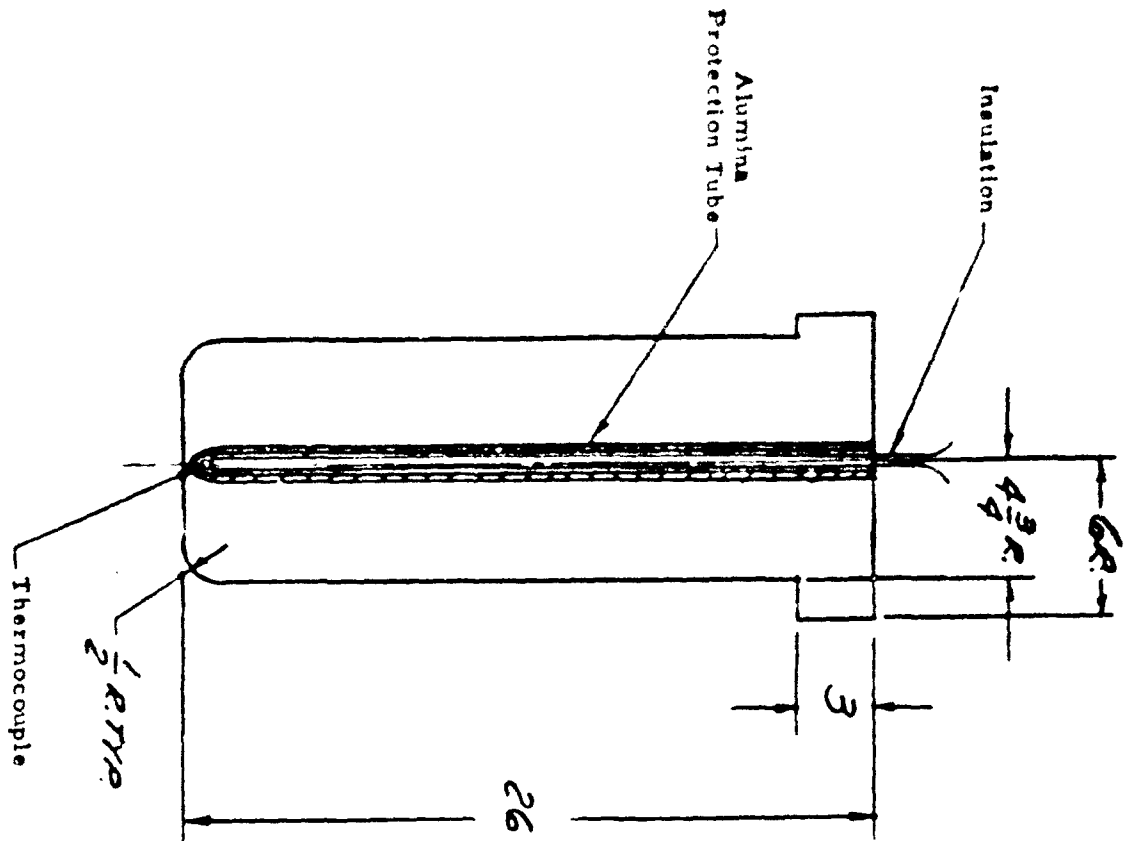


Figure 4 - Inside Cross-Section 10 Inch I.D. Furnace



Figures - Typical Plug and Pedestal

Pilot Line (Continued)

furnace had cooled to room temperature (cooling to room temperature would take 4 days.) Normally, the core was considerably swelled and the plug was bonded to the upper portion of the core due to solvent attack; thus neither the plug nor core was easily removed. The most successful method used was to forcibly extract the plug plus upper core half by means of an overhead block and tackle. The lower portion of the core was chipped away with a hammer. The remainder of the furnace insides were either lifted out or chipped away depending upon the extent of solvent attack. Once the furnace was reassembled, a slow initial warm-up cycle was necessary in order to remove water and prevent cracking of ceramic parts. The furnace was allowed to heat to 250 - 300°C at a rate of 15°C per hour and then held at that temperature for 24 hours, after which the furnace was brought rapidly to temperature.

Four 0.020 inch diameter platinum vs. platinum 13 percent rhodium thermocouples are used to either control the furnace or indicate the temperature at a desired location. The control thermocouple and one indicating thermocouple are located in the heating element region. These are shown in Figure 4. The control thermocouple is placed in the heating element area in order to sense and adjust temperature fluctuations before they affect crystal growth. A second indicating thermocouple is located in the plug, and the last, but most important thermocouple is located in the pedestal, see Figure 5. The pedestal thermocouple is positioned less than 1/4 inch away from the crucible floor, and was used to indicate "hold" and pour temperatures.

The pedestal thermocouple rotates with the pedestal during the soak period (fast rotation) and cooling cycle (slow rotation). It was, therefore, necessary to provide adequate voltage transmission to the potentiometer while the thermocouple was rotating. This was accomplished through use of a slip ring device which is shown in Figure 6. The thermocouple leads are soldered to brass rings which make continuous friction contact to copper wipers. This device was manufactured at Airtron and enables a continuous indication of the temperature throughout the crystal growth run.

The 10 inch furnace was equipped with an elevator and crucible rotating mechanism, which are shown in Figure 7. The elevator system is used to raise and lower the pedestal in order to insert and remove crystal growth runs. The elevator system is driven by a 3 phase AC motor, Type P, Model D56C, manufactured by Doerr Electric Co.\* It consists of a pedestal platform which is driven by four rotating screws. The crucible rotating mechanism is used to aid solution of the constituent oxides during the hold period. It consists of chain

---

\* Doerr Electric Co., Cedarsburg, Virginia

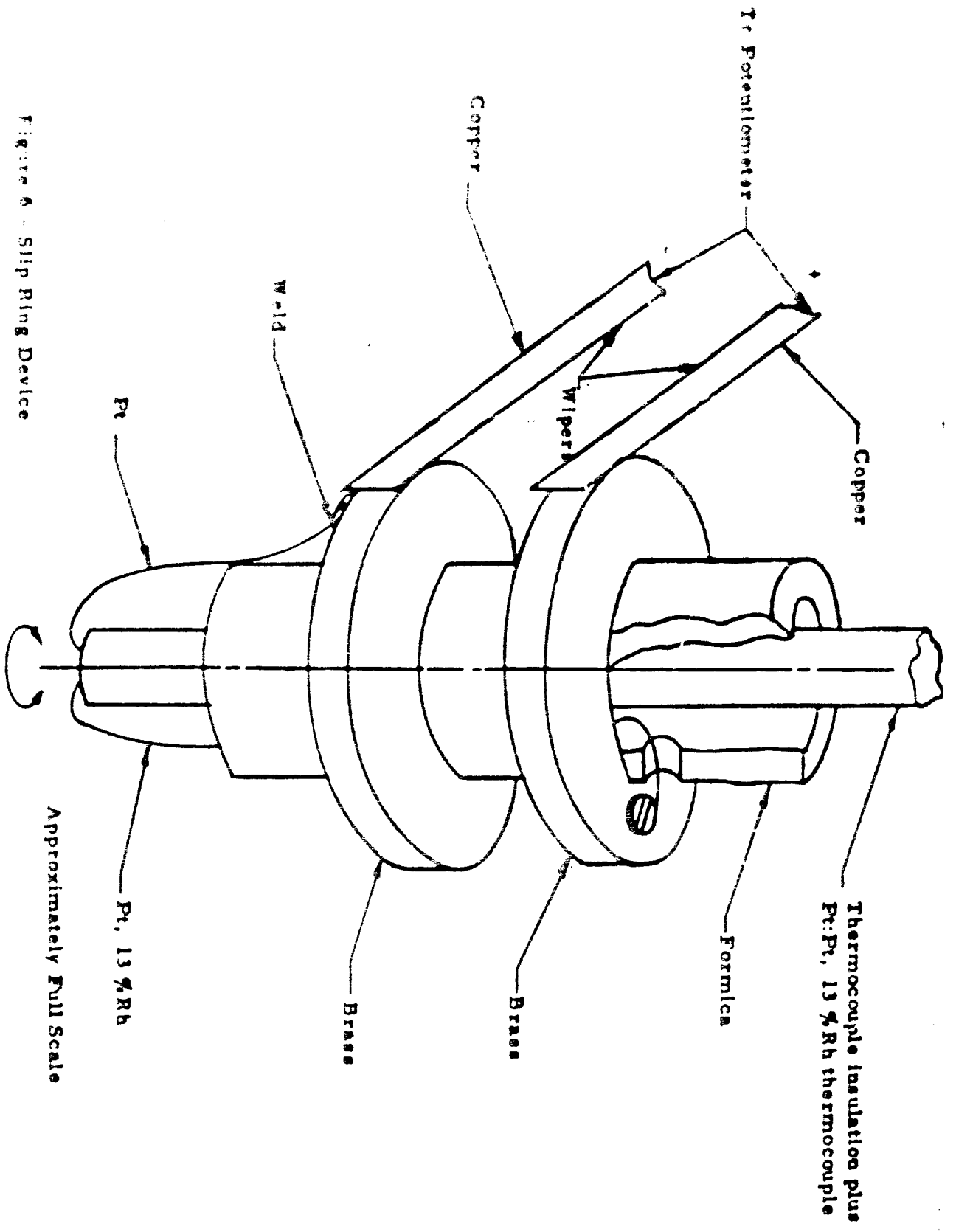


Figure 6 - Slip Ring Device



Pilot Line (Continued)

driven bearings mounted in the pedestal platform. The motor drive for the rotating system is equipped with an electric clutch to prevent abrupt starting and stopping of the pedestal. The motor, type MB-3P, and electric clutch, Part No. 304374-1, operate as one unit and are supplied by New England Gear Works and Eaton Manufacturing Co., respectively. The motor drives at 90 rpm to a 1 to 3 gear sprocket reduction which turns the pedestal at 30 rpm. The typical rotating cycle used is described in Section 2.1.6, Seed Crystal Growth Conditions.

Due to the weight of the melt plus crucible (55 to 75 pounds), a special device is needed for the pouring or unloading operation. A drawing of this device is shown in Figure 8. A set of metal jaws insulated with Fiberfrax sheet is clamped onto the crucible and supporting ceramic plate and the pedestal is lowered away. The unloader plus crucible is rolled down a track, then twisted so as to enable the liquid to pour slowly into a sand box.

Heating elements are a major consideration when attempting crystal growth on a large scale. During the earlier runs, Norton<sup>Δ</sup> "Hot Rods" and Carborundum<sup>Δ</sup> "Glo-bars" were used unsuccessfully. These elements were matched to the power input but usually did not last more than 6 to 8 weeks. With a life time of 6 to 8 weeks, it was impossible to be sure that a second run would proceed to completion.

Morganite<sup>++</sup> spiral cut heating elements (manufactured by Crucilite in England) are presently used. These double glazed 1 1/8 inch diameter elements are resistance matched to less than 2 1/2 percent and have an operating lifetime of about 6 months. These elements usually last as long as the furnace lining and are standard for the pilot line.

In order to insure identical aging of the heating elements, it would be ideal to have a completely parallel power hook-up. Unfortunately, the available power equipment and the resistances of commercial heating elements are not compatible with such a hook-up; therefore, the design shown in Figure 9 was used as an alternative. This alternating two-bank series parallel design should approximate uniform heating even though the two-banks may age differently. The elements are located 45° apart on a 16 inch bolt circle; this places the center of each element 2.5 inches from the outside diameter of the alumina core.

- 
- + New England Gear Works, South Hampton, Connecticut.
  - + Eaton Manufacturing Co., Kenosha, Wisconsin.
  - Δ Norton Co., Teterboro, New Jersey.
  - Δ Carborundum Co. Niagra Falls, New York.
  - ++ Morganite Co., 3302-3320 40th Avenue, Long Island City, New York.

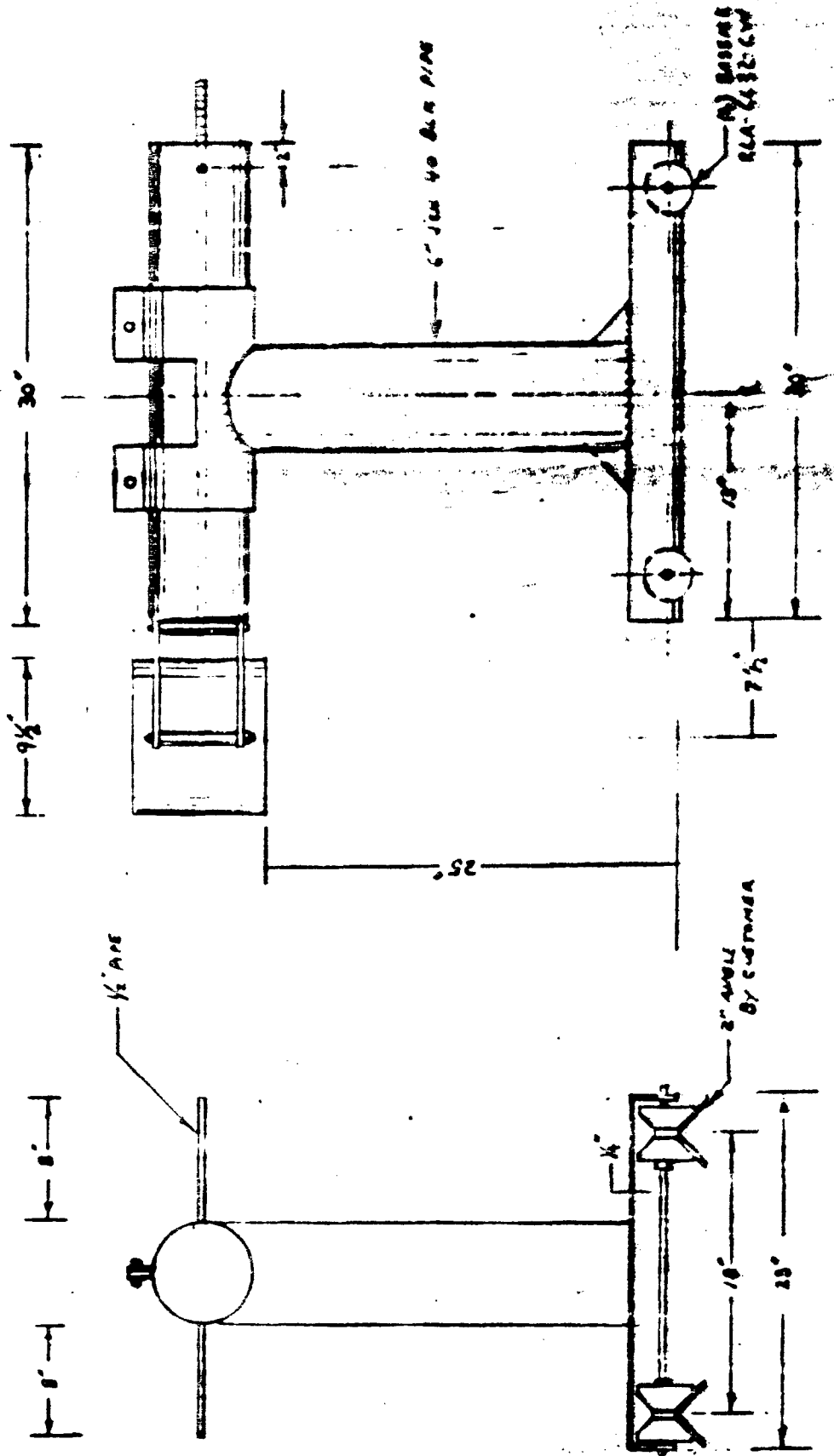
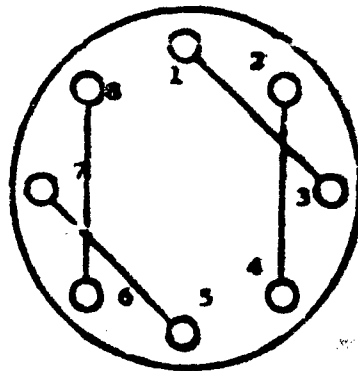


Figure 8 - Sampling Apparatus

RESEARCH DEVELOPMENT  
 DIVISION, N.J.

Top



Connect

- 1 to 3
- 3 to 5
- 2 to 4
- 6 to 8

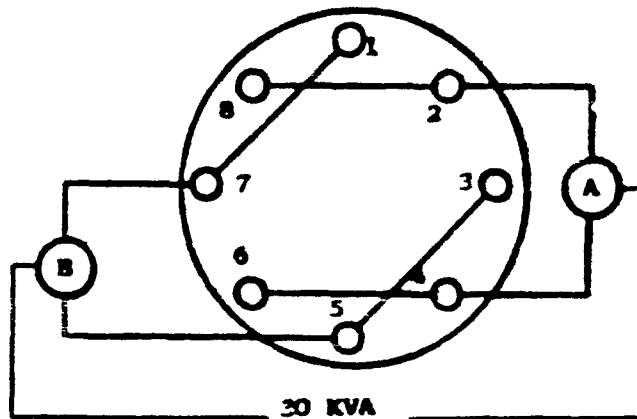
Note:

Parnace Lead in Wire - No. 6

Norton Type A Binding Post to Element Straps No. A-106

Norton Size A Strap to Element Clamps

Bottom



Connect

- 1 to 7
- 3 to 5
- 2 to 8
- 4 to 6

Power In

Phase Between 2  
4

Phase Between 5  
7

Note:

Transformer Output Voltage May Be Varied from 138-161 Volts

Figure 9 - Globar Hook-Up

Pilot Line (Continued)

The temperature control equipment, saturable reactor, power transformer and strip chart recorder (for temperature read out) were purchased from Minneapolis Honeywell Co.\* The Beck<sup>†</sup> program controller was also supplied through Minneapolis Honeywell. These components are shown with the appropriate interconnections to the furnace in Figure 10. Also shown are the elevator and rotating mechanism wiring.

The temperature control is accomplished through use of a platinum, platinum 13 percent rhodium thermocouple. The thermocouple wire is 0.20 inches in diameter, and is Englehard's standard grade. The location of the control thermocouple is shown in Figure 4. All the thermocouples, including the control thermocouple, are insulated with McDanel<sup>‡</sup> type AR2T116316 round, double bore insulation. The thermocouple plus insulation is placed in an alumina protection tube, type AFPT 14. The thermocouple is connected to an electronic null-balance recorder controller (see Figure 10), the calibrated accuracy of which is 0.3 percent of the span or  $\pm 0.12^{\circ}\text{C}$ . The actual cooling or temperature lowering is accomplished with a Beck control unit calibrated from 0.3 to  $10^{\circ}\text{C}$  per hour. Unfortunately, the Beck unit can only be used for cooling. Warm-up procedure, either from a cold furnace or after a run has been poured, must be accomplished by a manual control located on the Electro-Volt Controller, (see Figure 10). The warm-up procedure from a cold furnace has been previously described; warming up to "soak" temperature after a pour normally takes from 6 to 10 hours. Furnace power is regulated by the control unit through use of a saturable reactor, (see Figure 10).

2.1.3 The Three Inch Furnace

The four three inch furnaces were similar in design and construction to the ten inch furnace. As with the ten inch furnace, the three inch is used to designate the i.d. of the core. Because of the similarity to the ten inch furnace a complete construction schematic is not presented. Figure 11 shows the critical internal dimension and thermocouple position. The dimension of the core was such that 250 milliliter platinum crucibles were used as vessels for crystal growth. The position of the pedestal and crucible were varied throughout the course of the work; position data are included in Table III.

---

+ Minneapolis Honeywell Co., Route 22, Union, New Jersey.  
 † Harold Beck Co., 3640 North Second Street, Philadelphia 40, Penna.  
 ‡ Englehard Industries, 113 Astor Street, Newark, New Jersey.  
 Δ McDanel Refractories, Beaver Falls, Pennsylvania.

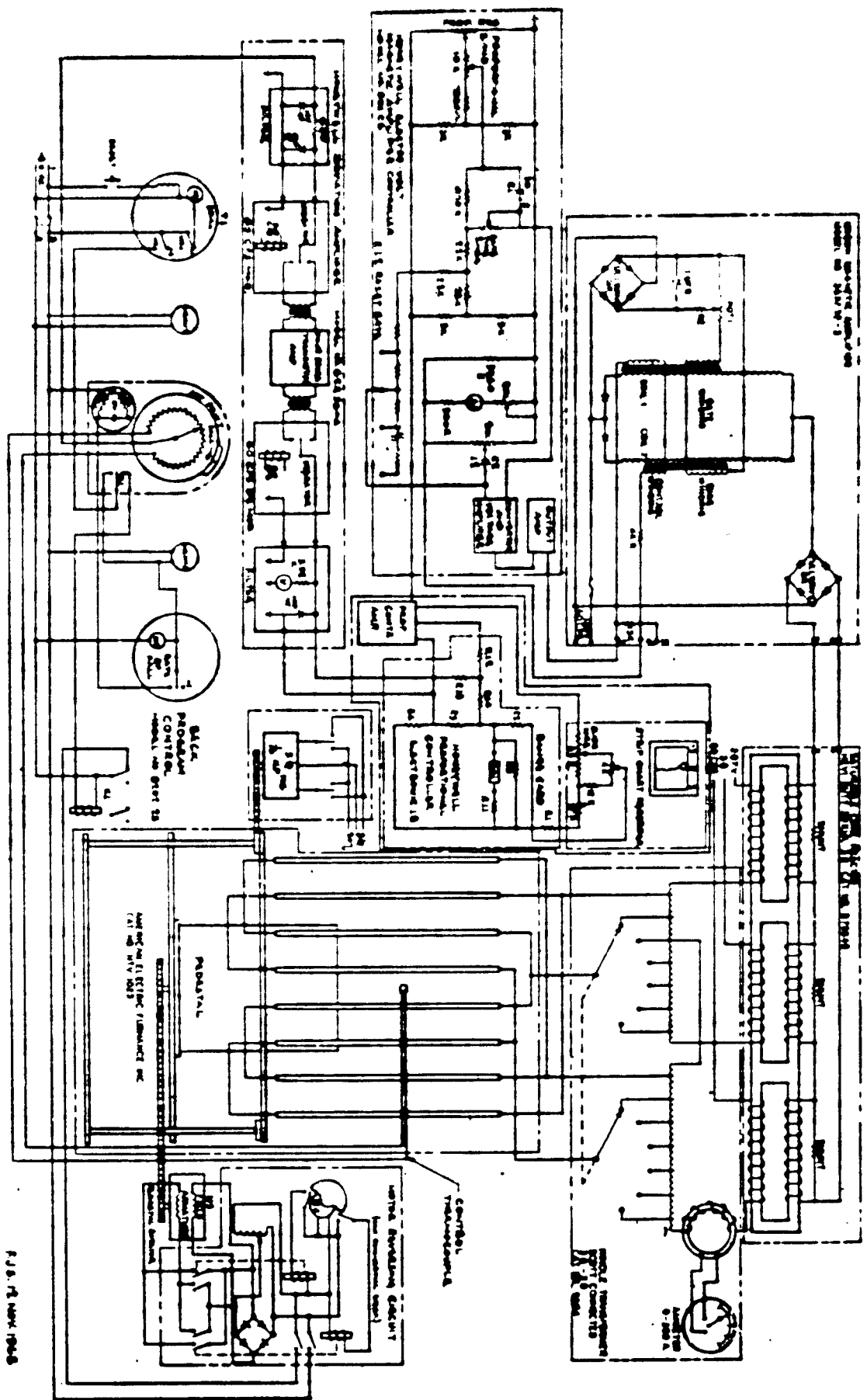


Figure 10 - Furnace Control Schematic

FIG. 10 NOV. 1948

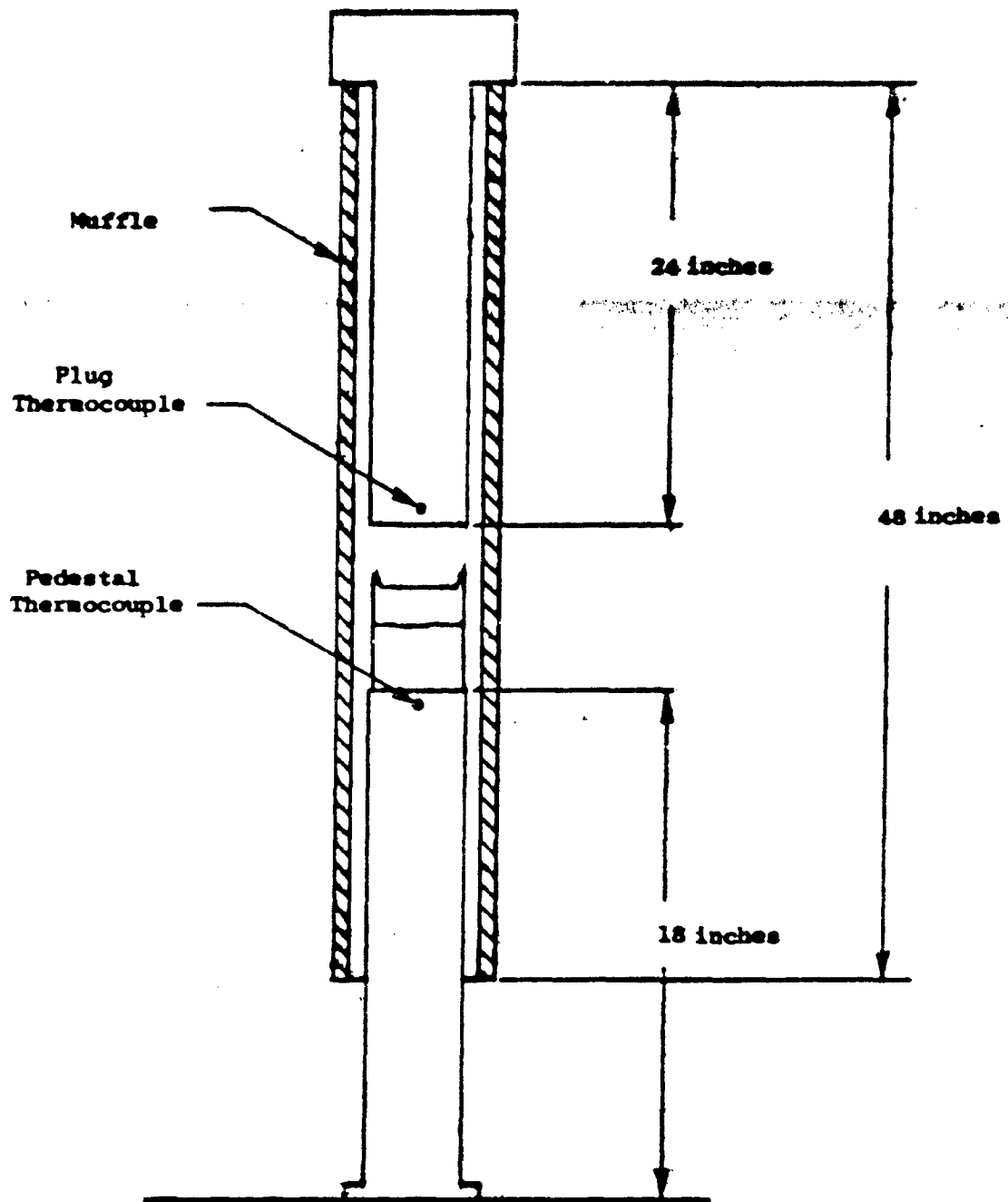


Figure 11 - 3 Inch Furnace Position Dimensions

### Pilot Line (Continued)

These furnaces are heated by six Globars wired as three series strings of two bars in parallel across the 208 volt line. (Figure 9) All are saturable core reactor controlled.

The temperature control units for these furnaces are all West Instrument Corporation, Model JSEG-3R controllers. These units consist of the temperature controller which is operated on the principle of a beam of light shining on a photocell. The beam is interrupted by a flag as the temperature approaches the set point. The proportional band which drives the magnetic amplifier and the saturable core reactor is determined by the amount of light incident on the photocell. The power input to the furnace is proportional to the photocell output. There is also a cam driven by a synchronous motor for programming. By incorporating various timers and interrupters in the circuits, it is possible to control the rate of change of temperature over a range of one-half degree per hour to fifty degrees centigrade per hour. The limit of control at constant temperature is about plus or minus two degrees centigrade.

While the temperature control is not nearly as sophisticated on the smaller furnaces, the better control is not really necessary. The very fine temperature control referred to for the 10 inch furnaces is necessary for any production type work. The smaller 3 inch inside diameter furnaces are used to obtain some of the process information which is applicable to the larger furnaces. Much of this information can be obtained on equipment which is not nearly as precise as the control equipment used on the larger furnaces. The very fine equipment will undoubtedly yield better crystals. The small furnaces are intended more to yield information than crystals. The process improvements are expected to yield more crystals per run as well as higher quality crystals.

The same kind of statement can be made about the elevators and stirrers for these furnaces. While the requirements are not as great; that is, the elevator is only required to lift a few pounds and the stirrer is required to rotate the same small mass of charge, it was felt that standard elevators and the stirrers with as many interchangeable parts as is feasible would allow the maximum utilization of equipment.

The elevator is simply a convenient method of admitting the sample to the furnace. The stirrer serves to reduce the length of time required to soak and dissolve zinc oxide in the lead fluoride. Stirring, for example, makes the zinc oxide go into solution in one or two hours at 1150°C where it would take several hours at 1250°C without stirring. It might not even be possible to dissolve the material at 1150°C without stirring. Early work by Nielsen<sup>7</sup>, indicates that zinc oxide should dissolve at 1150°C with no trouble. These temperatures are control thermocouple temperatures while Nielsen referred to

Pilot Line (Continued)

muffle or core temperatures. Even though the smaller furnaces, see Figure 12 for a comparison with the 10 inch furnace, do not require the elevator and stirrer power, it was decided that standardizing these components would be advantageous. For this reason, all the elevators are as nearly identical as furnace dimensions will permit.

2.1.4 Materials and Purity

For the growth of ZnO by the molten salt technique only two chemicals are required, ZnO and PbF<sub>2</sub>, which were purchased from Fisher Scientific Co. + and Baker and Adamson, ++ respectively. The zinc oxide was the Fisher CERTIFIED ACS Grade which is 99.8+% purity. The PbF<sub>2</sub> was B&A Reagent Grade which analyzed as 99.8+% PbF<sub>2</sub>.

Cleaning chemicals, acids for the platinum crucibles and NaNO<sub>2</sub> for the crystals were technical grade obtained from various chemical houses.

2.1.5 Weighing and Loading Procedures

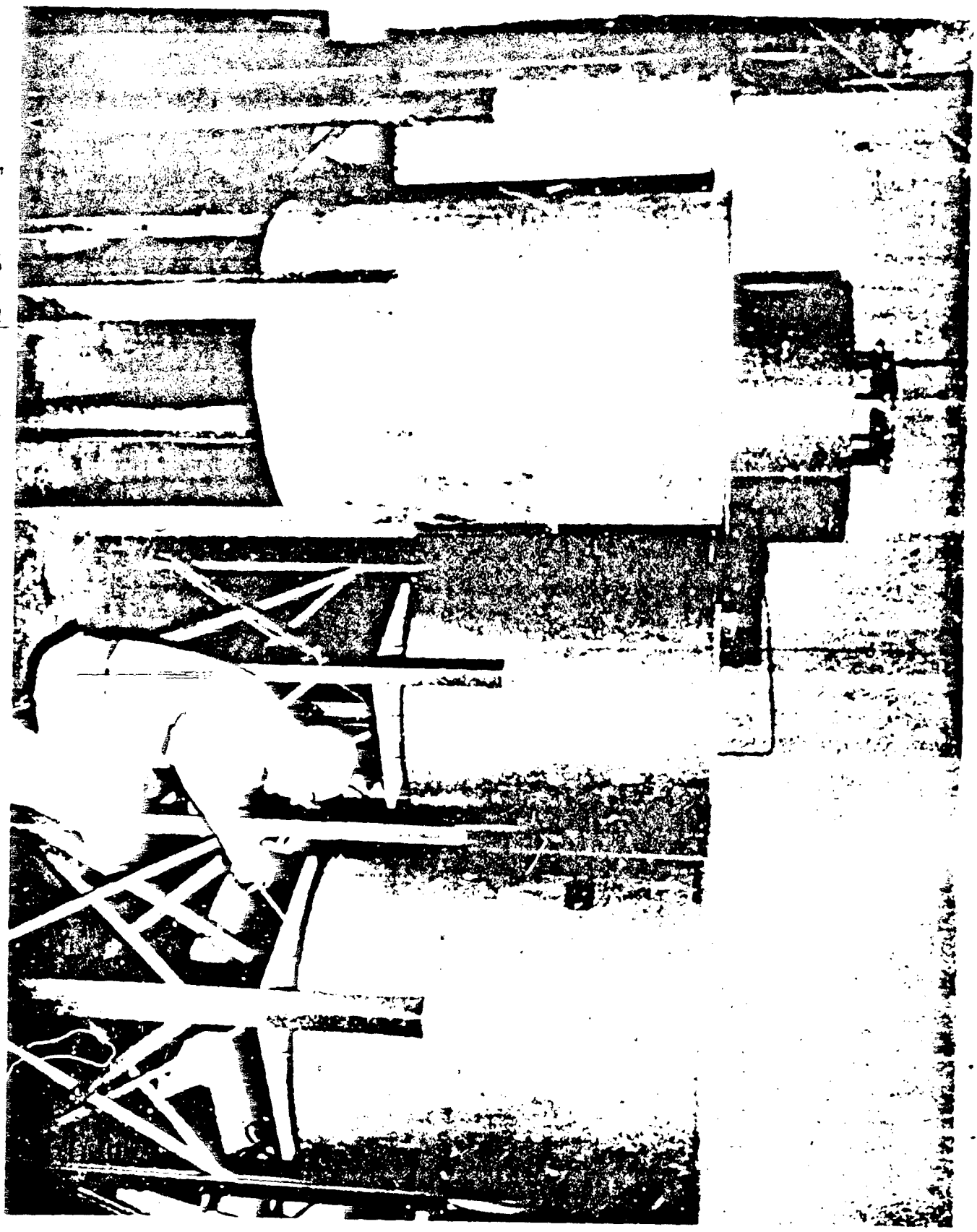
The ZnO and PbF<sub>2</sub> powders were carefully weighed on a chemical balance of suitable size. The balance used was different for batches for 3 inch, 6 inch and 10 inch furnaces. The general procedure in loading the crucibles was to pack the ZnO powder on the bottom of the crucible and to pack the PbF<sub>2</sub> on the top. By using this procedure it was felt that as the heavier PbF<sub>2</sub> melted and flowed downward it would help in dissolving the ZnO. A tight fitting cover was then placed on the crucible and the sides of the lid crimped so as to maximize the closure of the crucible.

The platinum crucibles<sup>Δ</sup> used in this work were of three sizes: 1) 8 inches in diameter by 8 inches high and .050 inch thick walls, 2) 5 1/4 inches in diameter by 5 1/4 inches high and .050 inch thick walls and 3) 3 1/2 inches in diameter by 2 1/2 inches high and .030 inch thick walls.

The usual or typical quantities of PbF<sub>2</sub> and ZnO charge to the three sizes of crucibles are in the same ratio as used by Nielsen and Dearborn<sup>7</sup> and are presented in Table I.

- 
- + Fisher Scientific Co. 1080 Lousons Rd., Union, New Jersey 07083.
  - ++ Baker & Adamson, General Chemical Division, Allied Chemical Corp. P.O. Box 70, Morristown, New Jersey.
  - Δ Baker Platinum Division, Englehard Industries, Newark, New Jersey.

Figure 12 - Photograph of Molten Salt Furnaces in Hydrothermal Pilot Line



Pilot Line (Continued)TABLE I

Typical Molten Salt Composition for ZnO Crystal Growth

	<u>Wgt ZnO (grams)</u>	<u>Wgt PbF<sub>2</sub> (grams)</u>	<u>Moles ZnO</u>	<u>Moles PbF<sub>2</sub></u>
3"	44	400	0.54	1.63
6"	322	2930	3.95	11.95
10"	1320	12000	16.20	48.92

In loading the ten inch furnace the cal was held in the jaws of the mechanical loader and placed on top of the pedestal. Loading of the 6" and 3" furnaces was more easily accomplished manually with tongs of the proper size and shape to hold the crucible.

2.1.6 Seed Crystal Growth Conditions

Again a general procedure and conditions are presented here in this section; individual experiments wherein various gradients were employed will be described in later sections.

In any of the furnaces used the pedestal with the can resting on top was raised into the preheated furnace. The pedestal position was varied in order to optimize the gradients for the best crystal growth.

The charged crucible was soaked at a temperature, usually 1150°C for a minimum of two hours while rotating the pedestal. The rotation cycle was as follows: 25 seconds clockwise, 5 seconds stop, 25 seconds counterclockwise, 5 seconds stop and repeat. It was found that without rotation much longer soak periods were required in order to obtain complete dissolution. At the end of the soak period this rotation was stopped and the cool-down began. Depending upon the size of the furnace and specific goal of each run the cooling rate was varied from 0.5°C/hour to 7°C/hour. In the smaller furnaces, the faster cooling rates of 3-7°C/hour were employed since the temperature control was probably limited to 1-2°C. In the large furnace rates down to 0.5°C/hour were employed. The cool down period was terminated at 1050°C which meant a cooling period of 24 to 300 hours depending upon the rate employed.

2.1.7 Unloading Operation

At about 1050°C - 1080°C, depending on the composition used, the crucible is rapidly withdrawn and the excess liquid is poured off the crystals.

### Pilot Line (Continued)

Preparations prior to the pouring operation are very important. The toxicity of lead fluoride vapors necessitates extreme care in handling. Three people (minimum) are required to pour a large run. One man operates the elevator and directs the movements of the unloading device; he also is responsible for removing the crucible cover. The second man handles the unloading device and does the actual pouring. A third man holds an exhaust snorkel directly above the crucible during the entire operation. The second and third men are equipped with appropriate gas masks (Model H, plus canister EA 81524, manufactured by Mine Safety Appliance Co.<sup>+</sup>). Also, during the entire pouring period, a high volume roof exhaust fan is in operation.

The actual pouring operation should be accomplished in less than 10 minutes to prevent the liquid from freezing. The sequence of events consists of the following:

- a. Prepare equipment, turn on exhaust fans, and put on gas masks, as described above.
- b. Lower pedestal and grab crucible with jaws of unloading device (1 - 2 minutes).
- c. Run pouring device down track and remove crucible cover (1/2 - 1 minute).
- d. Pivot unloading device and slowly pour liquid into sand box or water cooled metal container (4-5 minutes).
- e. If the crystals are floating, they should be prevented from escaping with the liquid. This is normally done by holding a metal rod across the rim of the crucible near the pouring area.

With the smaller crucibles the same health safety precautions were taken with the use of gas masks, and venting of the fumes. The flux pouring was essentially the same except that manually operated forceps were used to remove the crucibles and pour the flux.

#### 2.1.8 Crystal Separation and Cleaning

After the platinum crucible has cooled to room temperature, it is gently tapped with a plastic hammer to loosen the crystals which are attached to the wall and floor.

The usual flux removal technique for cleaning crystals employ one or more acids. Zinc oxide, though a refractory material is quite readily attacked by acids and so a different procedure had to be

---

<sup>+</sup> Mine Safety Appliance Co., 201 North Braddock Avenue, Pittsburgh, Pennsylvania

Pilot Line (Continued)

developed.. Simple mechanical removal of the flux by grinding, scraping etc. was not possible because of fragility of the thin ZnO plates.

A somewhat different approach was required to clean the ZnO crystals of any adhering  $PbF_2$  flux. The procedure which was developed was as follows:

1. The ZnO plates with adhering flux were placed in a stainless steel screen basket. (2" diameter)
2. This basket was then immersed into a 250cc platinum crucible which contains molten  $NaNO_3$  (mp 307°C).
3. After several minutes in molten  $NaNO_3$ , the basket was slowly withdrawn.
4. After cooling in air to room temperature the basket with the plates was placed in a beaker which was being flooded with hot water.
5. The cleaned plates were then washed with distilled water and air dried.

This procedure was quite satisfactory. The molten  $NaNO_3$  did not attack the ZnO crystal but did react with adhering  $PbF_2$  to form water soluble  $Pb(NO_3)_2$  and the just slightly less soluble  $NaF$ . The combination of molten  $NaNO_3$  followed by hot water proved to be a satisfactory approach to cleaning the molten salt ZnO plates.

## 2.2 Hydrothermal

### 2.2.1 Laboratory Facility

A pilot line for the hydrothermal growth of large ZnO crystals was designed and assembled. A 20-foot long x 4-foot wide x 4-foot deep pit with reinforced concrete walls was constructed in the laboratory to contain the autoclaves and furnaces when in operation. This pit provides personnel protection against scalding or fragmentation which could result from equipment malfunction. The pit contains six furnaces, four large ones for the large A-286 autoclaves and two for the small Waspalloy vessels, and a saturable core reactor for each furnace. At one end of the pit is located a sump and automatic pump in the event of ground water seepage into the pit. This sump area of the pit is also used for cleaning and cooling of the autoclaves. This equipment was obtained under Air Force Facilities Contract AF33(457)-12307.

The furnace heights are adjusted so that the tops of the autoclaves are just floor level. The pit area is covered by removable steel grill sections. Mounted on the nearest wall are the temperature controllers and programmers for the hydrothermal furnaces.

### Pilot Line (Continued)

A one-thousand pound capacity travelling hoist is mounted overhead so that the autoclaves may be readily moved.

The laboratory is also provided with chemical work benches for silver can preparation, loading and storage. A fume hood and large overhead exhaust fan supply ventilation for protection against chemical vapors.

A floor plan of the laboratory showing its hydrothermal and molten salt facility is shown in Figure 2. Figure 13 is a photograph of the pit area showing the larger furnaces and autoclaves.

#### 2.2.2 Hydrothermal Crystal Growth Autoclaves

In order to grow crystals weighing 150 grams or more as specified in the contract, it was necessary to purchase vessels of sufficient cavity size to contain such crystals. The cavity size was large enough so that crystals at least two inches in width could be grown in suitable silver cans.

Of the available materials for autoclave construction, that of maximum pressure and temperature (P-T) limits was chosen since, at the time of purchase, these variables for crystal growth were not known. It was also necessary to select a seal design capable of containing the high pressure temperature conditions. As a result of these criteria, the vessel as shown in Figure 14 was chosen, - the material of construction being A-286 whose pressure-temperature ratings are 30,000 psi and 590°C for 10,000-hour life.

The autoclaves were manufactured by Autoclave Engineers, Inc., Erie, Pennsylvania, who had developed what is called a "Modified Bridgman" seal. This seal is that used by Western Electric and others for quartz manufacture and believed to be the best workable, high temperature, high pressure seal. This seal is described as "self-energizing" since it relies upon the internal pressure developed by the fluid under growth conditions to provide for sealing force. The vessel is initially sealed by the main nut's downward thrust on the seal ring and then upward thrust on the piston by means of the set screws in the lock nut. Opposite screws are tightened in turn by means of a torque wrench to 10 ft. lbs. each. This sealing initially causes the seal ring to make line contacts with the autoclave body and plunger. As the internal pressure develops, the plunger is thrust upward causing the seal ring to deform elastically and produce surface contacts. This self-energized seal provides better sealing as the internal pressure increases.

During the early part of the program autoclave failure developed as a serious problem. One of the first four autoclaves failed because of a flaw in the original ingot from which it had been fabricated. The failure of the remaining vessels was caused by stress corrosion cracking.

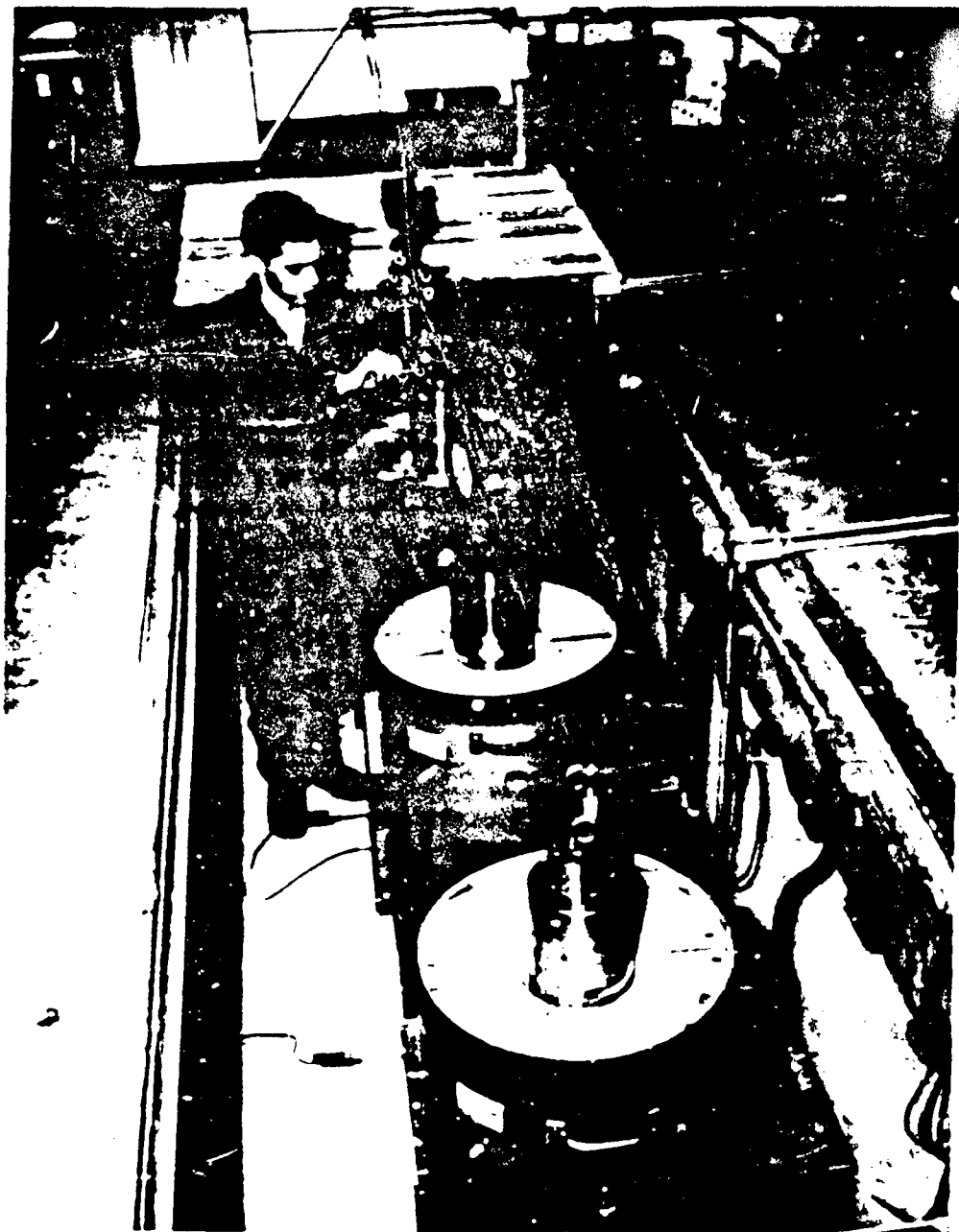


Figure 13 - Pit Area, Furnaces and Autoclaves

### Pilot Line (Continued)

Some form of stress and the presence of a corrosive atmosphere are the two elements necessary for the initiation of this particular type of failure. In the case of hydrothermal autoclaves used for crystal growth, the force is provided by the working pressure and the corrosive atmosphere is the result of occasional leaks in the noble metal (silver) container used to hold the caustic solutions. The three causes of leaks in the silver cans have been: 1) corrosion of the silver, 2) improper pressure balance leading to can rupture, and 3) faulty welding.

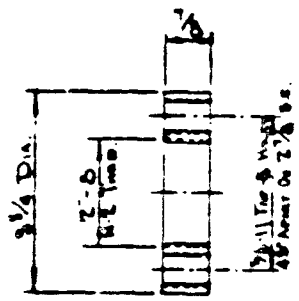
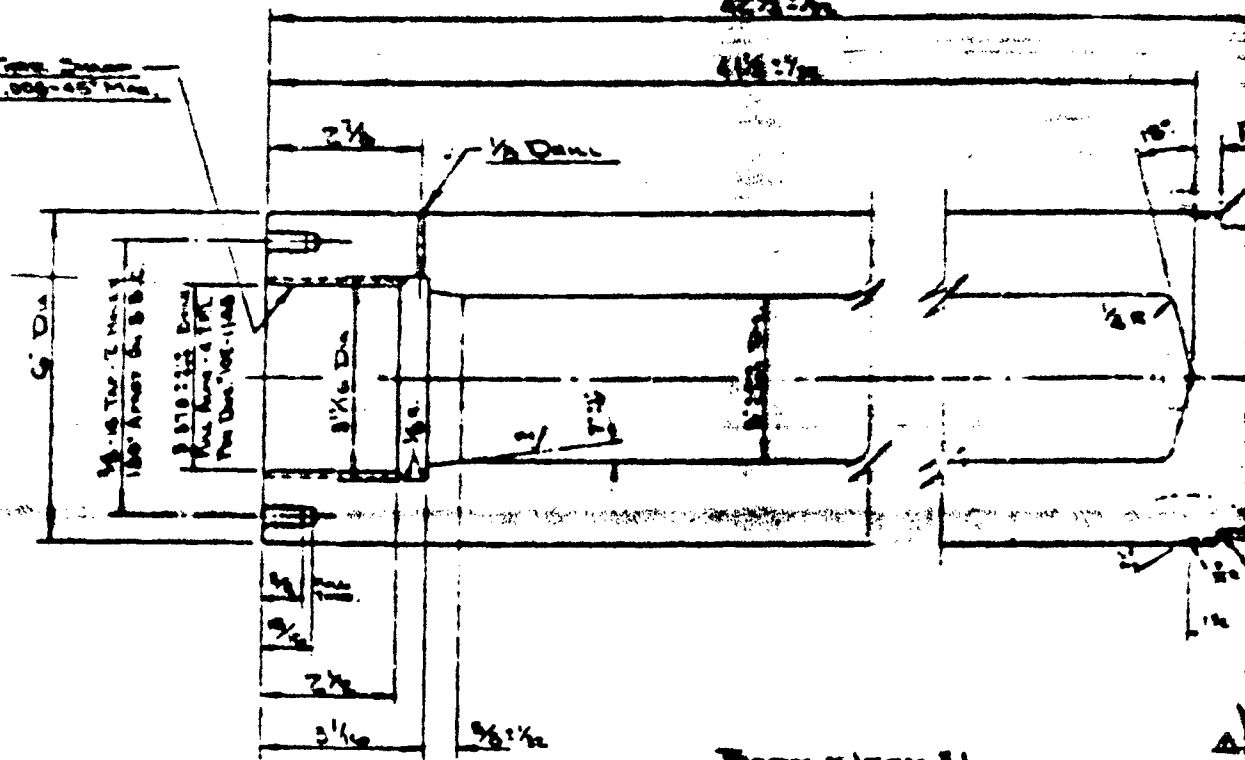
Experience has shown that even a limited exposure is sufficient to instigate this corrosive force and that failure can occur at some later date. A change in autoclave design was suggested to Autoclave Engineers to aid in extending the life of a vessel by preventing stress corrosion cracking from occurring too extensively. In order to do this, it was suggested that the bottom of the cavity be changed from conical to hemispherical. The conically machined tip was thought to be a place of high stress and particularly subject to attack by base. In the five vessels which failed on Contract AF33(657)-8795, the failure in each case was at the center of the bottom of the vessel.

This conical tip was also questioned in view of the rather thin wall at the bottom of the vessels. It was suggested that perhaps a thicker bottom (increased by one inch) would add extra strength to counteract any applied stress. Our experience with two Waspalloy autoclaves with 2.5 inch thick bottoms had been favorable in view of their long life even when subjected to basic solutions at higher pressures and temperatures. There were some differences in conditions to which the two types of vessels had been subjected. The Waspalloy vessels were used for ruby growth where the solvent is  $K_2CO_3$  solutions and the working conditions of 25,000 psi and 525°C; whereas, correspondingly, the A-286 vessels for ZnO growth were used with KOH solutions at 7,500 psi and 300°C.

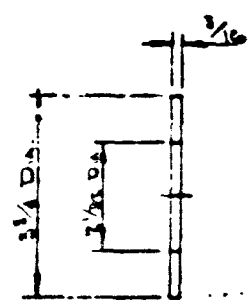
Autoclave Engineers concurred that these modifications certainly could not add to the problem and could probably help. Only slight addition in cost was necessary to cover production of the thicker hemispherical end, Figure 15. Two such vessels were purchased and used with satisfaction during the balance of the program. This design change has now been incorporated by Autoclave Engineers in all their standard crystal growth vessels.

One other difficulty is noted here since it involved an unpredicted behavior of the seal. While the seal ring does deform elastically at lower pressures and temperatures, it was found that plastic deformation occurred at higher temperatures and pressures (500°C and 20,000 psi) which were still well below the maximum temperature and pressure for which the vessels were rated. This deformation does not interfere with the vessel closure but does necessitate machining the seal ring after each use and careful preparation of all

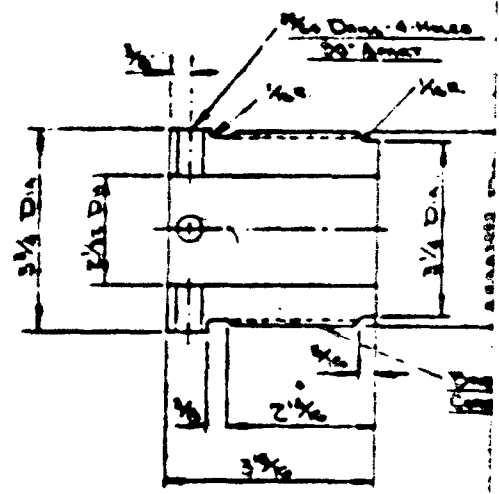
BRASS TUBE  
 GRADE 808-45 TYP.



LOCK NUT - ITEM #6



THRUST WASHER - ITEM #5



MAIN NUT - ITEM #4

BRASS ALL SHOWN COMPONENTS  
 GRADE 808-45 TYP. TO RIGHT DIA.  
 FRACTIONAL DIA. 1/16"  
 1/8" FRACTIONAL DIA.  
 ALL DIMENSIONS IN INCHES



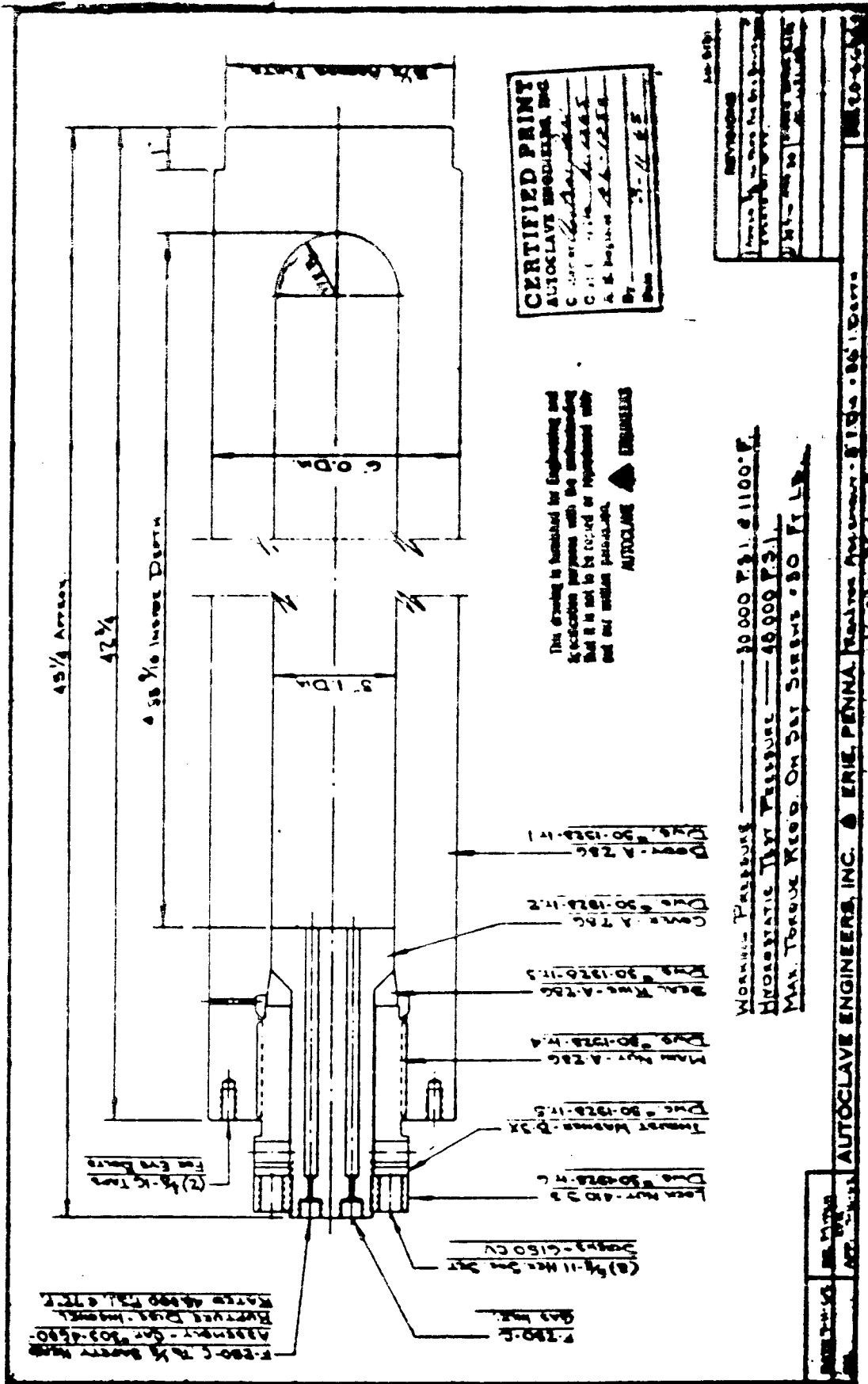


Figure 15 - Engineering Drawing of Autoclave with Newly Designed Bottom

### Pilot Line (Continued)

sealing surfaces prior to use. Machining, lapping tools, and techniques to produce reliable sealing of the autoclaves are discussed in section 2.2.8.

#### 2.2.3 Silver Cans

Noble metal containers or cans are used in order to prevent contact of the autoclave body with the basic solution used in ZnO crystal growth. This is necessary since the solution would corrosively attack the autoclave metals under hydrothermal conditions. The containers were made of seamless, fine silver tubing and flat circles of the same material. The baffle and seed rack were also made of fine silver. The first silver cans used were 2 inches in diameter by 24 inches long.

The design of the silver can was changed to a completely sealed system in the course of the program for two reasons: 1) in order to contain the large crystals and 2) it became apparent that better pressure balance could be achieved with a larger can. (See section 2.2.4). As the crystals increased in size it was noted that the crystal growth at the edges near the silver can was being affected by a restriction in flow of the fluid. Therefore it was desirable to make the silver can as large as possible. The second can design is shown in Figure 16. The silver materials for the fabrication of the cans were purchased from Handy and Harmon Co.<sup>+</sup> in the form of flats, tubing and wire. The dimensions of the cans, rack, baffle etc. are shown in Figure 17. After normal machining and cutting to the dimensions specified in Figure 17 the can and internal rack were fused together without a fluxing agent using a Miller Welder,<sup>++</sup> Model 330 AP, in an atmosphere of argon gas. The final sealing of the can after filling with seeds, nutrient and fluid is described in section 2.2.10.

#### 2.2.4 Large Can Technique

At the onset of this Contract, it had been the practice, when using noble metal cans, to adjust the volume of the can (internal volume) to be nearly equal to the remaining autoclave volume (external volume). The problem of using noble metal cans rests in the different equations of state for water and hydroxide or carbonate solutions. Since the equations are different, water and any aqueous basic solutions of the same percent fill and at the same temperature would generate different pressures. It has been found for all of the

-----  
<sup>+</sup> Handy and Harmon Co., New York, N.Y.

<sup>++</sup> Miller Co., Appleton, Wisconsin.

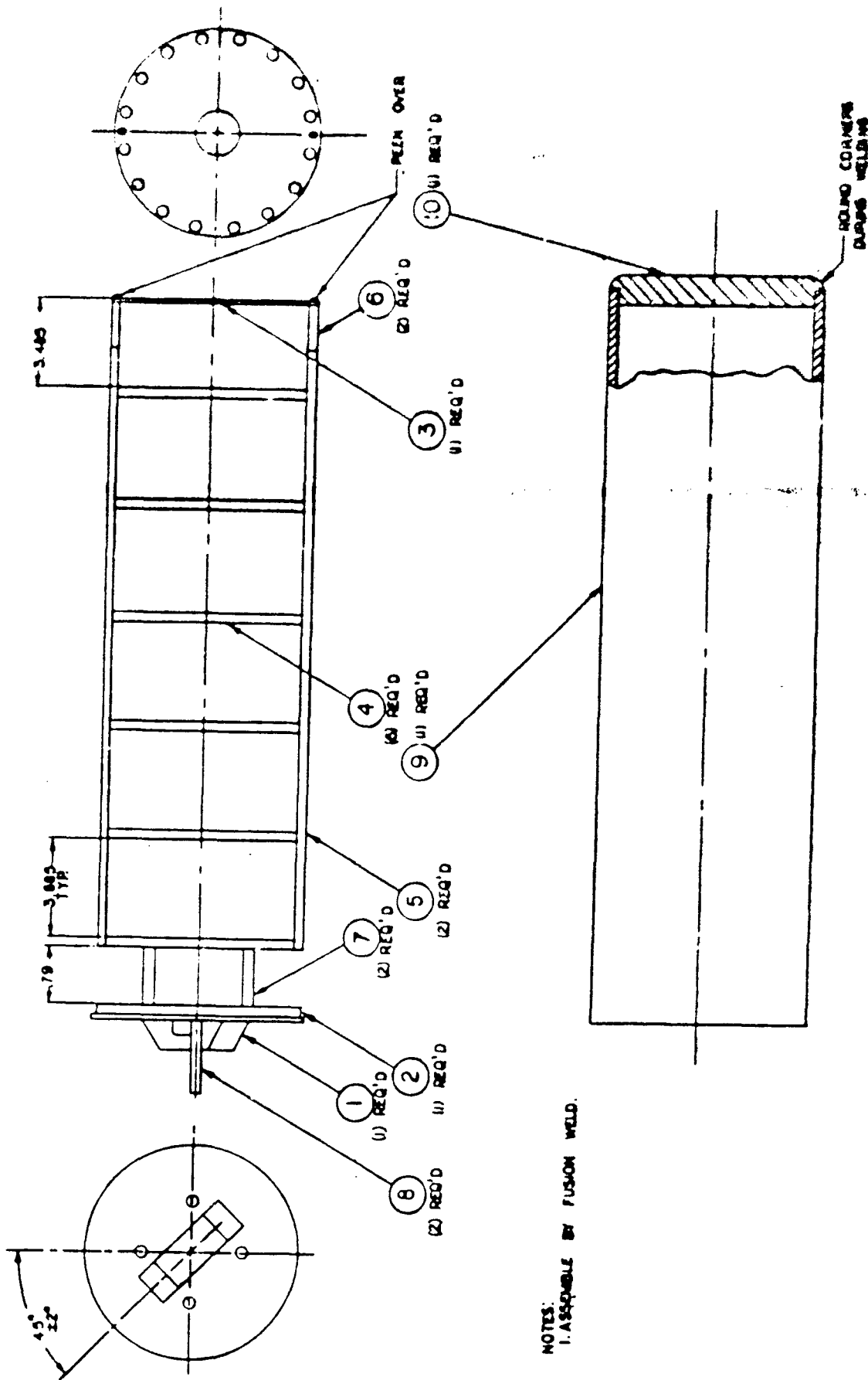


Figure 16 - Large Can Assembly



Pilot Line (Continued)

common hydrothermal solvents that the pressure generated by a solution is less than that of pure water.

As a result of these differences, an adjustment of the fills (internal to external) must be made so that at temperatures the same force is exerted by the base and water. Any grave imbalance of fill conditions would lead to severe compressive or expansive damage to the can which could lead to development of a leak. Because of the pressure-temperature behavior of these fluids, there is only one pressure and temperature condition at which there will be perfect pressure balance for any set of fills. See Figure 18.

The void external volume is obtained by measuring the volume of the autoclave when empty and subtracting the geometrically calculated volume of the can. The percent of this volume to be filled with water is defined as the external fill. The internal fill is similarly defined. It is obtained by calculating the volume of an empty silver can based on its geometry. From this value are subtracted the volume of the seed rack and baffle (calculated from geometrical forms) and the volume of seeds and nutrient (calculated from weights and density of ZnO). This value is then the void volume of the can and the percent to which it is filled with KOH solution is defined as the internal fill.

The figure is a somewhat exaggerated pressure-temperature diagram for water and a basic solution capable of exerting the same pressures at one temperature only. If one follows along the lines as if the vessels were warming; i.e., the temperature is increased, it will be noted that below the point (F,T) the external or water pressure is greater than the internal or base pressure and thus the can is under compression. At (P,T) the pressures are balanced so that the can is subjected to neither compressive nor expansive forces. Higher temperatures again cause an imbalance in pressure but now the can must expand. Even if the equations of state were known, the can would be subject to compression at the run warm-up and cool-down; however, the fills for the pressure-temperature balance point might be calculated rather than arrived at by experimental observation. Two other points are worth noting at this time.

In addition to not knowing the equation of state for the basic solution, any such equation would not be quite correct since at operating conditions the solutions contain 5 - 10 percent ZnO, and so a further perturbation of the equation would be necessary. Second, the treatment of this subject has been presented as though the systems were isothermal. For crystal growth, this is certainly not the case and some averaging of the equations would be necessary to apply the data.

The problems of severely working the silver can and matching pressures can be greatly alleviated by the use of a can which nearly fills the autoclave cavity. This technique was developed during

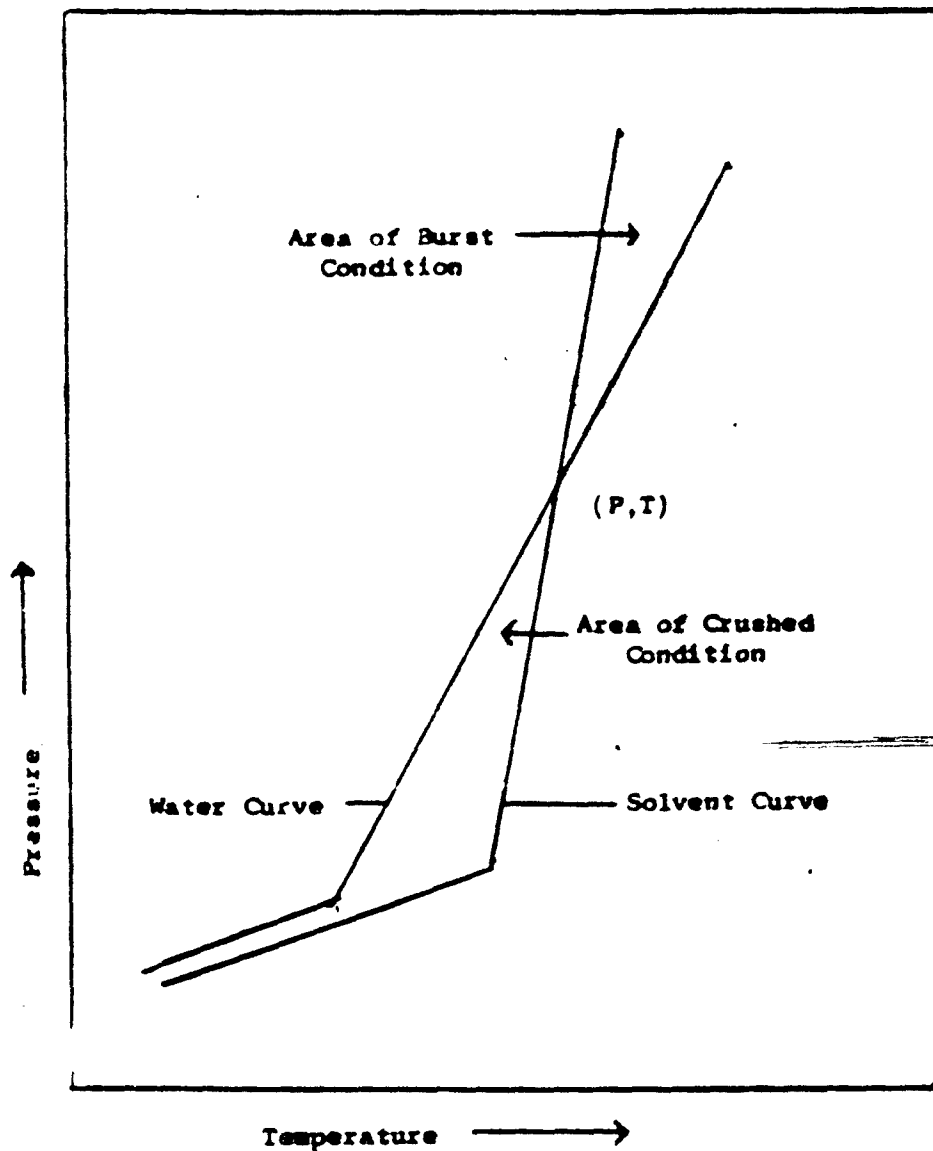


Figure 18 - Schematic for P-T Behavior of Water

Pilot Line (Continued)

the Contract when it was thought that the cans might sometimes be completely crushed when under growth conditions.

By using the large can neither of these conditions can occur as readily. For example, if the internal fill is larger than it should be by some reasonable value, the can will be under compression during the warm-up. When the crossover point is reached, and the temperature continues to increase, then the can undergoes expansion. Since the void volume is so small now a small percent change of the can's dimensions caused by expansion leads to a large percent decrease in the void volume. The large decrease in void volume also has the effect of producing a correspondingly large increase in pressure of the external volume and hence a restoration force. In other words, a small expansion of the can's dimensions leads to a relatively large increase in the external volume effectively raising its percent fill. Furthermore, due to the closeness of the fit, a bulge cannot occur in any one region and the expansion is spread out over the entire length of the can.

In the case of the internal fill being lower than it should, the can again will be under compression during the warm-up. When the operating temperature conditions are reached, the can is still under compression; however, the effect is now less since the small compression of the can leads to a large increase in the external volume. This increase in external volume essentially leads to a reduction of the fill and reacts to lower the compressive force.

With fairly accurate filling, only slight movement of the walls is required to produce balance. Thus, the gauge pressure is more nearly the internal pressure and the external fill acts only as a transmitting fluid.

For the low pressure work the internal fills were obtained from the data of Laudise et al<sup>8</sup> and the external fill from Kennedy's Tables. Fills for the high pressure work were acquired by extrapolation of the compressive fill data.

#### 2.2.5 Hydrothermal Furnaces

The furnaces used to heat the autoclaves are shown in Figure 19. The furnaces, originally designed and built by Research & Development Products, Inc., New Market, New Jersey, consist of clam shell type of heater sections constructed of Nichrome resistance wire cemented in a grooved ceramic, insulating wool materials and outer metal shells.

Since the bottom section of the autoclave must be the hotter section, it was found that the bottom should receive the greatest power and only slight or auxiliary heating was necessary in order to level out or adjust the proper temperature difference between sections.

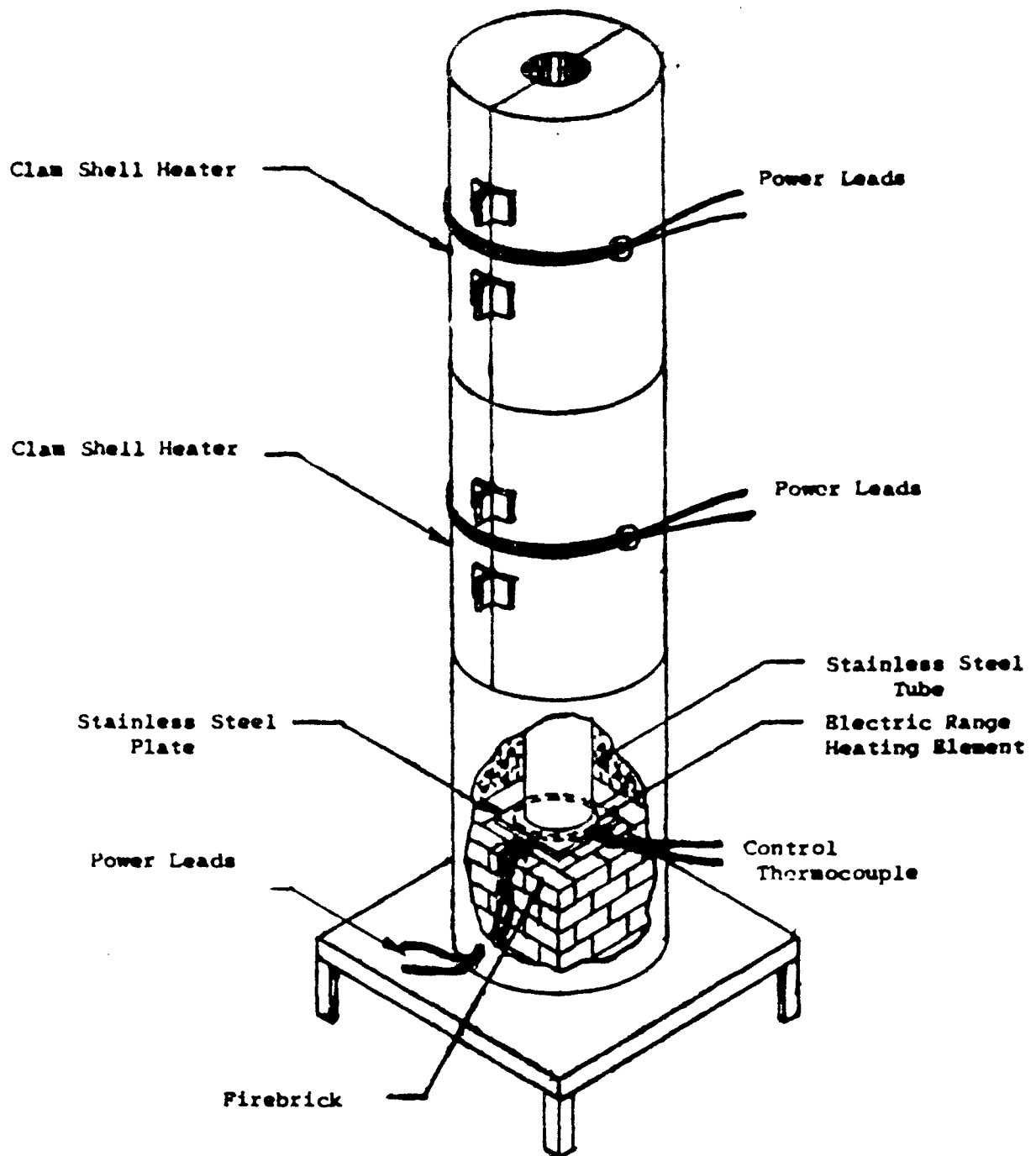


Figure 19 - Furnaces Used to Heat Autoclaves

Pilot Line (Continued)

After a number of failures in the bottom section, this section was redesigned so that the bottom of the vessel rested on an electric range heater. The main heat was applied to the bottom of the vessel by this electric range element. Figure 20. Better contact and more even heat distribution was achieved by placing an 8" x 8" x 1/2" stainless steel plate over this heater.

It was found that the amount of power for a fixed set of conditions varied somewhat for each combination of autoclave vessel, furnace and controller.

2.2.6 Temperature Control

The power to the electric range surface heating element or hot plate element is controlled by a saturable core reactor through a West Programmer Controller; a control thermocouple is cemented to the firebrick immediately below the hot plate element. The clam shell heater is also controlled by the West instrument by means of a manually set ratio for power distribution to each furnace element. This distribution of power is accomplished by the S-92 option of the West JSBG-3R Program Controller, which allows the output from one temperature controller to drive-up to three saturable reactors. In this case only two reactors are used. A schematic of the control system and furnace is shown in Figure 21. The control thermocouple supplies the input signal for the operation of the controller and driver.

The temperatures along the body of the autoclave were monitored during the course of the run by means of four thermocouples located at 1 1/2", 9 1/2", 21" and 34" from the bottom of the vessel. The temperature was measured using a Leeds and Northrup Millivolt Potentiometer, Catalogue No. 8690.\*

The functions of the various components shown in Figure 21 are discussed below. A & B are components of a Model JSBG-3R Temperature Controller manufactured by West Instrument Corporation, Chicago, Illinois.

A - The instrument uses a galvanometer detector powered directly by the thermocouple. An opaque "flag" attached to the galvanometer pointer is positioned so that it can diminish the light reaching the photocell. The photocell current is the input to a magnetic amplifier, rectifier combination which has a d.c. output proportional to the illuminated area of the photocell.

-----  
\* Leeds and Northrup, Philadelphia, Pennsylvania.

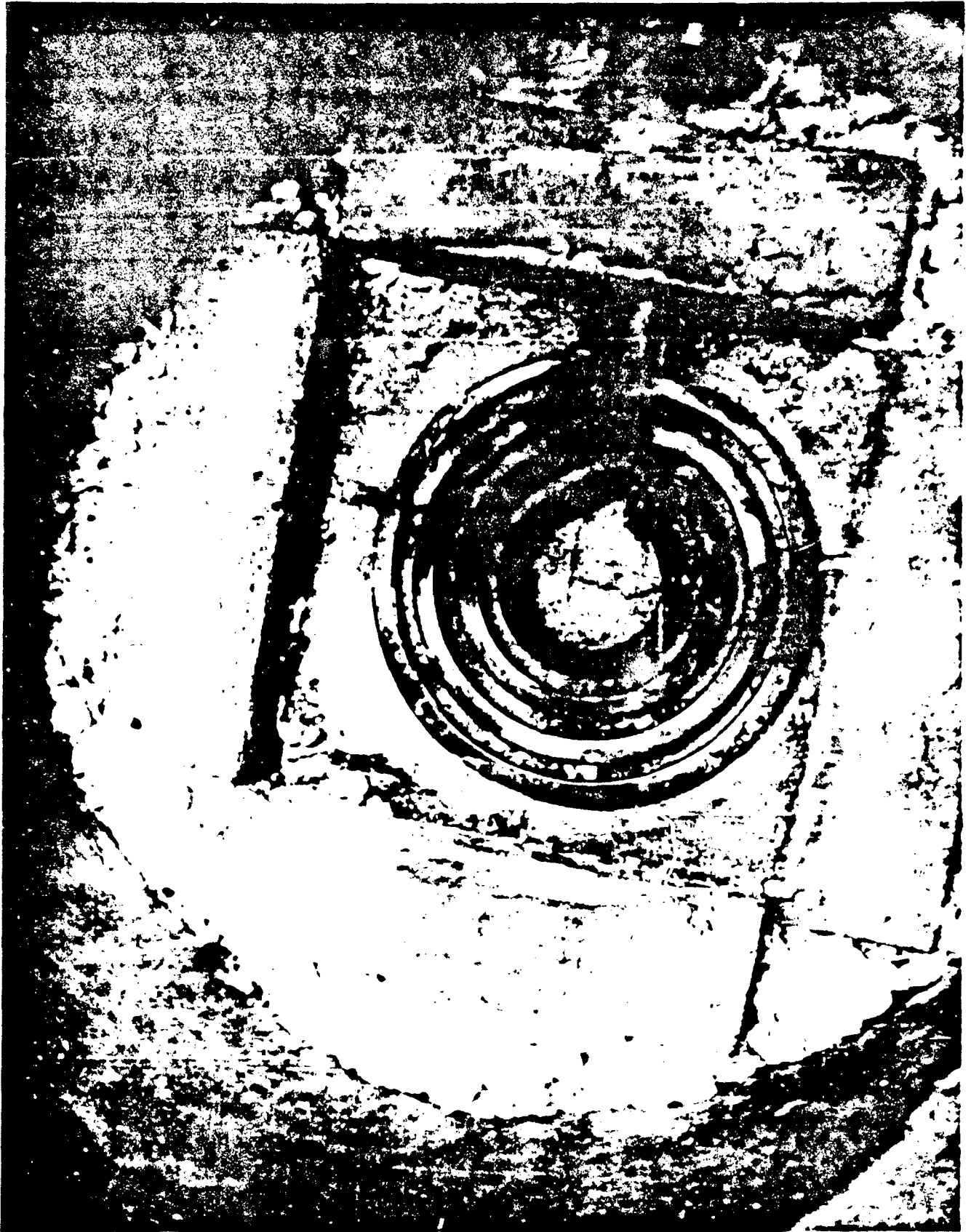


Figure 20 - Electric Range Element

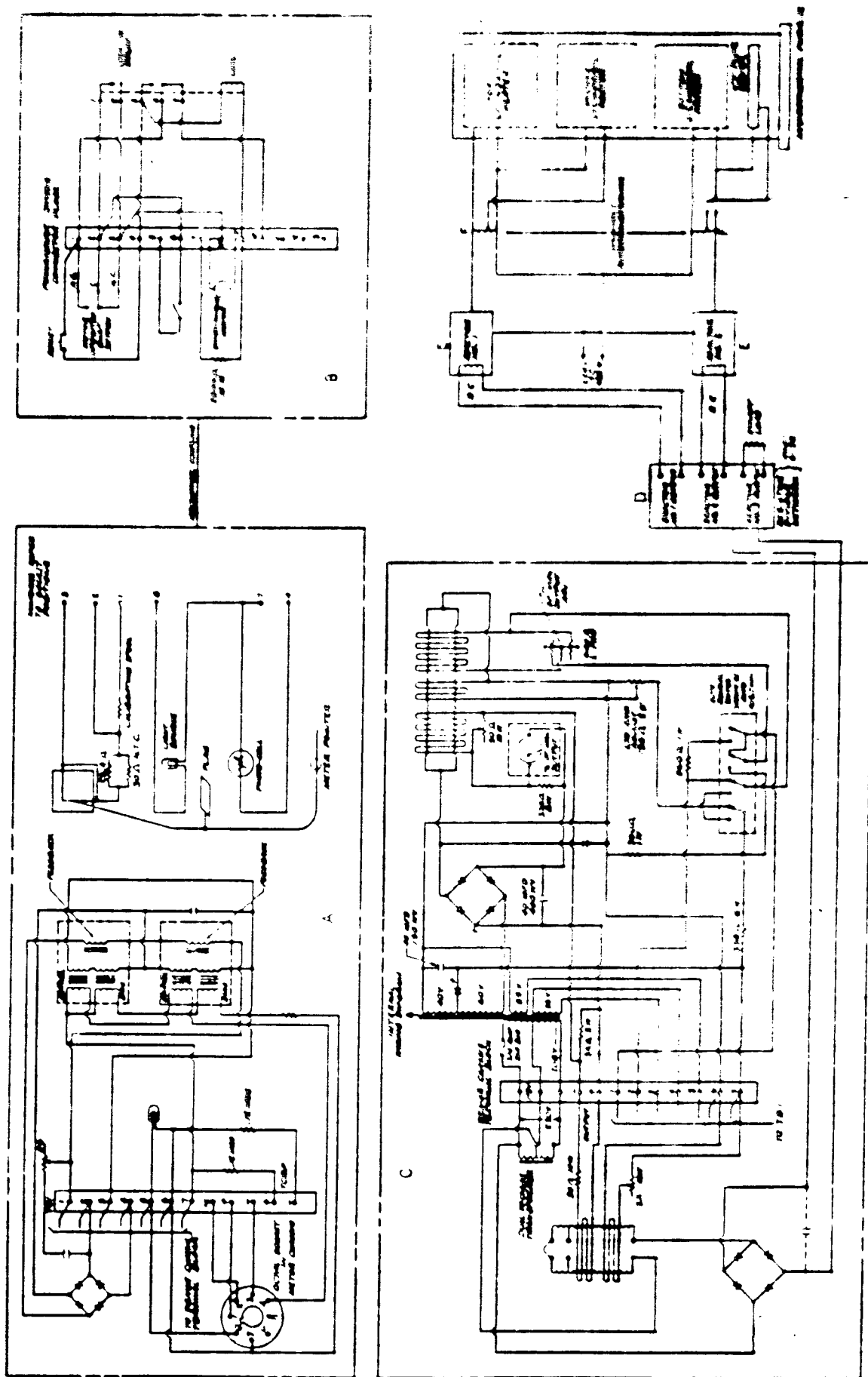


Figure 21 - Schematic of the Control System and Furnace

### Pilot Line (Continued)

B - The set point or control temperature is adjusted by moving the light-photocell unit either up-scale or down-scale causing the temperature indicator to "chase" the photocell. An aluminum can driven by a synchronous motor is mechanically connected to the light-photocell unit. The shape of the can controls the position of the light-photocell unit and thus the temperature.

C - The d.c. output of A is further amplified to a level sufficient to drive three saturable reactors. The reactor driver with auxiliary driver is manufactured by West Instrument Corporation.

D - The d.c. output from C is divided and matched to three loads, two reactors and a dummy load resistor. Individual adjustment of the fraction of the d.c. power reaching each reactor is provided for. This allows the relative power output of either reactor to be adjusted. The unit is an S-92 feature, manufactured by West Instrument Corporation.

E - The saturable reactors are rated for five KVA, 220 volt. The a-c current passing through the reactor is a direct function of d-c control current. The reactors were manufactured by West Instrument Corporation.

F - Directly connected to the furnace units are two, 2 KVA 220 volt variable auto-transformers, manufactured by Superior Electric Corporation, Bristol, Connecticut. The auto-transformers permit the adjustment of temperature differences between the top and middle cylindrical heater by limiting the power in the middle heater. In similar fashion the hot plates and bottom cylindrical heaters can be adjusted.

#### 2.2.7 Pressure Measurement

Pressure in the system is obtained by direct reading of Bourdon type gauges connected directly to the internal cavity of the autoclave. Since the walls of the silver cans are deformed under only slight pressure, the gauge pressure is a fairly accurate measure of the internal pressure of the can. Ashcroft Maxisafe<sup>+</sup> gauges (Autoclave Engineers, Inc., authorized vendor) with Monel Bourdon tubes and F250-C fittings were used.

#### 2.2.8 Equipment Developed During Contract

Use of the autoclaves and associate equipment required the development of some additional tools whose necessity had not been anticipated.

-----  
+ Autoclave Engineers, Erie, Pennsylvania.

Pilot Line (Continued)2.2.8.1 Autoclave Opener

Closure is achieved with manual force only, according to the technique described in Section 2.2.2. Operation of the autoclaves proved that the manufacturer's recommended technique and tools supplied for loosening the main nut after a run were far from adequate. In order to unscrew the main nut, and in some cases provide the only possible technique for removing it, a new anvil-type tool was developed (Figure 22). This tool was constructed so that it could easily be clamped onto the main nut by means of two bolts. When in place, two steel pins in the tool fitted into two opposing holes on the side of the main nut. The pins in these holes allowed for efficient transmission of the applied torque. For opening the autoclave, this torque is provided by striking the arms of the anvil openers with ten-pound hammers. No pressure-temperature or leak condition produced sealing of the vessel which could not be opened by this tool.

2.2.8.2 Can Extractor

Because of improper pressure balance or slow leaks in the entire system, there would occur in some cases a puffing up of the silver can. Due to the proximity of the autoclave walls, this expansion could not proceed too far. The movement of the can's wall could be stopped by the autoclave walls. As a result of this large expansive force, the silver can walls would be forced against the autoclave making removal of the can extremely difficult.

While this situation was true of the small can and vessel, it is even a greater problem in larger cans (3 inch diameter). In order to remove the cans after a run, an extractor (Figure 23) was designed and constructed which could be used with both vessel sizes. For the smaller can, a large screw was threaded into the top cap to provide a clamping handle. The cap of the larger can was provided with a large nut for easy removal. After clamping this handle in either case, the can is removed by driving the threaded rod with an electric drill. This instrument has removed cans which appeared to be impossible to remove manually.

2.2.8.3 Seal Area Lapping Tool and Polishing Tool

In order to regenerate and polish the sealing surface of the autoclave properly, it was necessary to design and develop two tools, - the final models of each are shown in Figures 24 and 25.

The lapping tool is made so as to generate a surface of the proper sealing angle ( $7^\circ$ ) whose bore was concentric with that of the threads. This particular alignment was found to be necessary since the bore used for the threads and that of the autoclave body are not necessarily uniaxial. Deviation from this geometric

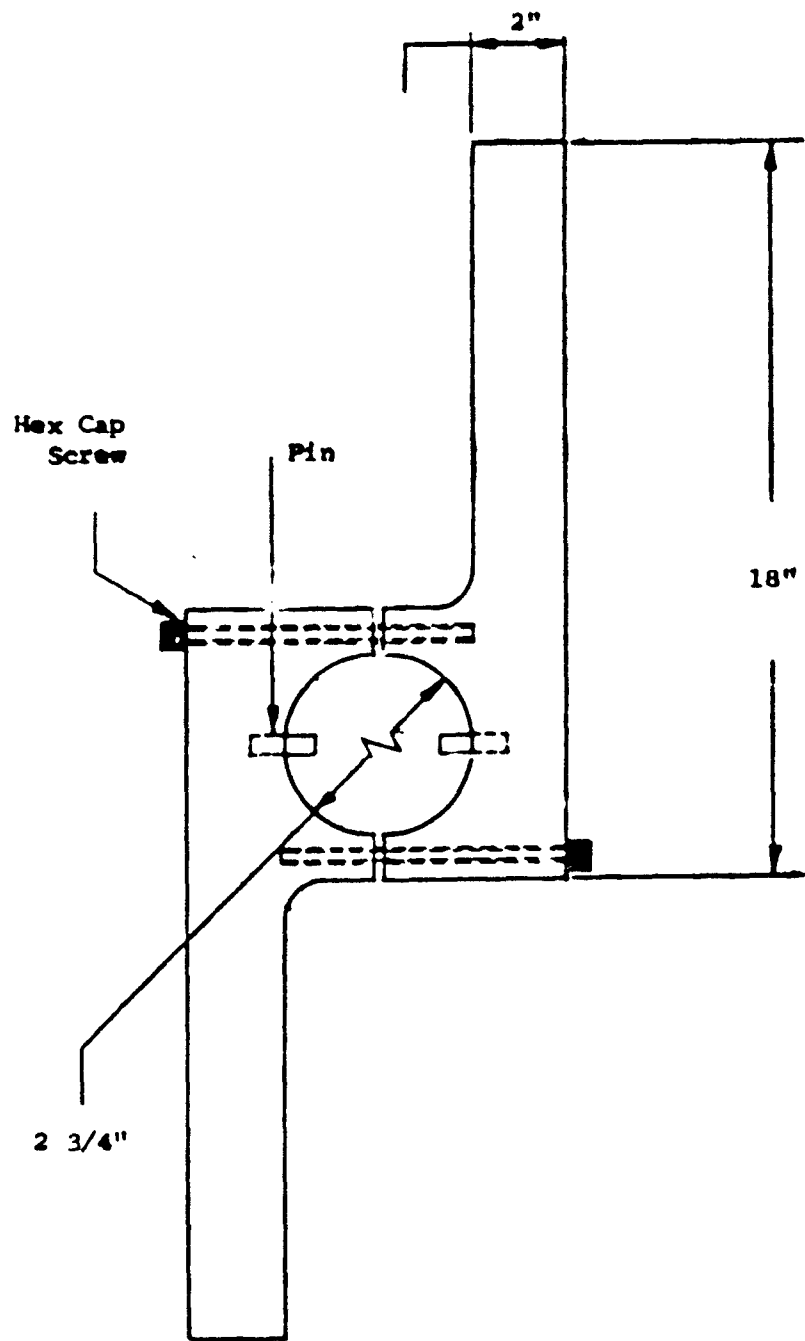


Figure 22 - Main Nut Opener

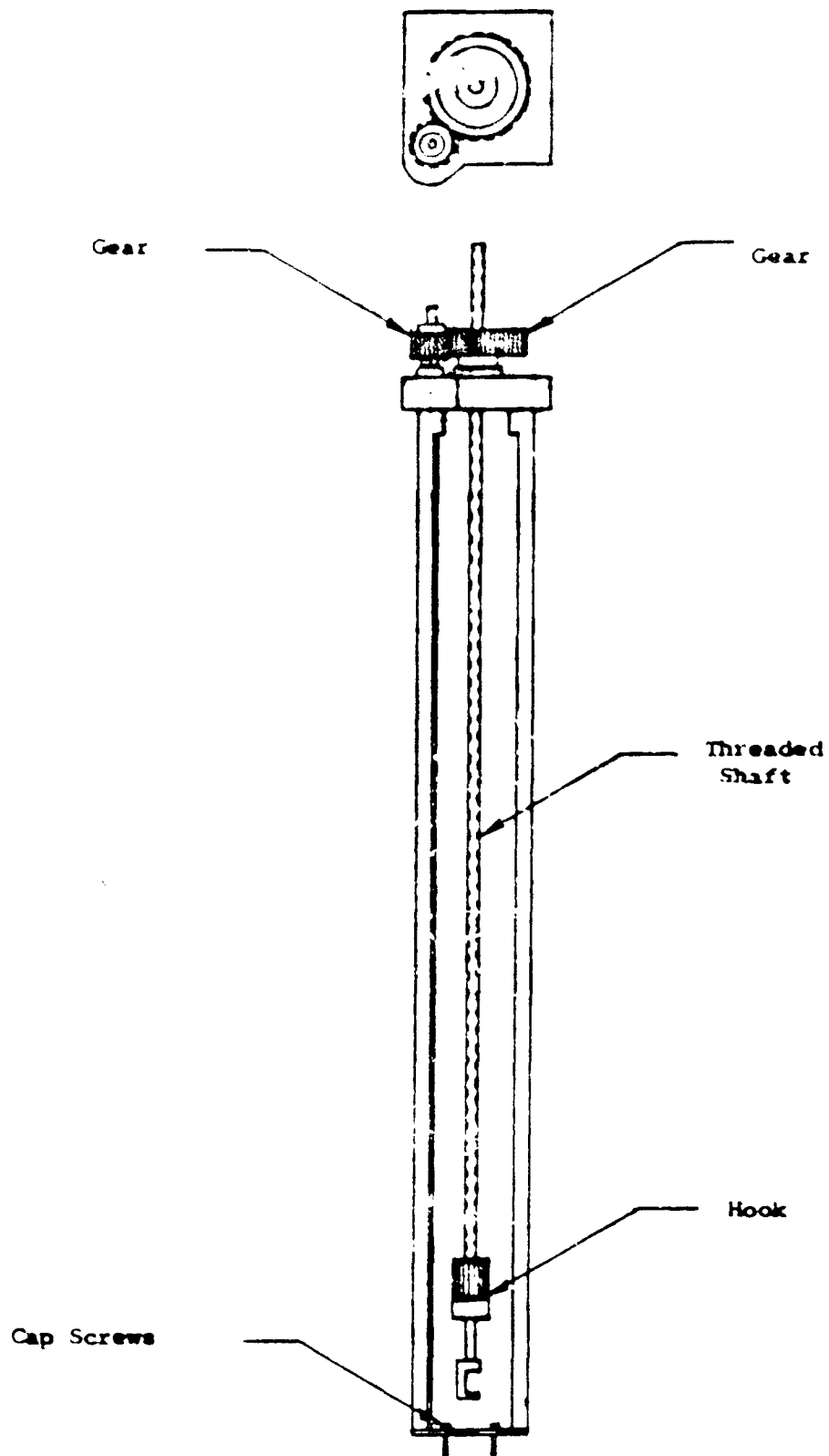


Figure 23 - Can Extractor

3" Dia. Autoclave Lap

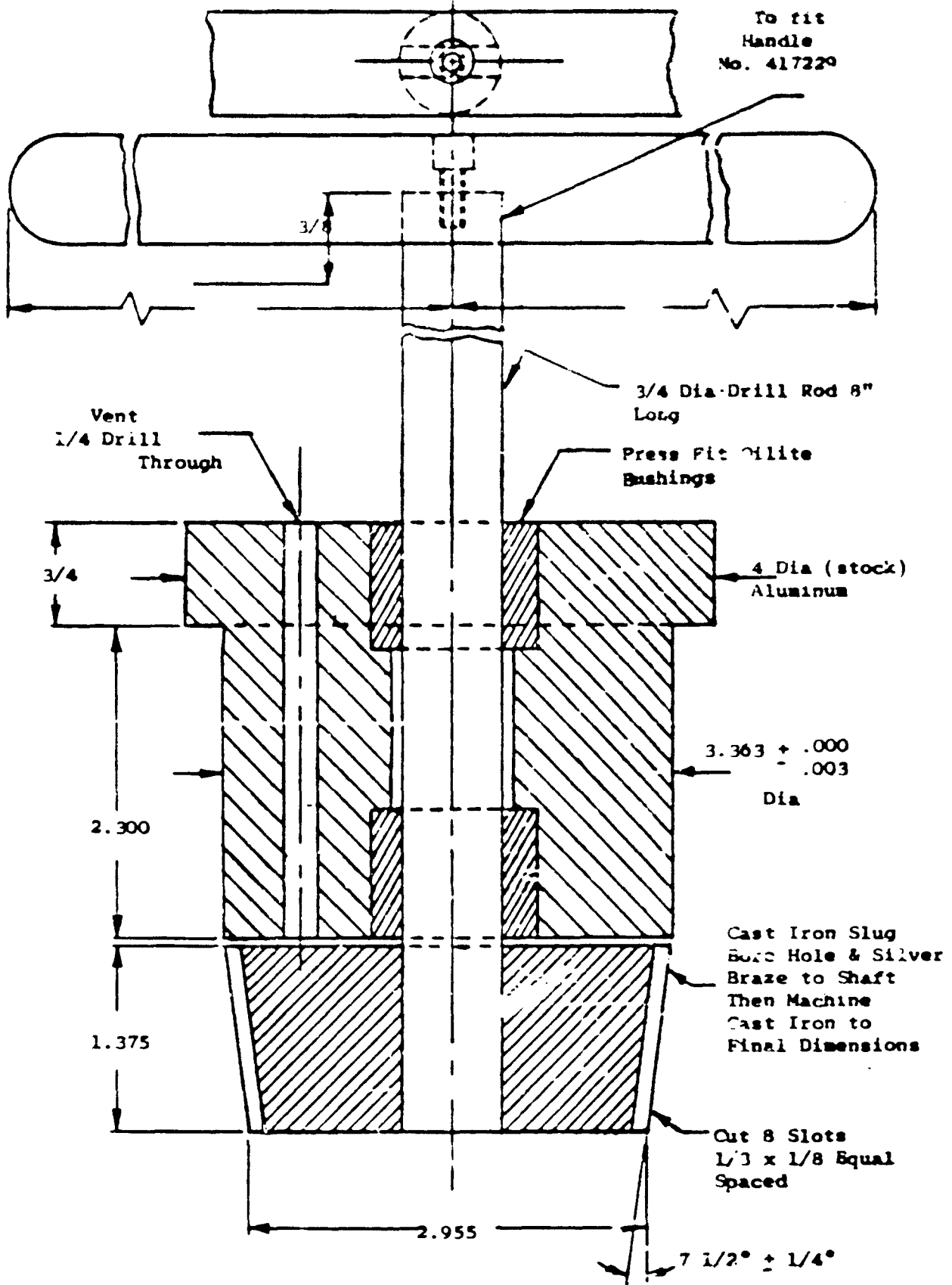


Figure 24 - Seal / ca Lapping Tool

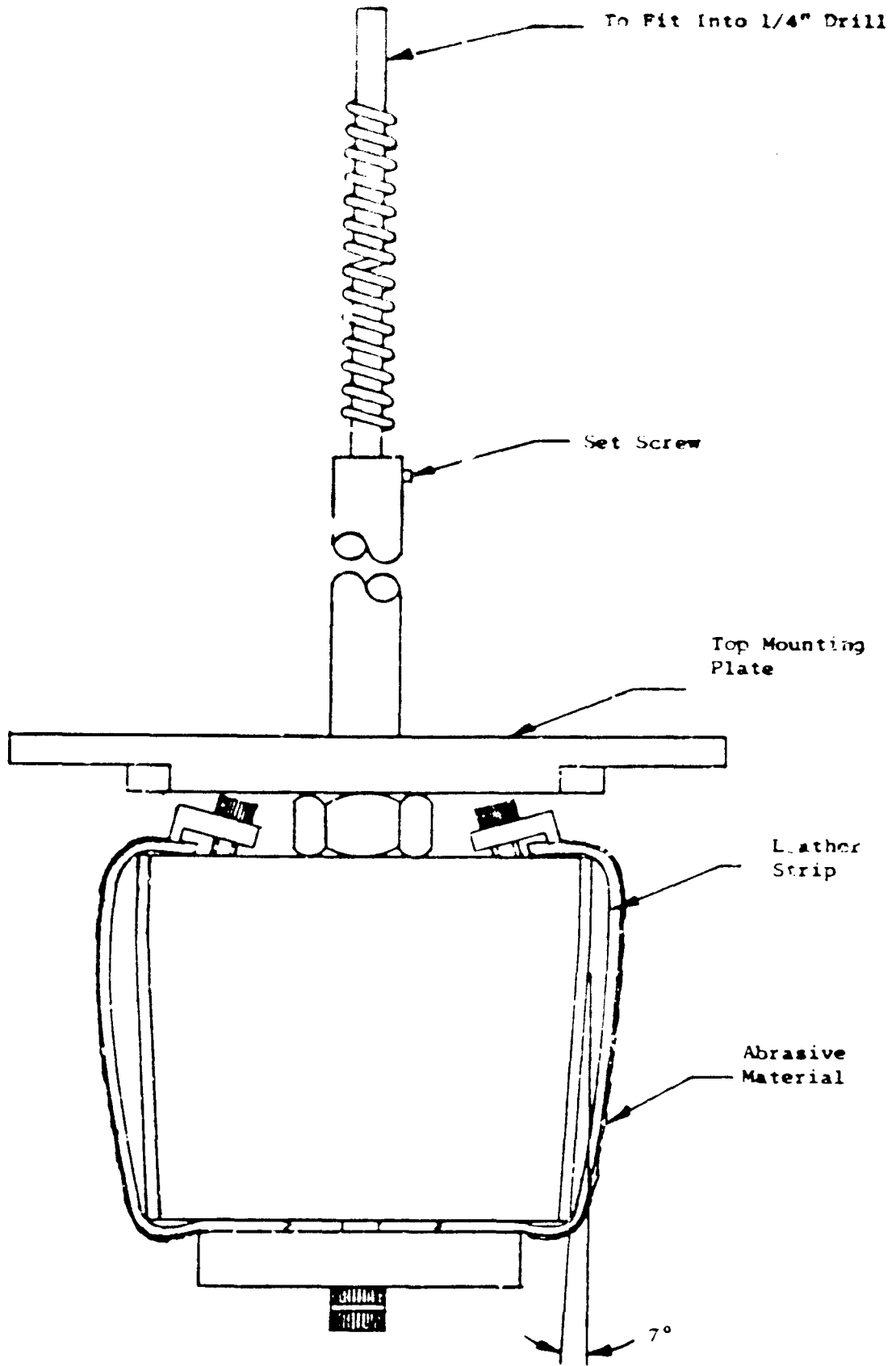


Figure 25 - Polishing Tool

### Pilot Line (Continued)

configuration leads to seal leaks. The lapping section of the tool is made of cast iron; the surface of the lap is regenerated periodically by milling. The guide in the body of the tool is made of aluminum and is fitted for one vessel specifically and used only for that vessel thereafter.

A polishing tool was also developed to be used after the seal surface had been ground with the lapping tool. The mirror polish produced by this tool was found to be essential in order to seal the autoclaves for use at combinations of high pressure-temperature conditions ( $>500^{\circ}\text{C}$  - 20,000 psi). In this case, after the autoclave has been suitably ground with the lapping tool, the polisher is placed in the seal area and driven at high speed by an electric drill. With experience, mirror finishes are easily attained in a matter of 2 to 3 minutes. No. 320 aluminum oxide abrasive is suspended in an oil slurry and used for both the lap and polisher.

### 2.2.9 Operating Procedure

#### 2.2.9.1 Preparation of Large Crystal Growth Autoclaves

After each run in the autoclaves, it was necessary not only to clean thoroughly the vessel but also to renew the sealing surfaces and angles. The vessel cavity was scrubbed with a large diameter ( $\sim 3$  inch) brush and liquid detergent; it was then rinsed by flushing with tap water and dried by a stream of compressed air. During each run the seal parts underwent plastic deformation to a greater or lesser extent resulting in permanent dimensional changes in all three seal parts. The ring, cover and autoclave seal areas had to be returned to original dimensions and surface finish each time the autoclave was used. If this was not done the seal became unreliable. The preparation of each part is discussed in turn below.

##### 2.2.9.1.1 Seal Ring

An expanding mandrel shown in Figure 26 was used to hold the seal ring during the remachining of the sealing surfaces. A modified vernier caliper shown in Figure 27 was used to measure the critical dimension which was the minor outside diameter of the taper. The ring was machined to the angles and dimensions shown in Figure 28. The angles are slightly different from those prescribed by the manufacturer (Figure 14) but only with the specifications depicted in Figure 28 could reliable sealing be attained. Both inner and outer angular surfaces were then polished using No. 180  $\text{Al}_2\text{O}_3$  U BOND METAL CLOTH from Sandpaper Inc., Rockland, Massachusetts.

##### 2.2.9.1.2 Cover

The sealing surface of the cover was remachined to the angle shown in Figure 14. Polishing of the surface was done using the same No. 180 cloth as above.

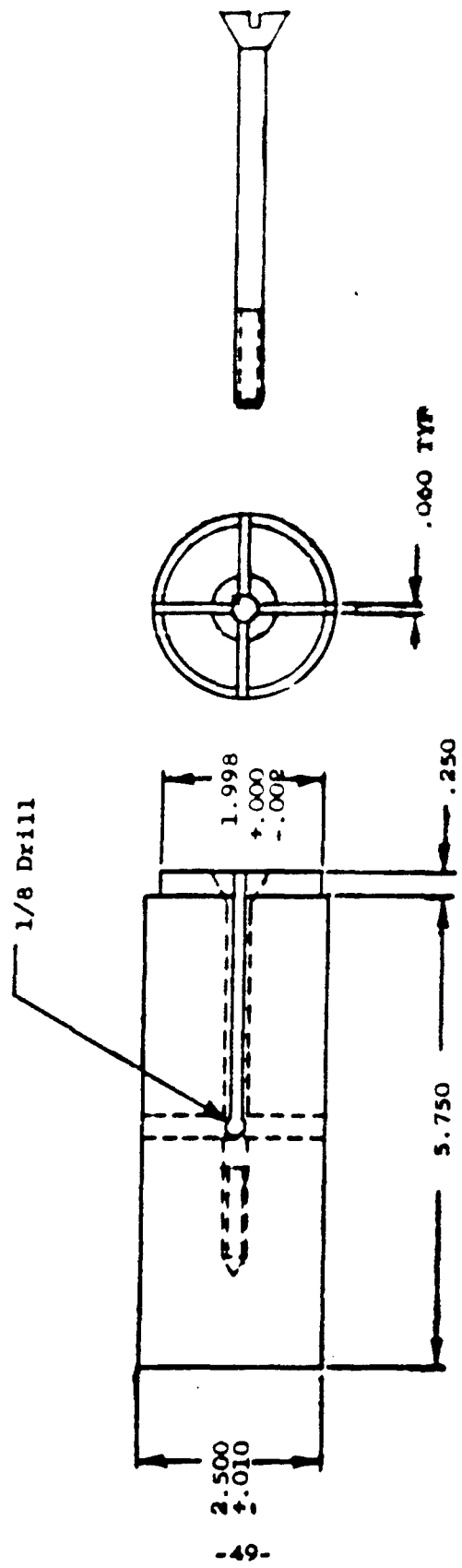
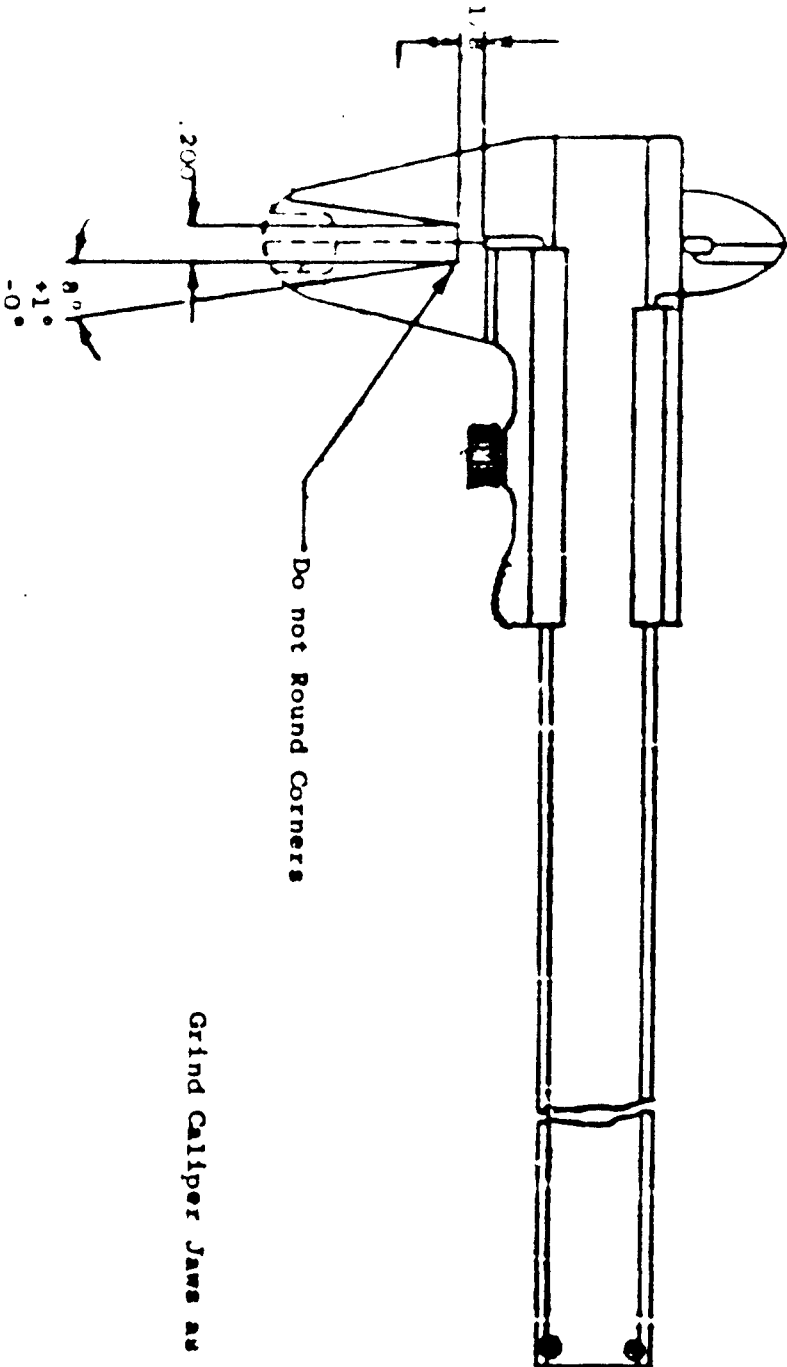


Figure 26 - Expanding Mandrel for Remachining Seal Rings



Grind Caliper Jaws as Shown.

Figure 27 - Seal Ring Caliper

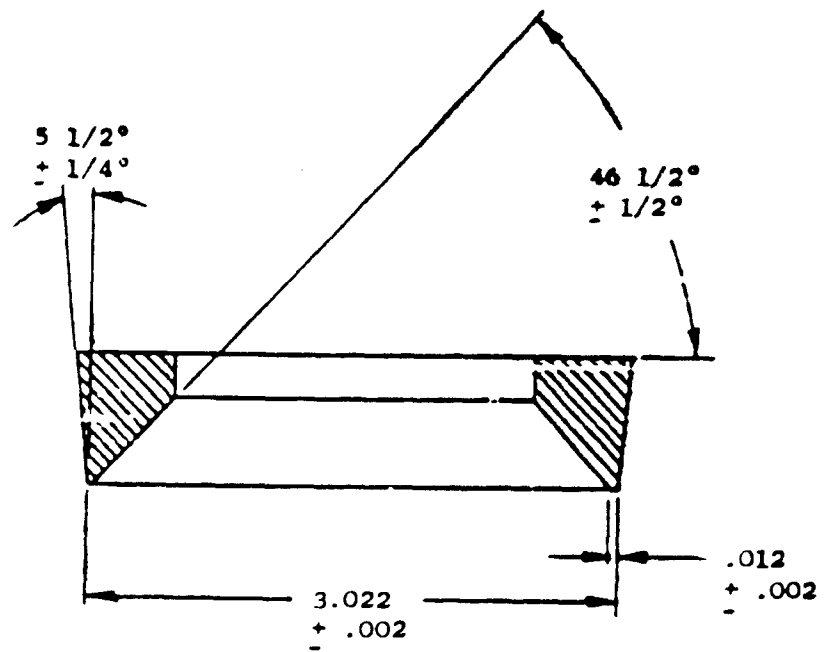


Figure 28 - Seal Ring

2.2.9 1.3 Autoclave Seal Area

The seal area of the autoclave was lapped with a mixture of 2 volumes of SAE 20 machine oil plus 1 volume of NORTON No. 320 aluminum oxide abrasive using the lapping tool shown in Figure 24. Lapping was continued until all traces of former seal marks were removed. The seal area was then polished using WET-ORDRY TRI-M-ITE PAPER No. 320 SILICON CARBIDE (TM Co., St. Paul, Minnesota) and SAE 20 machine oil. The paper was fixed to the polishing fixture shown in Figure 25. An electric drill controlled by a variable transformer drove the polishing fixture at 200 to 300 RPM. A good polish was required, i.e. no visible flaws with the unaided eye.

All parts were scrubbed with detergent<sup>+</sup> and hot water to remove any residual grit. Prior to assembly all surfaces were wiped with Kimberly-Clark type 900-S Kimwipes saturated with acetone. The vessel was then sealed according to the manufacturer's directions.

2.2.10 Nutrient Preparation

ZnO nutrient was prepared from commercially available ZnO powder. Fisher<sup>++</sup> CERTIFIED ACS grade was used. Depending upon the quantity of nutrient required and the availability of a sintering furnace two sizes of platinum crucibles were employed, either a 250 ml for the three inch furnace or the 5 1/4" x 5 1/4" can for the six inch furnace. The ZnO powder was packed into the can and the can placed in the furnace operating at 1100 - 1200°C. After 2-3 hours at temperature the can was removed. The result of this operation was a cylinder of sintered ZnO. This cylinder was then crushed in a silver metal tube; 1/4 inch to 1/2 inch pieces were the most desirable nutrient size.

2.2.11 Solution Preparation

The solution used for the growth of crystals was 6 molal and was prepared by adding 1009.8 grams of Fisher CERTIFIED ACS grade KOH to 3000 grams of water. Typically the solution was also 0.1 M with respect to LiOH which was prepared by adding 4.19 grams of Fisher CERTIFIED ACS grade LiOH·H<sub>2</sub>O to the 3000 grams of water.

2.2.12 Seed Preparation

Zinc oxide seeds for the final and most successful portion of the program were produced from hydrothermally grown crystals. The crystals were mounted and cut perpendicular to the <0001> axis

-----  
<sup>+</sup> Lux Liquid, Lever Brothers, New York, New York.

<sup>++</sup> Fisher Scientific Co., 1080 Lousons Rd., Union, New Jersey. Lot No. 745324 or 714125.

Pilot Line (Continued)

yield large area plate whose thicknesses were 50 to 100 mils. The plates were then cleaned with methanol and a small hole was drilled near one edge of the seed. A 20 mil wire was placed in the hole and the seeds suspended on a silver ring for etching. The ring with the seeds were submerged in hot 10 molar NaOH ( $\sim 90^\circ\text{C}$ ) for 5 minutes. The ring and seeds were then flushed in flowing tap water, rinsed in deionized water, and finally air dried, ready for attachment to the seed rack.

2.2.13 Preparation of Silver Can-loading of Autoclaves

Just prior to loading the cans for a run, the silver pieces were cleaned of grease and oil with detergent, washed with concentrated HCl, thoroughly rinsed with deionized water and then allowed to dry.

Most hydrothermal ZnO crystal growth runs were in excess of one month duration. This provided ample time given even a very small leak in the silver can to cause serious damage to the autoclave. In fact, an autoclave could easily be rendered useless in a single run. Testing for leaks in the system before use was a prime requirement for successful operation of a crystal growth system.

During construction of the cans all welds in sub-assemblies were subjected to a dye-penetrant test<sup>+</sup> and any suspicious areas were welded and tested again. The seeds were attached to the seed rack with 20 mil fine silver wire and the nutrient and zinc metal were placed in the bottom of the can. The seed rack and baffle sub-assembly was then welded to the can body. Any pressure within the can generated by the heat of welding was relieved through the twin vent tubes in the cover. The cover to body weld was then dye-checked and rewelded if necessary.

One hundred milliliters of deionized water were placed in the can through one of the vent tubes. The ends of both vent tubes were then flattened with heavy pliers and the tips fused, thus sealing the can.

The can was then weighed to  $\pm 1/2$  gram. Final leak testing was done by heating the can to 110 to  $120^\circ\text{C}$  with a Briskeat<sup>++</sup> type D heating tape operating at 70 to 80 volts from a variable transformer. The can was kept hot for 15 to 16 hours and then weighed again. If there had been no loss of weight the ends of the vent tubes were cut and the test water boiled out. When all the water was removed, the KOH solvent was introduced through one of the tubes which were then flattened and sealed.

-----  
 + Spotcheck, Penetrant Type SKL-HP, Spotcheck Developer Type SKD-NF, Magnaflux Corporation, Chicago, Illinois.  
 ++ Scientific Glass Co., Bloomfield, New Jersey.

#### Final Run (Continued)

The can was then placed in the autoclave, along with the appropriate external fill of deionized water. The vessel was closed, the pressure gauge attached and the vessel was placed in the furnace ready for operation.

#### 2.2.14 Warm-up

Two different warm-up schemes were used in the course of this work: (a) programmed and (b) "as fast as possible." The programmed procedure was used only in the early part of this work when the operating pressure was low. In this case, the vessel was heated at a constant rate to operating conditions over 24, 48 or 96 hours by using the temperature programmer modification on the West Controller.

During the warm-up a low gradient was maintained between the bottom and top sections of the autoclave. Since the seeds were so thin in the early part of the program it was found that by using the slow warm-up with a low temperature gradient that most or all of the seeds would be dissolved before arriving at growth conditions.

Drastic seed dissolution was prevented by heating the vessel to operating conditions "as fast as possible", with a high temperature gradient. This was accomplished by having the power inputs on the controller fixed at their ultimate position for operation and then switching on the controller.

Operating conditions were approached within 2-3 hours with an additional 3-4 hours required for the entire assembly of furnace, vessel, etc. to attain thermal steady state. This procedure prevented seed dissolution, and was used for the major part of the program.

#### 2.2.15 Shut-down

At the end of the run, the power was switched off and the autoclave was air cooled; when zero gauge pressure was indicated, cold water was then passed over the vessel until it reached room temperature. The vessel was opened with the main nut released by the opener (Figure 22). The silver can was removed manually from the autoclave or with the extractor (Figure 23). The cap was sawed off and the ladder removed from the can. The crystals were removed from the holder by cutting the wire and then thoroughly rinsed in water until all the base was washed away. The crystals were then allowed to air dry prior to weighing and measuring the thickness with a micrometer.

## 3.0 CRYSTAL GROWTH

### 3.1 Molten Salt

#### 3.1.1 Background for Program

It had been demonstrated by Nielsen and Dearborn at Bell Telephone Laboratory that fairly large (1-2 inch) high quality plates of ZnO could be grown using the molten salt technique. After joining Airtron Dr. Nielsen and Mr. G. Townsend continued growing zinc oxide plates by the same method. There was no apparent difficulty in using this technique to grow ZnO crystals which would provide seeds for the hydrothermal crystal growth.

The initial success did not continue and it became more and more difficult to obtain the plates of size, quality and thickness previously observed using the same growth parameters. The difficulties were manifested by the decreasing frequency of successful runs, crystals of smaller area, and a large decrease in plate thickness.

Attempting to cope with the degeneration of the system a course was set upon to investigate thermal gradient effects, furnace effects and batch size effects.

This difficulty in producing plates by the molten salt approach was also noted by Laudise.<sup>11</sup> Both laboratories then approached the seed problem by using hydrothermal crystals as a source of seed plates.

#### 3.1.2 Crystal Growth Experiments

Initially the work began by simply duplicating the composition and procedures used by Nielsen and coworkers. This work was quite successful and large plates were easily grown (Figures 29 and 30). During this first phase both three inch and six inch furnaces were used for crystal growth.

At that time not all of the furnaces in the pilot line were equipped with rotating pedestals. It was found that without rotation it was not possible to dissolve ZnO at 1150°C, even with a twenty four hour soak period. On the other hand with rotation only a two hour soak period was necessary to dissolve all the material.

In order to optimize crystal quality and yield, a series of experiments was begun in which the pedestal position and therefore crucible was varied in the furnace. The purpose in changing the position of the pedestal was to alter the thermal gradients in the melt. By so doing it was possible to have either the top or bottom of the melt in the hottest part of the furnace. The objectives were to see if the number of nucleation sites could be reduced so that the crystal once nucleated could be induced to increase in basal area and thickness, and to eliminate dendritic growth. The other important



Figure 23 - Photograph of Large Zinc oxide Crystal Prior to Cleaning

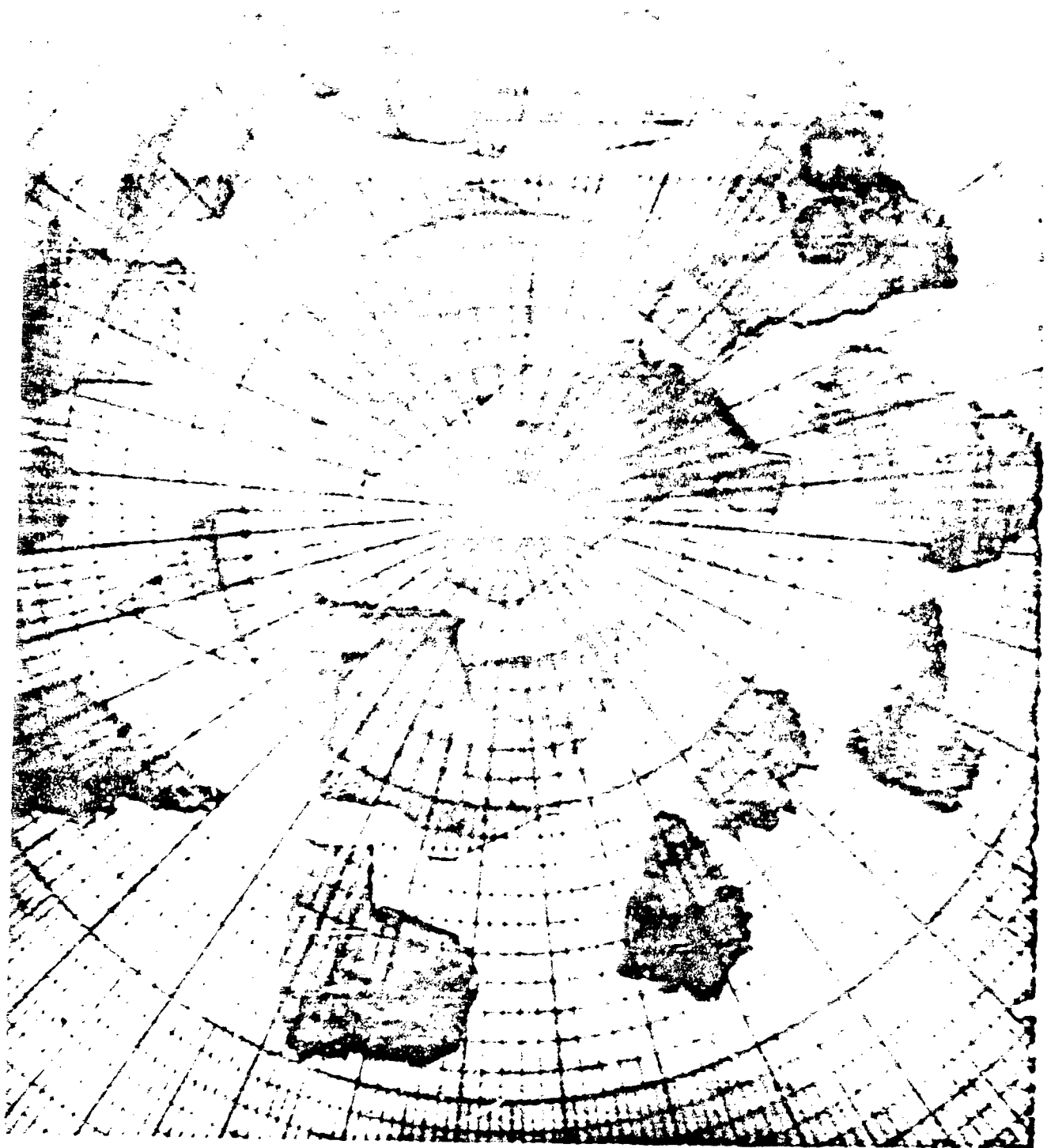


Figure 30- Zinc Oxide Crystals Grown from  $PbF_2$

### Crystal Growth (Continued)

growth variables e.g. cooling rate were also varied in order to accomplish the same objectives.

The data for the runs in this period are presented in Tables II and III.

The conditions used where the best plate was obtained are as follows:

The starting mixture was composed of 25 mole percent ZnO and 75 mole percent PbF<sub>2</sub>. The container was a 5 1/4" x 5 1/4" crucible with cover which was run in the 6 inch furnace. The pedestal position was such that the bottom of the platinum can was just above the lower portion of the furnace hot zone. In terms of gradients this would mean that the temperature at the surface of the melt was higher than any other part of the flux. The contents of the crucible were soaked at 1150°C for two hours with stirring. The timing was stopped and the furnace cooled at 1°C per hour. At 1050°C the crucible was removed and the solution poured into a sand bath.

With the continued decrease in plate yield, thickness and quality, more variation of gradients, batch size, melt composition and soak temperatures were attempted. No significant improvement was obtained by any of these changes, Table IV.

#### 3.1.3 Controlled Nucleation and Crystal Growth

As the ZnO - PbF<sub>2</sub> system continued to degenerate considering the size quality and thickness of the plates, more thought was devoted to how to control the factors involved in nucleation and growth of ZnO plates. A program was begun to see if these objectives could be accomplished in a molten salt system.

In addition to growing platelets of ZnO which float on the surface of the melt, it had been observed that in some runs the platelets also appeared to grow in a vertical position rather than horizontally. The presence of the vertical plates, Figure 31, supports the analysis that the heat flows in the vertical furnaces in such a manner as to result in vertical gradients. In order to control nucleation and subsequent crystal growth, it is necessary to control not only the amount of the gradient, but also the direction of the gradient. While large plates have been grown in some cases in vertical gradients, originally large plates were grown in horizontal furnaces which probably had lateral gradients.

##### 3.1.3.1 Vertical Gradient Method

A vertical furnace that is cylindrical in construction and further has radial symmetry about its axis, both in construction materials and in heat dissipation, has only one significant gradient, which is in the vertical direction.

TABLE II

Molten Salt Crystal Growth Runs

Run	Crucible Position	Soak Temp. (°C)	Soak Time (hrs)	Cooling Rate (°C/hr)	Removal Temp. (°C)	Comments
1	+8	1205	4	14.0	850	Polycrystalline plate, ZnO not completely dissolved - dendritic growth.
2	+6	1220	4	8.3	875	Flawed plate ZnO not completely dissolved, dendritic growth.
3	+7	1330	16	8.3	850	Tiered plates attached by flux, dendritic growth.
4	+5	1300	16	5.6	950	Polycrystalline plate.
5	+4	1250	15	5	1000	Some good areas, much polycrystalline.
6	+4	1200	4	9	1025	Much undissolved.
7	+3	1180	3	10	1050	Parallel plates cracked.
8	+2	1100	9	6.7	1000	Parallel plates, much flux inclusion.
9	+1	1150	4	4.8	1025	Much strain cracking.
10	0	1150	4	2.4	1025	Large area excellent, see Figure 1.
11	-1	1150	5	0.5	1055	Large plate with heavy inclusions.
12	+1	1150	8	2.0	970	Many plates, wall nucleation.
13	+1	1190	8	3.0	1025	Wall nucleation number of plates developed.

\* Crucible Position column numbers indicate position of the center of the can relative to the center of the furnace in inches.

TABLE III

Molten Salt Crystal Growth Runs

<u>Run</u>	<u>Crucible<sup>o</sup> Position</u>	<u>Soak Temp.</u>	<u>Soak Time (hrs.)</u>	<u>Cooling Rate °C/hr.</u>	<u>Pour Temp. (°C)</u>	<u>ΔT (°C)</u>	<u>N<sup>o</sup> Plates</u>	<u>N<sup>o</sup> Dendrites</u>	<u>Comments</u>
10-4	+2"	1150	5	2.5	1000	80-85	30	70	Some plates heavily flux included, mostly dendrites.
10-5	+2"	1150	5	0.5	1025	80-85	--	100	No plates, den- dritic.
10-6	+1"	1150	5	0.5	990	75-80	10	90	Some small plates, no flux included, mostly dendrites.
10-7	0	1150	5	0.5	1000	70-75	--	100	No plates, den- drites.
10-8	-1	1150	5	0.5	1050	60-65	--	100	Dendrites.
10-9	0	1150	5	1.0	1025	70-75	20	80	Some plates, no flux included, dendrites.
10-10	+1	1150	5	2	1030	75-80	15	85	Plates have flux included den- drites attached.
10-11	+1	1160	5	3	1050	75-80	20	80	Thin plates some good areas.
10-12	+2	1150	5	3	1025	80-85	5	95	Almost no plates.
10-13	+2	1190	5	5	1045	80-85	10	90	Flux included, no usable plates.

Table III (Continued)

Run	Crucible <sup>a</sup> Position	Soak Temp. (°C)	Soak Time (hr.)	Cooling Rate °C/hr.	Pour Temp. (°C)	$\Delta T$ (°C)	% Plates	% Dendrites	Comments
10-14	+1 1/2	1150	5	5	1055	70-75	35	65	Flux included, some good areas.
10-15	+1	1160	5	5	1035	75-80	25	75	Flux included.
10-16	+1 1/2	1160	5	5	1040	70-75	80	20	Some good areas 1 - 2 cm <sup>2</sup> .
10-17	+1 1/2	1160	5	7	1050	70-75	75	25	Some good areas.
3-2	+3	1150	4	1.5	1025	30	70	30	Good plates, thin.
3-3	+3	1160	4	0.5	1025	30	40	60	Plate with dend- rites.
3-4	+3	1150	4	1.0	1000	30	--	100	Lost cover, dendrites.
3-5	+2	1155	4	1.0	990	25	20	80	Plate with some dendrites.
3-6	+1	1150	4	1.0	1025	20	5	95	Lost cover, mostly dendrites.
3-7	0	1160	4	1.0	1010	15	0	100	Dendrites.
3-8	+1	1160	4	1.0	1020	20	30	70	Plate with some dendrites.
3-9	+1	1160	16	2.0	1030	20	50	50	Thin plates, some dendrites.
3-10	+1	1155	4	2.0	1050	20	--	100	Lost cover.

Table III (Continued)

Run	Crucible <sup>a</sup> Position	Soak Temp.	Soak Time (hrs.)	Cooling Rate °C/hr.	Pour Temp. (°C)	ΔT (°C)	% Plates	% Dendrites	Comments
3-11	+1	1160	4	2.0	1020	20	--	100	Low cover.
3-12	+2	1160	4	3	1010	30	60	40	Many small plates.
3-13	+2	1160	4	2.5	975	30	60	40	Small plates dendrites.
3-14	+1	1170	4	3.5	1000	20	40	60	Dendrites with many small plates.
3-15	+1	1170	4	3.5	1025	20	40	60	Dendrites with small plates
3-16	+1	1160	4	5	1050	24	75	25	Thin plates multi- ple nucleation.
3-17	+1	1165	4	5	1035	25	80	20	Thin plates.
3-18	0	1170	4	5	1040	15	40	60	Mostly dendrites.
3-19	0	1170	4	5	1025	15	40	60	Mostly dendrites.
3-20	+3	1150	4	5	1030	35	40	60	Multiple nucleation cool walls.
3-21	+3	1150	4	5	1035	35	40	60	Mostly dendrites.
3-22	+1 1/2	1170	4	7	1025	25	80	20	Thin plates, some dendrites.
3-23	+1 1/2	1160	4	7	1040	25	90	10	Thin plates, 1-2 cm <sup>2</sup> good area.

Table III (Continued)

Run	Crucible Position	Soak Temp.	Soak Time (hrs.)	Cooling Rate °C/hr.	Pour Temp. (°C)	ΔT (°C)	% Plates	% Dendrites	Comments
3-24	+1 1/2	1170	24	3	1030	25	90	10	Thin plates.
3-25	+1 1/2	1175	4	3	1025	25	80	20	Thin plates.
3-26	+1 1/2	1170	4	3	1035	25	90	10	Good but thin 1-2 cm <sup>2</sup> good area.
3-27	+1 1/2	1180	4	5	1040	25	80	20	Thin plates, almost no dendrites.
3-28	+1 1/2	1185	4	7	1025	25	95	5	Thin - multiple nucleation.
3-29	+1 1/2	1180	100	3	1035	25	90	10	Programmer failed.
3-30	+1 1/2	1175	4	5	1030	25	95	5	Thin plates, 1-2 cm <sup>2</sup> good area.
3-31	+1 1/2	1180	4	7	1020	25	90	10	Thin plates.
3-32	+1 1/2	1180	4	5	1035	25	85	15	Thin plates.
3-33	+1 1/2	1180	4	5	1025	25	85	15	Thin plates, 1-2 cm <sup>2</sup> good area.
3-34	+3	1190	4	5	1025	35	25	75	Mostly dendrites.
3-35	+3	1180	4	5	1030	35	25	75	Mostly dendrites.
3-36	+2	1150	4	5	1025	30	50	50	Plates with attached dendrites.

Table III (Continued)

Run	Crucible # Position	Soak Temp.	Soak Time (hrs.)	Cooling Rate °C/hr.	Pour Temp. (°C)	$\Delta T$ (°C)	% Plates	% Dendrites	Comments
3-37	+2	1180	4	5	1040	30	60	40	Plates with attached dendrites.
3-38	0	1170	4	5	1035	15	15	85	Almost all dendrites.
3-39	0	1165	4	5	1035	15	25	75	Dendritic.
3-40	+1	1160	4	5	1040	20	60	40	Plates with attached dendrites.
3-41	+1	1150	4	5	1025	20	60	40	Plates with attached dendrites.
3-42	+1 1/2	1170	4	5	1035	25	75	25	Thin plates, some dendrites.
3-43	+1 1/2	1175	4	5	1020	25	90	10	Thin plates, 1-2 cm <sup>2</sup> good area.
3-44	+1 1/2	1150	4	5	1035	25	81	15	Thin plates.
3-45	+1 1/2	1160	4	5	1025	25	90	10	Thin plates.
3-46	+1 1/2	1150	4	5	1030	25	95	5	Good but thin.

\*Crucible Position column numbers indicate position of the center of the can relative to the center of the furnace in inches.

TABLE IV

Molten Salt Crystal Growth Runs

Run	Furnace	Crucible Position	Soak Temp. (°C)	Soak Time (hrs)	Cooling Rate (°C/hr)	Pour Temp. (°C)	ΔT (°C)	% Plates	% Dendrites	Comments
10-18	10"	1 1/2" above center	1190	5	5	1025	70-75	60	40	Considerable dendritic growth.
10-19	10"	2" above bottom	1185	5	2	1025	25	70	30	Plates well formed but thin (bottom cool).
6-10	6"	4" above bottom	1180	4 stir	5	980	--	--	--	No real plate formation.
6-11	6"	2" above bottom	1160	4 stir	4	1000	--	25	75	Wall and bottom nucleation.
6-12	6"	3" above bottom	1150	4 stir	3	1050	--	20	80	Wall and bottom nucleation.
6-13	6"	3" above bottom	1160	5 no stir	3	1025	--	30	70	Thin plates but cool walls and bottom.
6-14	6"	4" above bottom	1160	5 no stir	1	1010	--	30	70	Thin plates - some usable.
6-15	6"	4" above bottom	1160	5 no stir	2	1030	--	30	70	No good plates.
6-16	6"	4" above bottom	1180	5 no stir	1	1035	--	30	70	Cool walls and bottom.
3-47	3-2	1 1/2" above center	1165	5	5	1025	35	60	40	Considerable dendritic growth.

Table IV (Continued)

Run	Furnace	Crucible Position	Soak Temp. (°C)	Soak Time (hrs)	Cooling Rate (°C/hr)	Pour Temp (°C)	ΔT (°C)	% Plates	% Dendrites	Comments
3-41	3-1	Center	1190	4	5	1020	15	10	90	Dendritic growth.
3-42	3-2	1" above center	1170	4	5	1035	35	40	60	Very thin and fragile - much dendritic growth.
3-50	3-1	1" above center	1180	4	5	1020	10	20	80	Almost no plates
3-51	3-1	1 1/3" above center	1200	4	5	1025	5	15	85	No real plate formation
3-52	3-2	1" above center	1200	4	5	1040	30	35	65	Considerable dendritic growth, some plates.
3-53	3-1	1 1/2" above center	1200	4	5	1010	5	20	80	Almost all dendritic growth.
3-54	3-2	1" above bottom	1200	4	2	1035	-20	65	35	Very thin - bottom cool.
3-55	3-2	2" above bottom	1200	4	5	1010	-25	70	30	Bottom cool - wall nucleation but some thin plates.
3-56	3-2	2" above bottom	1200	4	4	1020	-15	65	35	Some plates - considerable dendritic growth.
3-57	3-1	1" above bottom	1200	4	5	1000	-25	40	60	Very little plate formation.

Table IV (Continued)

Run	Furnace	Crucible Position	Soak Temp. (°C)	Soak Time (hrs)	Cooling Rate (°C/hr)	Plat. Temp. (°C)	ΔT (°C)	% Plates	% Dendrites	Comments
3-58	3-1	2" above bottom	1200	4	5	1050	-20	50	50	Multiple nucleation.
3-59	3-2	1" above bottom	1200	4	5	1025	-25	60	40	Much dendritic growth.
3-60	3-2	2" above bottom	1200	4	4	1040	-20	65	35	Some good plates paper thin.
3-61	3-2	2" above bottom	1200	4	4	1025	-15	65	35	Dendrites attached to plates (used high ZnO concentration).
3-62	3-2	3" above bottom	1200	4	2	1015	-10	65	35	Considerable dendritic growth (high ZnO concentration).
3-63	3-2	3" above bottom	1200	4	3	1050	-5	60	40	Considerable dendritic growth (high ZnO concentration).
3-64	3-1	1" above bottom	1160	4	5	1040	-15	60	40	Very thin polycrystalline wall nucleation (high ZnO).
3-65	3-2	2" above bottom	1200	4	6	1050	-10	65	35	Plate formation improved - high ZnO concentration.
3-66	3-1	2" above bottom	1170	4	6	1050	-20	60	40	Plate looks good - considerable dendrite formation - high ZnO.

Table IV (Continued)

Run	Furnace	Crucible Position	Soak Temp. (°C)	Soak Time (hrs)	Cooling Rate (°C/hr)	Pour Temp. (°C)	ΔT (°C)	% Plates	% Dendrites	Comments
3-67	3-1	3" above bottom	1200	4	2.5	1025	-15	50	50	Multiple nucleation high ZnO concentration
3-68	3-2	3" above bottom	1200	4	2.5	1025	-5	60	40	Thin plate, considerable wall nucleation - high ZnO.
3-69	3-1	4" above bottom	1200	4	8	1050	-10	40	60	Wall nucleation - high ZnO.
3-70	3-1	4" above bottom	1200	4	4	1050	-5	45	55	Some plate formation - high ZnO - wall nucleation.
3-71	3-2	3" above bottom	1200	4	4	1090	-10	60	40	Some plate formation - high ZnO.
3-72	3-2	3" above bottom	1200	4	2	1010	-10	55	45	Thin plates, some dendrites - low ZnO.
3-73	3-1	4" above bottom	1200	4	2	1040	-5	50	50	Small plates, some dendrites, low ZnO.
3-74	3-1	4" above bottom	1100	4	4	1050	-10	40	60	Small plates - polycrystalline, medium ZnO.
3-75	3-1	4" above bottom	1200	4	3	1040	-5	50	50	Small plates - medium ZnO, wall nucleation.

Table IV (Continued)

Run	Furnace	Crucible Position	Soak Temp. (°C)	Soak Time (hrs)	Cooling Rate (°C/hr)	Pour Temp. (°C)	ΔT (°C)	Plates	Dendrites %	Comments
3-76	3-1	3 1/2" above bottom	1200	4	2	1050	-10	--	--	Almost no crystals, refiner. ZnO.
3-77	3-1	4" above bottom	1200	4	3	1050	-5	50	50	Small crystals around edge, medium ZnO.
3-78	3-1	4" above bottom	1200	4	2	1030	-5	60	40	1" diameter plate and dendrites, medium ZnO.
3-79	3-1	4" above bottom	1200	6	1.4	1050	-5	50	50	Small plates, medium ZnO.
L1	Lindberg	Horizontal furnace - front	1200	24	5	1020	---	10	90	Too much evaporation.
L2	Lindberg	Horizontal furnace - middle	1200	24	5	1020	---	20	80	Too much evaporation
L3	Lindberg	Horizontal furnace - back	1200	24	5	1020	---	10	90	Too much evaporation.
L4	Lindberg	Horizontal furnace - front	1200	6	15	850	---	--	--	Interrupter failed.
L5	Lindberg	Horizontal furnace - back	1200	6	15	850	---	--	--	Interrupter failed.

Table IV (Continued)

Run	Furnace	Crucible Position	Soak Temp. (°C)	Soak Time (hrs)	Cooling Rate (°C/hr)	Turn Temp. (°C)	$\Delta T$ (°C)	# Plates	# Dendrites	Comments
L6	Lindberg	Horizontal furnace - middle	1200	6	15	850	---	--	--	Interrupter failed
L7	Lindberg	Horizontal furnace - back	1200	4	4	1025	---	60	40	24.7% percent ZnO.
L8	Lindberg	Horizontal furnace - front	1200	4	4	1025	---	20	80	25.5% percent ZnO.
L9	Lindberg	Horizontal furnace - middle	1200	4	4	1025	---	50	50	26.3% percent ZnO
L10	Lindberg	Horizontal furnace - front	1190	6	6.5	1000	---	20	80	Too much evaporation.
L11	Lindberg	Horizontal furnace - middle	1190	6	1.5	1000	---	40	60	Too much evaporation.
L12	Lindberg	Horizontal furnace - back	1190	6	1.5	1000	---	50	50	Too much evaporation.

High concentration 27% percent  
 Medium concentration 26% percent  
 Low concentration 25% percent

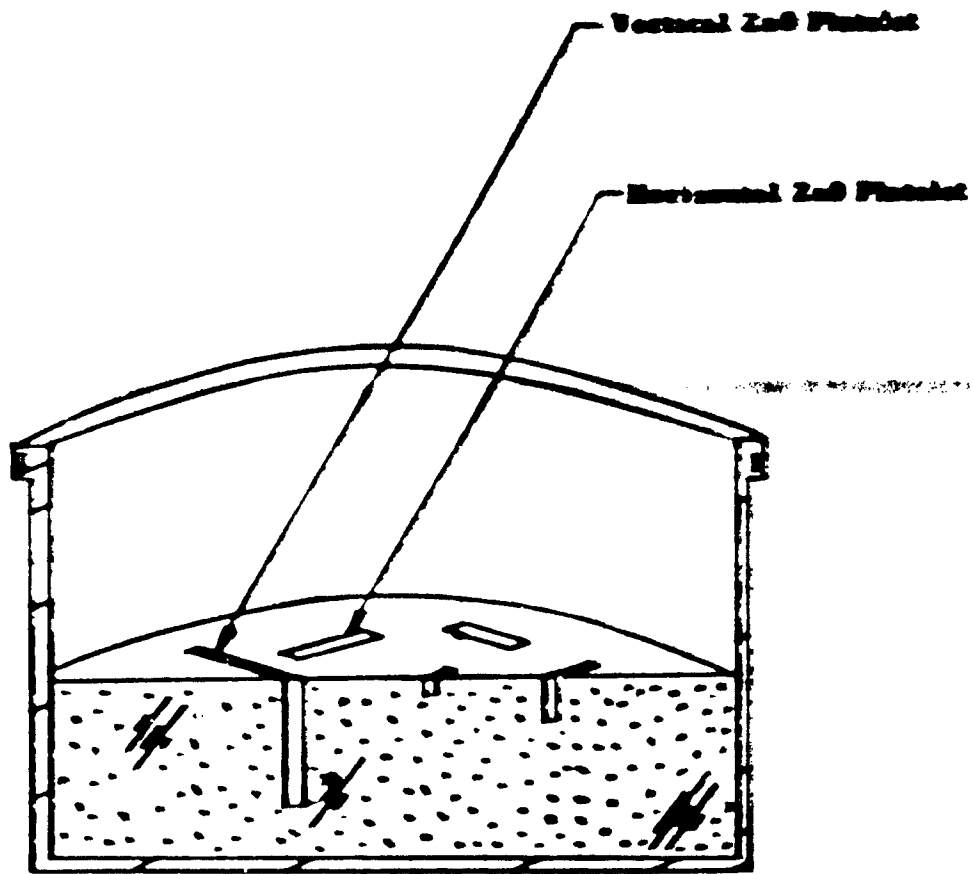


Figure 31 - Cross Section of Molten Salt Crucible  
Showing Growth Directions of Zinc Oxide  
Platelets

### Crystal Growth (Continued)

The center of the furnace is the hottest point, and temperature decreases with distance away from the center. A crucible placed above the center would have the bottom higher in temperature than the top, while below the center the opposite conditions would prevail.

Routine batch weight for a  $ZnO + PbF_2$  run is obtained by filling the crucible with the maximum amount of powdered chemicals which, after melting is only about one-third of the diameter in depth, or quite shallow. Since the temperature gradient is vertical, the temperature difference tends to be established from top to bottom of the melt; however, since the melt is so shallow this difference is small. Therefore, increasing the depth of the melt would increase the temperature difference between top and bottom of the melt.

Also, evaporation of  $PbF_2$  from the melt raises the  $ZnO$  content of the melt which can cause nucleation when it is unwanted, i.e., during the soak period. The rate of  $PbF_2$  evaporation should be dependent on surface area of the melt and surface temperature only. For the same surface and surface temperature the rate of evaporation is independent of melt depth.

Therefore, the increase in  $ZnO$  concentration for a given amount of  $PbF_2$  evaporation can be greatly reduced simply by increasing the depth of the melt in the crucible.

Generally "double batch" runs were made with only limited success (Table V). It was considered more profitable to pursue the use of lateral gradient in order to grow plates on the surface of the melt in the crucible.

#### 3.1.3.2 Lateral Gradient Method

Evaporation of  $PbF_2$  from the surface of the melt causes a thin skin of melt to be enriched in  $ZnO$ . With the appropriate vertical gradient, at some temperature during the growth cycle, crystallization should occur at the coolest point in the  $ZnO$  enriched surface layer. Though it is conceivable that some other region of the melt could nucleate before the surface skin, in practice, the melts are quite shallow, i.e., depth approximately one-third the diameter, and a significant temperature difference between the top and bottom of the melt seems unlikely.

If the rate of growth across the surface of the melt was to be controlled, it was only reasonable that a lateral gradient be employed to produce the nucleation site near the edge of the crucible.

Modification of the Lindberg furnace (a furnace with a horizontal muffle) to provide a variable lateral gradient was accomplished. Additional thermocouples were installed on

TABLE V

Molten Salt Crystal Growth Runs

Run	Furnace No.	Charge	% Loss	Cool Rate °C/hr.	Soak Temp. (°C)	Soak Time (hours)	Withdrawal Temp (°C)	Comments
189	H-3	D	NA	6 & 2	1200	5	1050	No growth.
190	H-2	S	10.6	NA	1210	24	1210	No growth.
191	L	S <sup>+</sup>	9.5	5	1150	4	1060	Tiny crystal plates.
192	H-2	S <sup>-</sup>	15	2.6	1210	5	1055	Tiny crystal plates.
193	L	S	10	2.5	1150	4	1050	Tiny crystal plates.
194A	H-3	D	2	2.1	1200	5	1000	No plate growth.
194B	H-3	D	--	2.2	1150	2	1055	Small plates.
195	L	S	5	2.5	1150	4	1070	Small plates.
196	H-3	D	7	5	1200	5	1040	Large plates.
197	L	S <sup>+</sup>	10	2.5	1160	4	1060	No plate growth.
198	H-3	D	15	5	1200	12	1040	Large plate.
199	L	D	--	2.5	1150	4	1020	No growth.
200	L	D	7	2.5	1150	4	1080	No growth.
201	H-3	D	--	5	1200	5	1050	Large thin plate.
202	H-3	D	--	5	1200	5	940	Medium plate.

Table V (Continued)

Run	Furnace No.	Charge	% Loss	Cool Rate °C/hr.	Soak Temp. (°C)	Soak Time (hours)	Withdrawal Temp. (°C)	Comments
203	H-3	D	--	5	1200	5	1040	Large plate.
204	H-3	D	--	5	1200	5	1030	Large plate.
205	6"	S	--	5	1200	5	1025	Medium plate.
206	H-3	S	--	4	1200	5	1050	No growth.
207	6"	S	--	4	1200	5	1050	Medium plate.
208	H-2	D	--	4	1200	5	1050	Small plate.
209	H-3	S	--	4	1200	5	1060	No growth.
210	H-2	D	--	6	1200	5	1060	No growth.
211	6"	S	--	3.5	1200	5	1050	No growth.
212	H-3	D	--	4	1200	5	1050	No growth.
213	H-2	S	--	4	12--	5	1050	Small thin plate.
214	H-2	D	--	3.1	1200	5	1050	No growth.
215A	L	S	25	3.1	1200	5	1050	BiO <sub>3</sub> - small plate.
215B	L	S	12	3.1	1200	5	1050	Small plate.
216	H-2	S	40	3	1200	5	1050	Medium plate.
217A	L	S	22	3	1200	5	1050	Medium plate-BiO <sub>3</sub> added.
217A	L	S	16	3	1200	5	1050	Medium plate.

Table V (Continued)

Run	Furnace No.	Charge	% Loss	Cool Rate °C/hr.	Soak Temp. (°C)	Soak Time (hours)	Withdrawal Temp. (°C)	Comments
218	H-2	S	--	2.5	1200	5	1050	Medium plate.
219	H-5	S	9	2.5	1200	5	850	No growth.
220	H-2	S	--	5	1200	5	1055	No growth.
221	H-5	S	--	4	1200	5	1050	No growth.
222	L	S	--	4	1200	5	1050	No growth-B <sub>2</sub> O <sub>3</sub> added.
223	H-3	S	--	2.5	1200	5	1050	No growth.
224	H-2	S	--	2.4	1200	5	1050	No growth.
226	6"	D	13	3	1150	8	1050	No growth.
227	6"	D <sup>+</sup>	5	5	1150	5	1050	No growth.

S - Single charge - 49.5 gms. ZnO, 400.5 gms. PbF<sub>2</sub>, 450.0 gms. total.

D - Double charge - 99.0 gms. ZnO, 801.0 gms. PbF<sub>2</sub>, 900.0 gms. total.

+ and - refer to slightly greater or lesser amounts of ZnO.

### Crystal Growth (Continued)

either side of the position where the crucible is placed, Figure 32. By means of these thermocouples, the actual gradient across the diameter of the crucible could be measured at any time during a run.

Tests showed a gradient of 35°C across the crucible; therefore at a cooling rate of 5°C per hour solidification should advance from the nucleation site on one side of the crucible to the opposite side of the crucible in seven hours.

Another attempt was made to achieve lateral gradients in a vertical furnace by removing two of the heating elements from the circuit. In essence this created a cool side on the muffle. A temperature gradient of 7°C across the melt was achieved, in Furnace H-3. This gradient was measured by means of two thermocouples which were strapped to the pedestal, Figure 33. In cooling the furnace, therefore, nucleation should occur only on one edge and continue across the top of the melt.

Some success was achieved using this furnace and technique. The plates though somewhat larger were still thin. While the importance of thermal gradient effects proved to be significant it became clear that such gradients were not the only factor in determining the size, thickness and quality of ZnO plates grown by this technique.

As the hydrothermal crystal growth improved it appeared that, although the gradient control could be developed to produce larger crystals, the hydrothermal seed problem would most readily be resolved by utilizing the hydrothermal system to generate its own seeds.

## 3.2 Hydrothermal

### 3.2.1 Low Pressure Crystal Growth

Shortly after the program was begun Laudise, Kolb and Caparaso<sup>8</sup> published a paper in which they described a set of conditions at which ZnO crystals could be grown using the hydrothermal technique. As such the conditions provided an excellent "jumping-off point" for the contract. After several preliminary experiments with the autoclave pressure testing, furnace calibration and pressure balance, the first attempts were made to grow crystals. The major differences between the two laboratories were in the sizes and types of autoclaves. The ZnO crystal growth was developed at Bell Telephone Laboratories using rather small chambered silver-lined Morey type vessels (maximum internal cavity size 1-3/16" diameter x 6-7/8" long). The Airtron vessels have been previously described in this report.

The first attempts at crystal growth failed using the Bell Telephone Laboratories' parameters. The most apparent reason for failure was in the warm-up procedure. The warm-up procedure employed by Bell Telephone Laboratories was what would be considered slow,

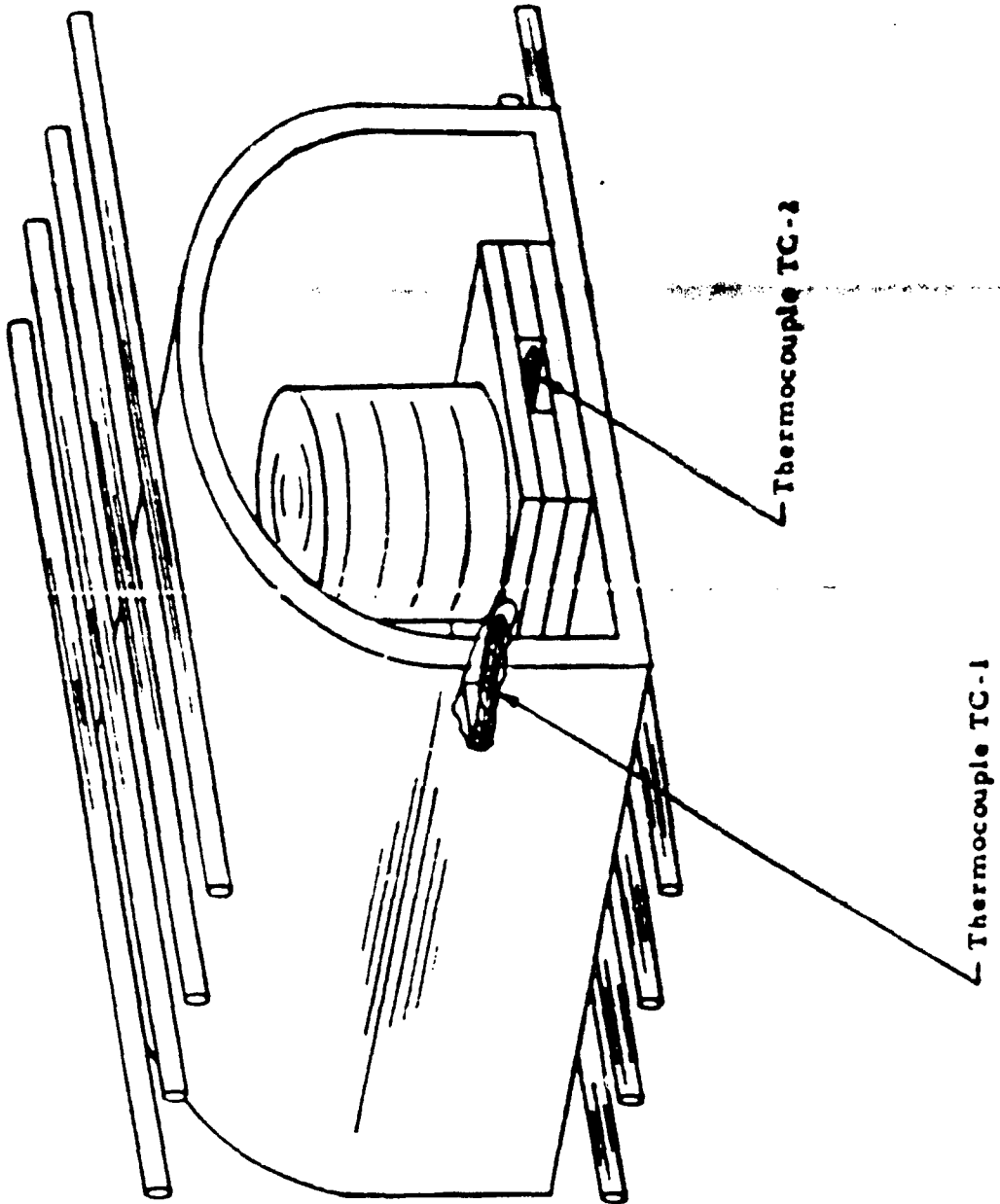


Figure 32 - Diagram of Lindberg Furnace with Lateral Gradient Measuring Thermocouples in Place

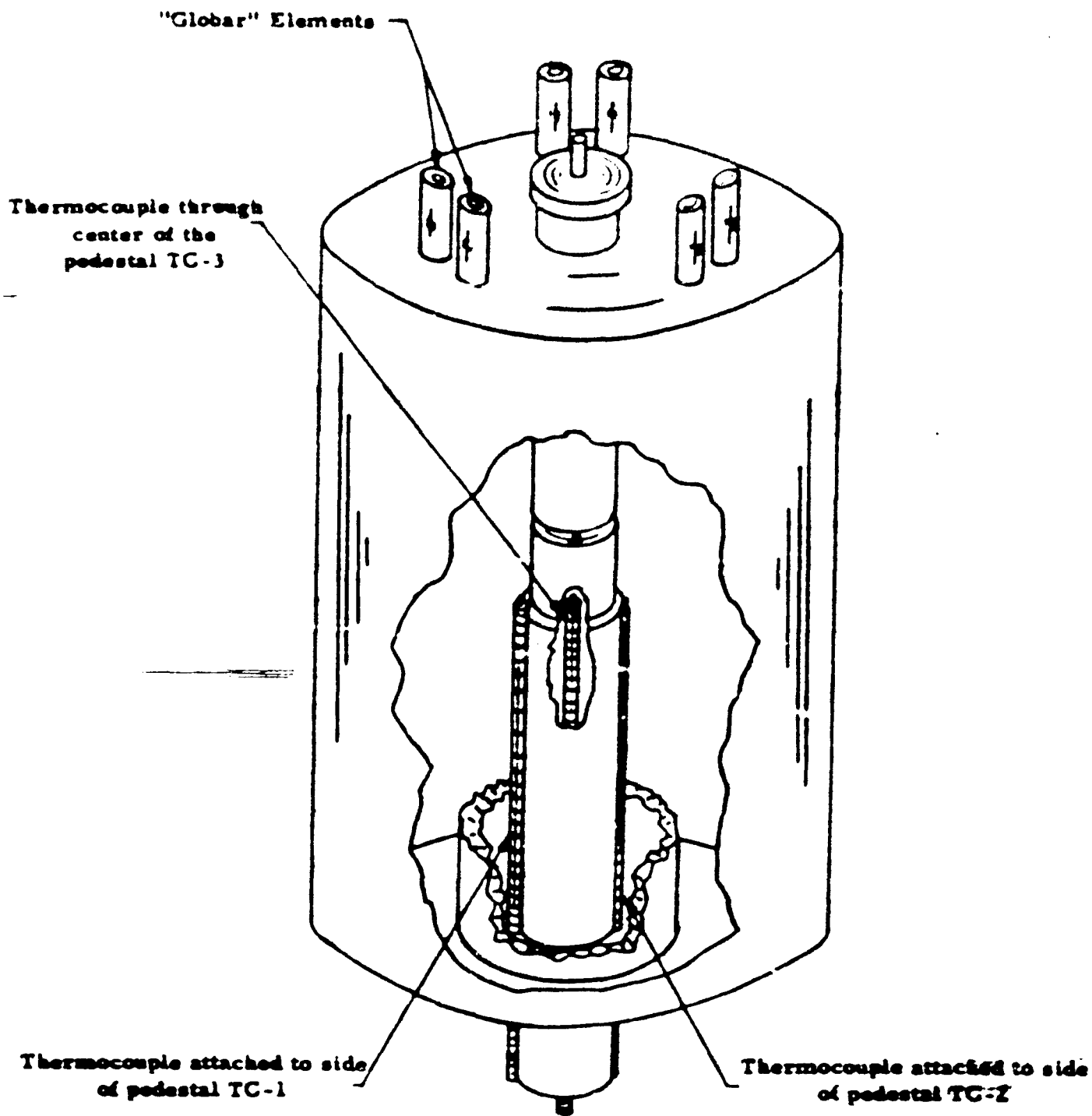


Figure 33 - Three Inch Furnace Showing Thermocouple Positions for Measuring Lateral Gradient

Crystal Growth (Continued)

i.e. over a twenty-four hour period. Because of the difference in autoclave geometry, silver liners, etc. this approach did not work at Airtroon. Instead it was found that with this procedure in many cases the seeds would be completely dissolved. This was not unreasonable since the seeds were only 10-15 mils thick and the volume of solution was approximately 1.3 liters.

After some experimentation with warm-up procedure it was found that the best technique at Airtroon was to warm up the vessel to operating conditions as quickly as possible. In this way the seeds were retained and the growth of crystals began. The data for the initial growth runs with the warm-up procedure experiments is presented in Table VI, and a photograph of some typical crystals are shown in Figure 34 .

Once having obtained a suitable warm-up procedure the following task remained:

- 1) To improve the quality of the crystals.
- 2) To eliminate the corrosive attack of the silver container (see section 3.2.4).
- 3) To attempt to obtain uniform growth rates at all seed positions by baffle area changes, and changes in the amounts and position of insulation.
- 4) To maximize the growth rate yet maintain or improve the crystal quality.
- 5) To develop high quality seed crystals of large basal area by successive hydro-thermal growth runs. (see section 3.2.2)

Work on the above objectives was performed during runs No. 44 through No. 63. The operational crystal data for these runs is presented in Tables VI and VII. With regard to objectives 2 and 5 the results and discussions of these are presented in separate sections of this report. An idea of the improvement in quality during this period can be obtained by comparison of the crystals shown in Figure 34 (Run No. 39) and Figure 35 and Figure 36 . Figure 36 is the top section of a crystal from Run No. 51 in which the seed was removed.

The improvement in growth rate uniformity can be seen from the data presented in Tables VIII and IX which summarizes the growth rate for each crystal for Runs No. 46 through No. 54. In general it was found that the seed(s) in the uppermost position were the fastest growing. This is to be expected since it is the one which sees the greatest  $\Delta T$ . The seed(s) nearest the baffle exhibit the lowest growth rate because it is the one with the lowest  $\Delta T$ . In order to obtain a

TABLE VI

Crystal Growth Operational Data

Run	Solvent	Nutrient	Internal fill (silver can) %	External fill %	Baffle Area %	Warm-up Time (hrs)	AT (°C)	Results	Comments
27	6 molar KOH pre-saturated with ZnO 0.2 molar LiOH added	ZnO entered at 1150°C for 2 hrs., broken into 1/4" to 3/8" chunks	83	70.6	8	24	18	Some growth	Weld leaked seeds thickened.
28	"	"	83	70.6	8	24	17	Some growth	Weld leaked, thin seeds dissolved.
29	"	"	83	70.6	10	24	24	Some growth	Weld leaked.
30	"	"	83	70.6	10	24	26	Growth on seeds	Hot plate and slide units, fill error, can crushed.
31	"	"	83	70.6	12	24	8	No growth	Used slide heat- seeds dis- solved to hot plate.
32	"	"	83	70.5	12	24	50	Almost no growth	Took insulation out of center section of fur- nace.
33	"	"	83	70.6	10	32	36	Seeds thick- ened.	1 day at opera- ting conditions.

Table VI (Continued)

Run	Solvent	Nutrient	Internal fill (silver can) %	External fill %	Baffle area %	Warm-up time (hrs.)	$\Delta T$ (°C)	Results	Comments
34	6 molar KOH presaturated with ZnO	ZnO sintered at 1150°C for 2 hrs., broken into 1/4" to 3/8" chunks	83	70.6	10	32	45	Seeds thickened	Operated 1 day to check pressure balance.
35	"	"	83	70.5	10	45	40	Seeds thickened	Hot plate only - check warm-up procedure.
36	"	"	83	70.6	10	45	58	Spontaneous nucleation	Can puffed - fill balance off - exterior low.
37	"	"	83	71.5	12	32	40	Some growth	Can puffed.
38	"	"	83	75	10	96	75	Spontaneous nucleation	Autoclave seal leaked, can burst - autoclave overheatd.
39	"	"	83	76	10	96	40	Some growth on 13 seeds	Best.
40	"	"	83	77.0	10	96	50	Some growth	Autoclave seal leaked, grinding incorrect.
41	"	"	83	77.9	10	96	45	Some growth	Balance looks good.

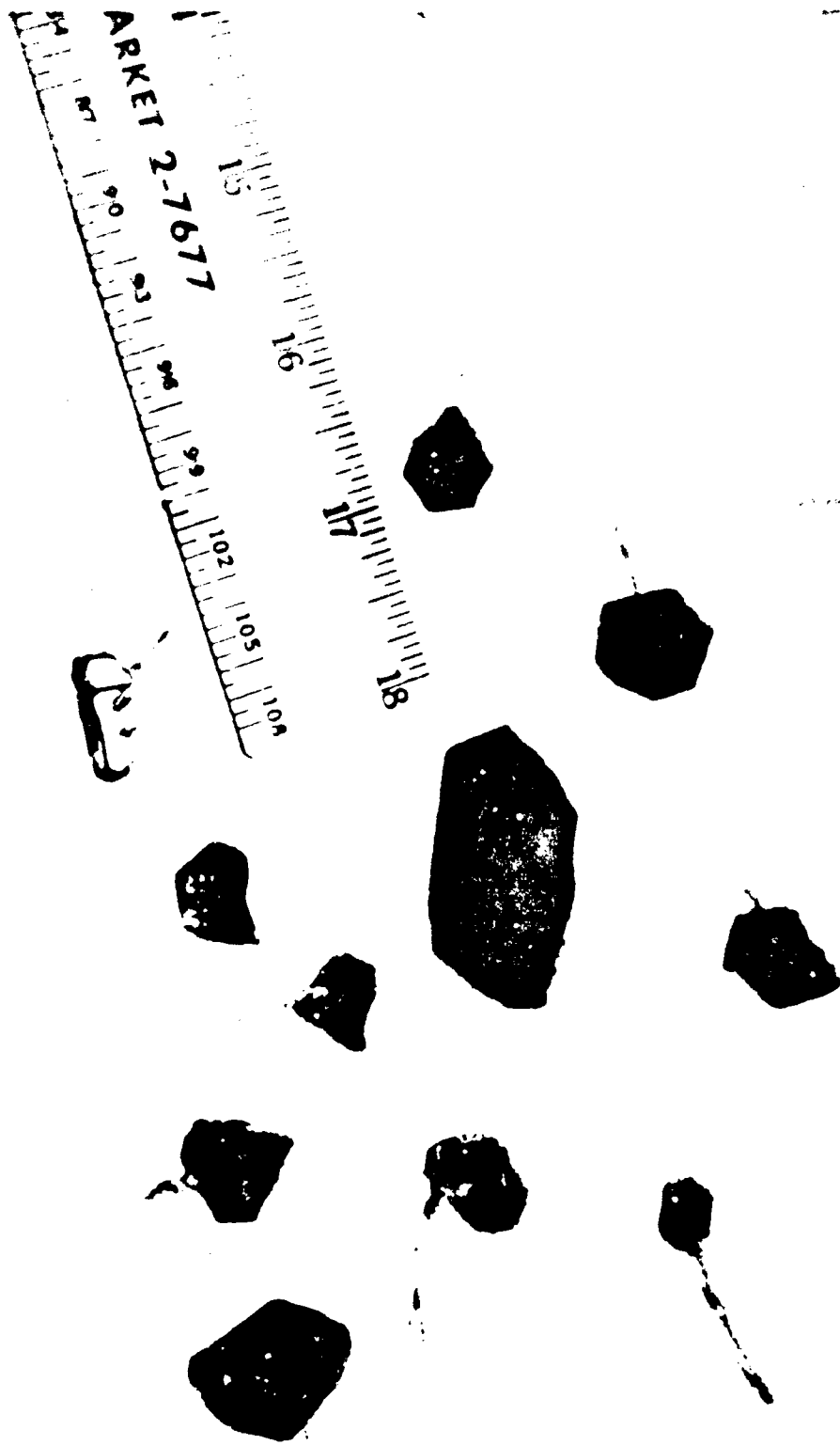


Figure 34 - Hydrothermally Grown Zinc Oxide Crystals

TABLE VII

Crystal Growth Operational Data

Run No.	T <sub>B</sub> (°C)	T <sub>M</sub> (°C)	T <sub>T</sub> (°C)	Δt (°C)	P (psi)	LiOH Conc. (m)	Operating Time (days)	Average Growth Rate (mils/day)	<000>	Remarks
42	---	---	---	---	---	---	---	---	---	Leaked
43	---	---	---	---	---	---	---	---	---	Leaked.
44	338	304	288	50	7500	0.2	28	10.6		
45	330	294	293	37	7500	0.2	29	5.9		
46	325	295	295	30	6400	0.2	7	7.6		
47	325	285	295	40	8300	0.2	11	14.4		First hydrothermal seeds.
48	335	300	305	35	6900	0.2	22	9.0		Seeds from No. 46.
49	315	290	295	25	7500	0.2	28	11.7		
50	330	300	310	30	6500	0.2	43	6.3		
51	325	294	296	31	7700	1.0	34	7.9		Seeds from No. 49.
52	326	295	290	31	17000	0.2	6	26.0		First high pressure run.
53	325	299	295	26	7700	0.2	31	9.1		
54	328	299	297	29	10500	0.2	22	10.7		
55	330	299	295	31	7500	0.2	14	19.7		

Table VII (Continued)

Run No.	T <sub>B</sub> (°C)	T <sub>M</sub> (°C)	T <sub>T</sub> (°C)	ΔT (°C)	P (psi)	L1OH Conc. (m)	Operating Time (days)	<0001> Average Growth Rate (mils/day)	Remarks
56	---	---	---	--	----	----	--	--	Leaked.
57	---	---	---	--	----	---	--	--	Leaked.
58	332	317	317	15	6500	0.2	13	3.5	
59	328	313	313	15	9000	1.0	42	7	Au plated can.
63	332	317	317	15	9000	1.0	33	1-2	No silver attack. VMOP - seed development.
64	400	388	388	12	19400	0.2	15	18-23	Silver attack. Plated growth - VMOP.
60	341	326	327	15	19700	1.0	5	1	1 inch vessel, 7.5% baffie.
61	---	---	---	--	----	0.2	--	---	Failed during warm-up.
62	415	393	390	25	23000	0.2	11	31	1 inch vessel, 15% baffie.

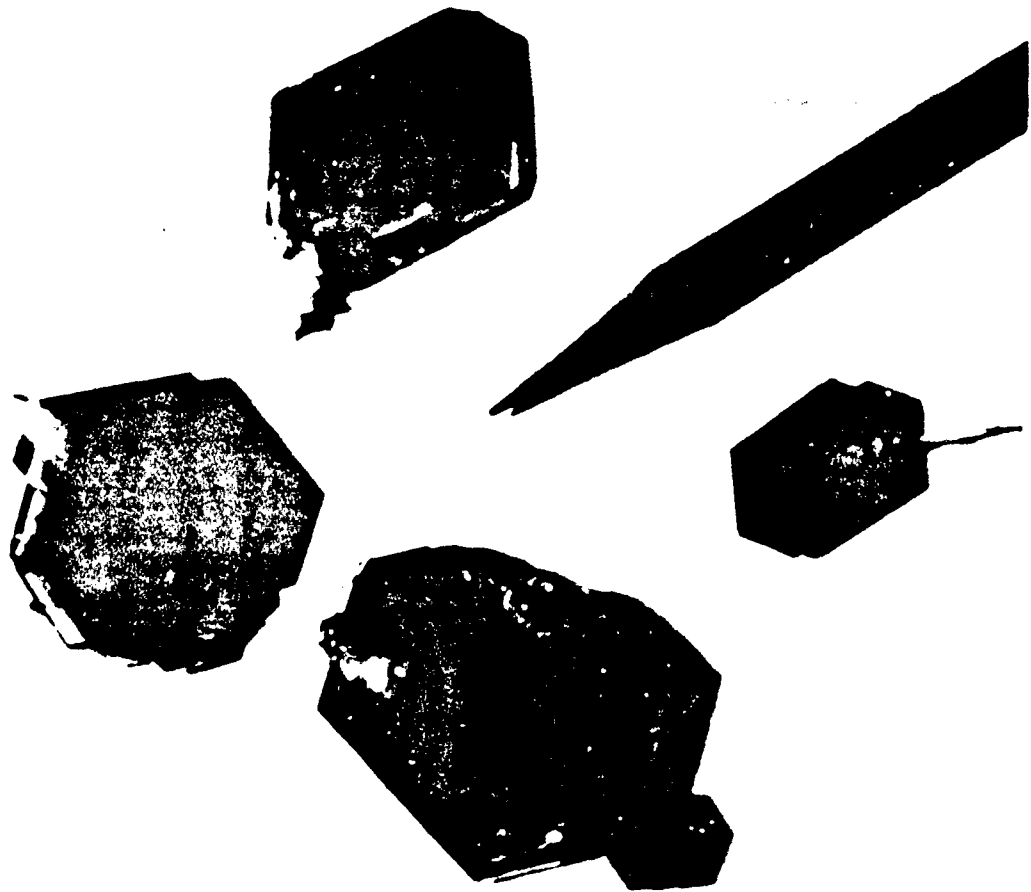


Figure 35 - Hydrothermally Grown Zinc Oxide Crystals

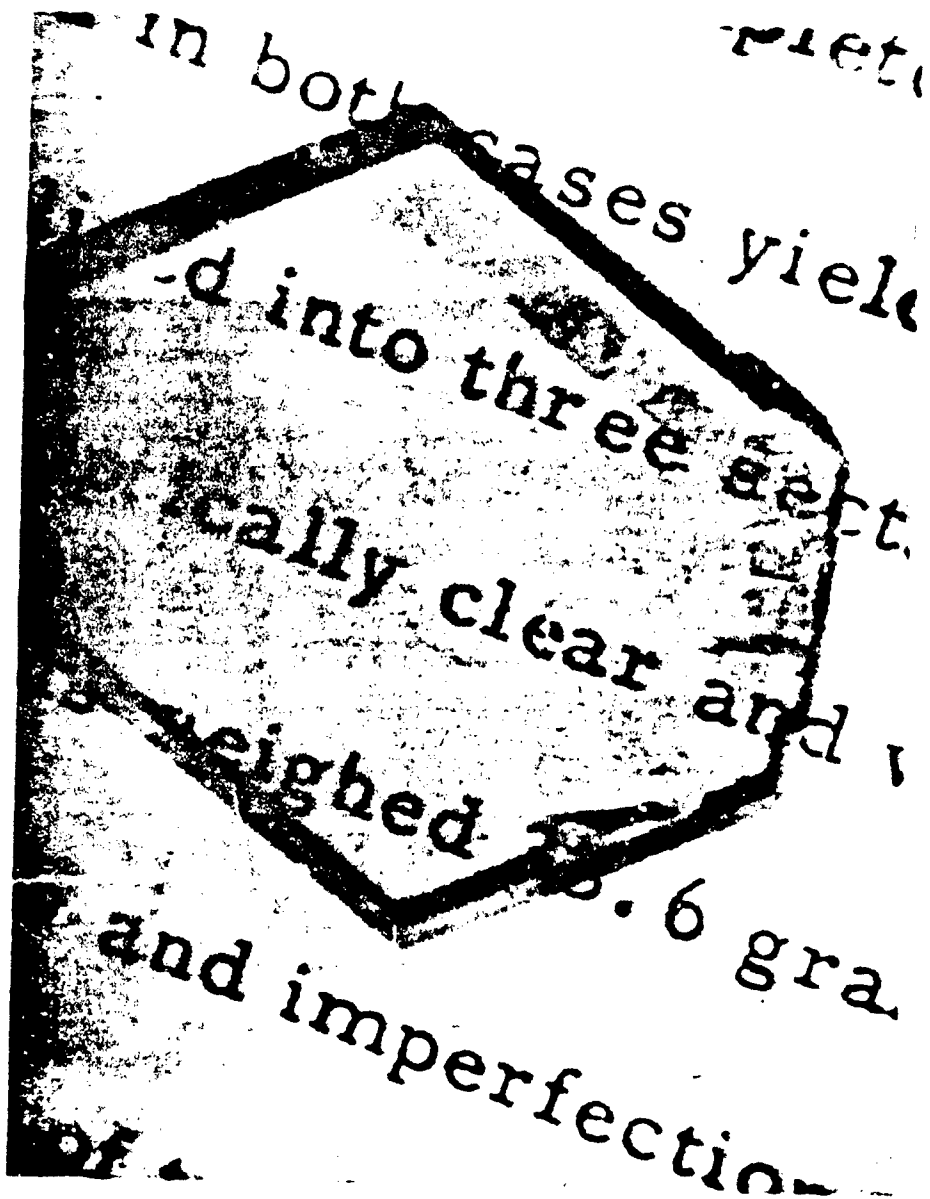


Figure 36 - High Quality Crystal from Run No. 51  
with Seed and  $c^-$  Side Removed

TABLE VIII

Seed and Crystal Data for Run No. 44

<u>Rack Position</u>	<u>Weight (grams)</u>	<u>Total Thickness (mils)</u>	<u>(0001) Thickness (mils)</u>	<u>(000I) Thickness (mils)</u>	<u>Total Growth Rate (mils/day)</u>	<u>&lt;000I&gt; Growth Rate (mils/day)</u>	<u>&lt;000I&gt; Growth Rate<sup>e</sup> (mils/day)</u>
1	12.9	395	241	154	14.1	8.6	5.5
1	3.9	303	166	137	10.8	5.9	4.9
2	4.4	324	179	145	11.6	6.4	5.2
2	8.1	400	255	145	14.3	9.1	5.2
2	7.1	403	267	136	14.4	9.5	4.9
3	4.4	306	178	128	10.9	6.3	4.6
3	4.0	287	165	122	10.3	5.9	4.4
4	1.8	245	136	109	8.8	4.9	3.9
4	5.4	279	187	92	10.0	6.7	3.3
5	1.3	149	125	24	5.3	4.2	0.9
5	2.2	173	117	56	6.2	4.2	2.0

Table VIII (Continued)  
Seed and Crystal Data for Run No. 45

<u>Rack</u> <u>Position</u>	<u>Weight</u> <u>(grams)</u>	<u>Total</u> <u>Thickness</u> <u>(mils)</u>	<u>(0001)</u> <u>Thickness</u> <u>(mils)</u>	<u>(0001)</u> <u>Thickness</u> <u>(mils)</u>	<u>Total</u> <u>Growth Rate</u> <u>(mils/day)</u>	<u>&lt;0001&gt;</u> <u>Growth Rate</u> <u>(mils/day)</u>	<u>&lt;0001&gt;</u> <u>Growth Rate</u> <u>(mils/day)</u>
1	33.6	233	176	57	8.0	6.1	2.0
2	20.1	206	153	53	7.1	5.3	1.8
3	5.7	191	116	75	6.6	4.0	2.6
4	17.5	190	151	39	6.6	5.2	1.3
5	9.5	153	113	40	5.3	3.9	1.4
6	5.3	109	109	0	3.8	3.8	0
6	2.2	118	118	0	4.1	4.1	0

\*Neglecting Thickness of Seed.

TABLE IX

Seed and Crystal Data for Runs No. 46 Through 54

<u>Run No.</u>	<u>Rack Position</u>	<u>Seed Weight (gms)</u>	<u>Seed Thickness (mils)</u>	<u>Crystal Thickness (mils)</u>	<u>Growth Rate (mils/day)</u>	
46	1	3.1	--	53	8	
	2	5.6	--	62	9	
	3a	3.0	--	47	7	
	3b	1.6	--	50	7	
	4a	4.3	--	71	10	
	4b	2.4	--	84	12	
	5	1.0	--	36	9	
	6a	1.6	--	44	6	
	6b	1.7	--	54	8	
	7a	1.8	--	48	7	
	7b	1.7	--	49	7	
	47	1	21.1	64	273	19
		2	24.7	57	244	17
3a		12.5	59	235	16	
3b		14.4	49	236	17	
4a		11.5	--	180	16	
4b		5.3	--	163	14	
5a		6.2	--	150	13	
5b		8.0	--	154	11	
6a		5.0	--	169	15	
6b		5.1	--	125	11	
7a		4.2	--	147	11	
7b		4.4	--	138	13	
48		1	18.5	53	259	9
	2	34.1	62	322	12	
	3a	16.3	47	233	4	
	3b	10.0	50	243	9	
	4a	21.4	71	295	10	
	4b	5.5	84	200	5	
	5	10.4	36	289	11	
	6a	9.8	44	238	9	
	6b	9.8	54	254	9	
	7a	9.1	48	225	8	
	7b	10.0	49	244	9	
49	1	55.1	55	400	12	
	2	20.8	44	365	11	
	3	56.8	42	450	15	
	4	10.5	43	343	11	
	5	18.3	48	382	12	
	6	50.0	40	371	12	
	7	12.2	49	293	9	

Table IX (Continued)

<u>Run No.</u>	<u>Back Position</u>	<u>Seed Weight (gms)</u>	<u>Seed Thickness (mils)</u>	<u>Crystal Thickness (mils)</u>	<u>Growth Rate (mils/day)</u>
50	1	96.7	322	655	8
	2	59.5	236	588	8
	3	41.5	295	562	6
	4	27.8	109	418	7
	5	32.1	153	409	8
	6a	27.0	238	442	5
	6b	16.4	200	391	5
	7a	28.8	243	477	5
51	7b	25.7	254	461	6
	8	26.3	289	521	6
	1	4.9	39	372	10
	2	7.6	65	381	9
	3	6.6	54	404	10
	4	5.1	43	315	8
	5	5.9	60	261	6
	6	5.1	39	277	7
52	7	5.7	55	223	5
	8	1.6	21	98	2
	1	0.7	10	197	31
	2	5.0	63	217	26
	3	1.3	30	216	31
	4	3.7	135	418	47
	5	2.2	32	182	25
	6	2.8	34	193	27
	7	2.9	36	190	26
	8	1.5	30	155	21
53	9	.8	64	145	14
	10	1.8	35	153	20
	1	11.7	80	426	11
	2	8.4	57	425	12
	3	7.4	54	338	9
	4	8.9	61	392	10
	5	8.2	63	325	8
	6	11.0	88	353	8
54	7	7.5	53	309	8
	8	5.2	47	280	7
	1	8.4	44	348	14
	2	9.4	53	307	12
	3	9.1	43	325	13
	4	7.9	47	273	10
	5	9.3	50	278	10
	6	5.5	37	227	9
	7	8.4	49	127	8

Crystal Growth (Continued)

uniform growth rate it is necessary to make the growth chamber as nearly isothermal as possible. This could only be accomplished by adjusting the baffle area (5 - 10%) and experimenting with the quantity and position of insulating material on the top of the autoclave.

During this period it was found that at rates in excess of 15 mils/day the crystal quality was generally poor and that the slower the rate the higher the quality. The lower quality was manifested by crevice flawing resulting from differences in growth of the  $\langle 10\bar{1}1 \rangle$  and  $\langle 0001 \rangle$  directions.<sup>8</sup> While the presence of  $\text{Li}^+$  aided in reducing this crevice flawing, growth rates of 15 mils/day were still too great to result in high quality.

The crystal structure of ZnO is such that the  $\langle 0001 \rangle$  and  $\langle 000\bar{1} \rangle$  are not equivalent and therefore the growth rates in the two directions are not equivalent. It was found that the rates in the  $\langle 0001 \rangle$  or  $c^+$  were 2-3 times faster than the  $\langle 000\bar{1} \rangle$  or  $c^-$ . In addition to the anisotropy of growth rate the quality defects were of a different nature. The crevice flawing previously described occurs in the  $c^+$  direction. The defects on the  $c^-$  faces were in the forms of dendritic growth along the  $\langle 10\bar{1}1 \rangle$  direction.

The anisotropy of the electrical resistivity of material in the  $c^+$  and  $c^-$  sides of the seed will be discussed in a later section of this report (4.2.1).

The following summary gives the conditions which were found suitable for the growth of high quality crystals at low pressure conditions at that time:

Crystallization Temperature-----	~800°C
Nutrient Temperature-----	~330°C
$\Delta T$ -----	~30°C
Pressure-----	8000 psi
Solvent-----	6N KOH
Lithium Concentration-----	1.2-2.0 M
Seeds-----	High quality
Warm-up-----	As fast as possible
Nutrient-----	Sintered ZnO powder
Baffle Area-----	7.5-10%
Autoclave-----	3 in. i.d.
Silver can-----	2.0 in o.d.
Internal fill-----	83%
External fill-----	78%

3.2.2 Hydrothermal Seed Development

During the course of the contract a program was begun to use the hydrothermal system to produce large area seed crystals. This program had not been anticipated at the beginning of the contract since in its original concept the large seeds were to be obtained by

### Crystal Growth (Continued)

the molten salt technique. As the contract progressed, however,

- 1) the molten salt technique failed to yield reproducibly large high quality crystals.
- 2) it was found that hydrothermal crystals could be sliced and used as seeds for subsequent runs.
- 3) at conditions where high quality growth was produced a "healing effect" of cracks and other defects took place during the crystal growth and,
- 4) in addition to obtaining growth in the ( $c^+$ ) and ( $c^-$ ) directions, significant lateral growth i.e. in the (a) and (m) directions, also took place thus enlarging the basal area of the crystals.

It therefore seemed appropriate to begin a program wherein the largest hydrothermal crystals of reasonably good quality would be sliced into a seed crystal and used in the subsequent run.

This program was begun using a high quality seed whose area was  $9.2 \text{ cm}^2$ . Table X summarizes the data for the development of the seeds giving an indication of the increase per run over a four run period. Figure 37 also shows several crystals from subsequent runs to indicate the increase in crystal size from run to run. The increase in size as shown in the figure and table is indicative of the way in which the program progressed. Finally in the growth of large 150 gram crystals the basal area of the crystals was greater than  $28 \text{ cm}^2$ . The average growth rate in the (a) and (m) directions during this period was found to be 4-5 mils per day.

One problem which was discovered in the lateral growth during this period was concerned with the observations of a phenomenon known as "electrical twinning." This growth defect was first noted in the crystals grown in run No. 59 which utilized a gold plated can.

The crystals were examined with a U-V mineral-light (3660A\*) which caused almost the entire (0001) surface of the crystal to have a yellow fluorescence. The (000 $\bar{1}$ ) surface only fluoresced below that area where the (0001) surface did not fluoresce. Further examination of the crystal surfaces showed that on both sides of the crystal the areas which fluoresced were smooth, and not flawed. It appeared that these smooth areas which fluoresced might be (0001) faces and that a reversal of crystallographic orientation had occurred. Such a reversal would account for these observations such as shown in Figure 38. Etching the crystals in sodium hydroxide solutions was found to reveal the differences in orientation quite nicely. On the (000 $\bar{1}$ ) surface the etch produces a matte appearance while the (0001) surface remains shiny. The etch rate is also greater for the <000 $\bar{1}$ > than the <0001> and as a result an etched (0001) surface, the material just described, will have islands of (0001) surface where this orientation

TABLE X

SUMMARY OF DATA FOR BASAL AREA INCREASE

<u>Exp. No.</u>	<u>Basal Area (cm<sup>2</sup>)</u>	<u><math>\Delta A</math> cm<sup>2</sup></u>	<u>Rate (cm<sup>2</sup>/day)</u>
51	9.2	---	-----
53	12.4	3.2	0.103
54	15.4	3.1	0.141
55	19.4	3.9	0.278

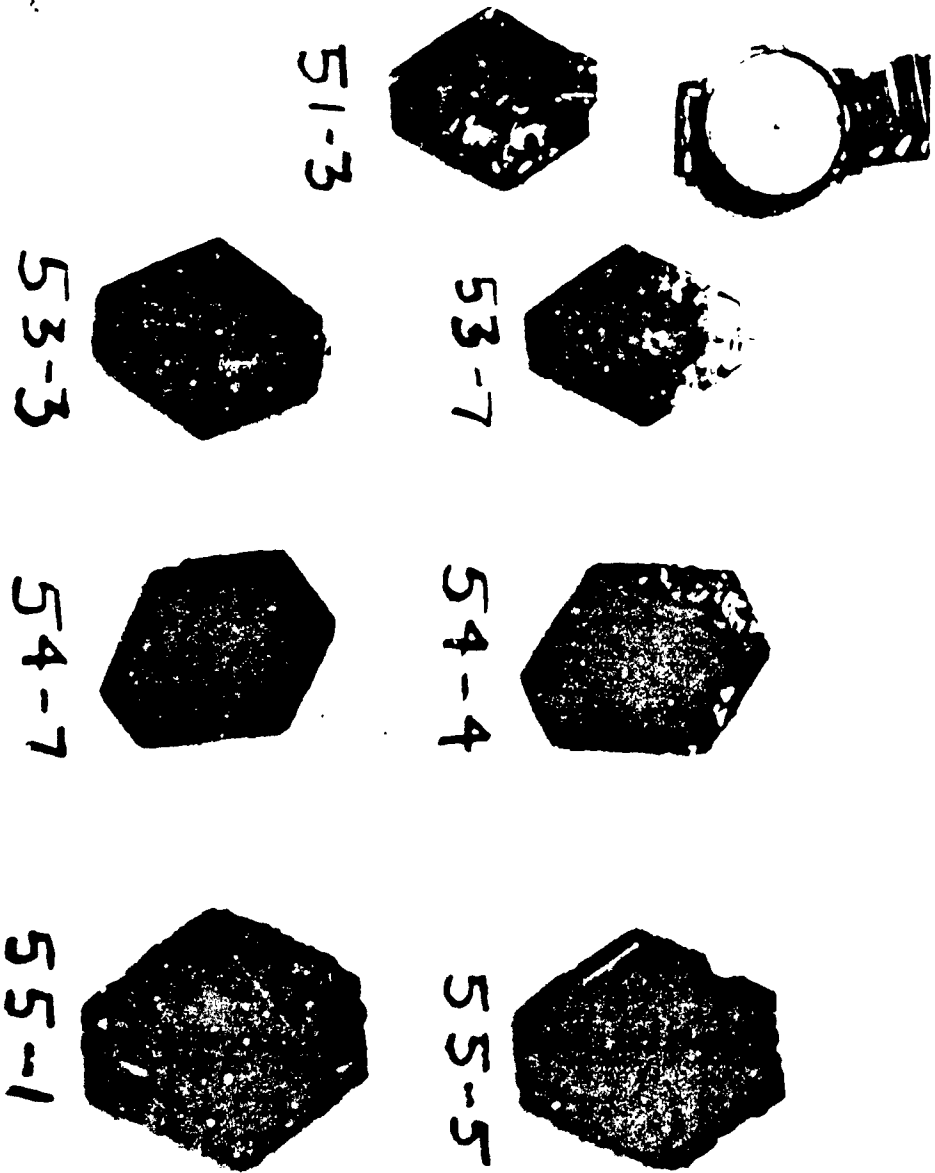


Figure 37 - Crystals from the Seed Development Runs Showing Basal Area Increase

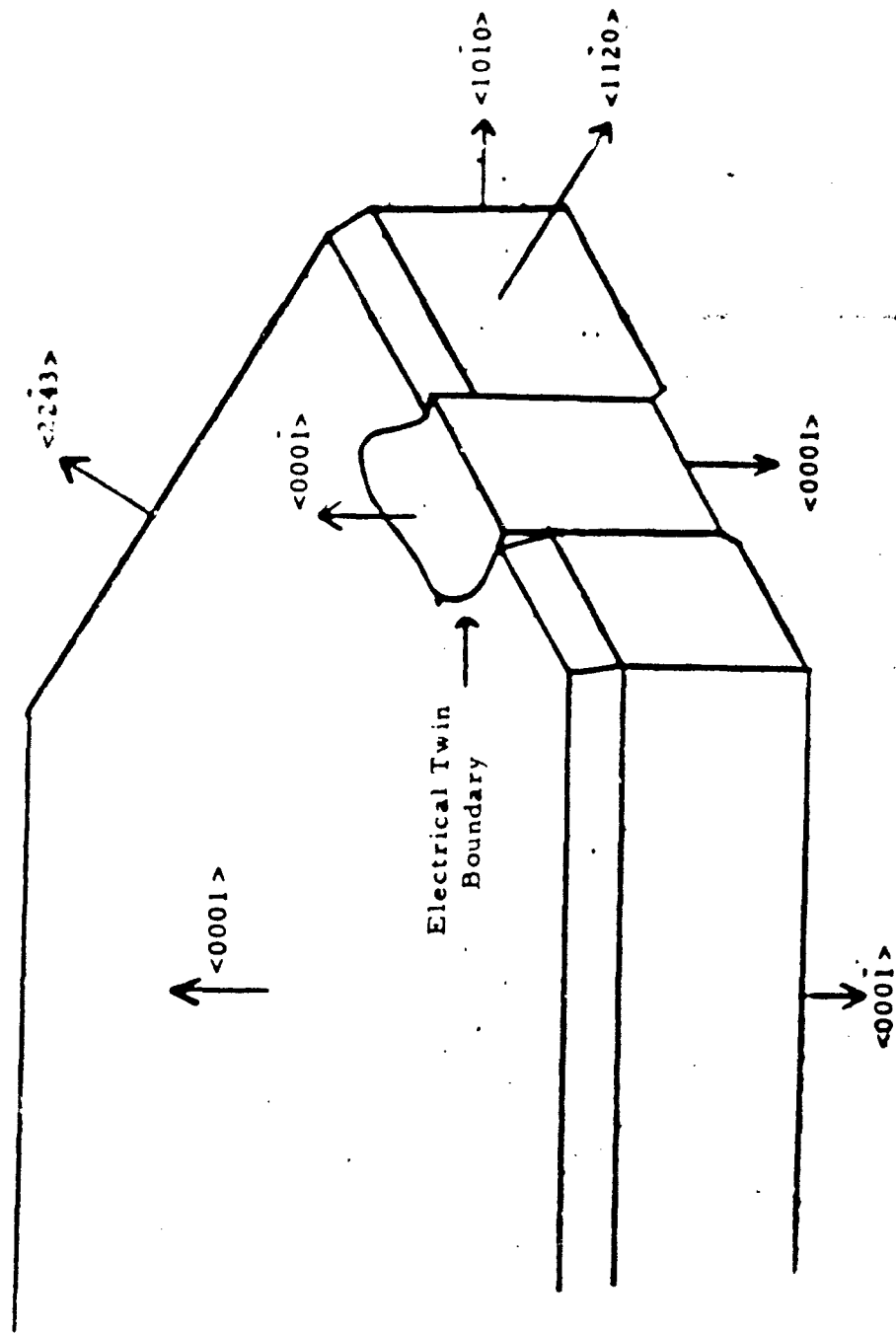


Figure 30 - Schematic Drawing of Electrical Twinning of ZnO

### Crystal Growth (Continued)

reversal occurs. This type of orientation reversal has been found to occur in quartz and is called "electrical twinning."

Etching of ZnO crystals in 10 M NaOH at 90°C for 15-30 minutes was found to develop different etch figures or patterns of the opposing pole faces. The figures are somewhat different than those reported by Mariano and Hanneman<sup>2</sup> who used a HNO<sub>3</sub> etch. In this case the (0001) faces etch very quickly leaving the surface with a somewhat dull finish. The (000 $\bar{1}$ ) faces etch more slowly and are shiny except for the pit produced by the etch. Typical etch structures are shown in Figures 39 and 40 for the (000 $\bar{1}$ ) and (0001) faces, respectively. The patterns on the (000 $\bar{1}$ ) surface is formed by the production of hillocks on the surface having the appearance of small hemimorphs in agreement with the natural crystal morphology. Two patterns are present on the (000 $\bar{1}$ ) surfaces. One is the pits which appear as hexagonal or parallelogram-shaped pits with flat bottoms. The other is a pattern or network of lines which may be slip lines and due to the microscopic imperfection of the crystals.

These etch patterns clearly reveal the existence of pole reversal in the crystals when the various sections are examined microscopically. The areas of such electrical twins on a grown crystal are shown in Figure 41 .

Unfortunately the seed development program was slowed down by the discovery of such twins. The edge of the seed plate thereafter was trimmed of any of the "electrically twinned" material thus reducing the basal area. Nonetheless the program's success is notable when the final seed plate area and large crystal growth are considered.

#### 3.2.3 High Pressure Crystal Growth

The dramatic increase in growth rate with increased pressure in the hydrothermal growth of ruby<sup>13</sup> led to speculation of what might happen in the case of ZnO. The only reason at that time for operating below 10,000 psi was that this was the region used by the Bell Laboratory workers, who were limited by the pressure capability of their vessels.

The first high pressure ZnO run attempted at Airtron produced relatively high quality crystals and at what appeared to be higher growth rates.

Subsequent runs indicated that the rate is undoubtedly more dependent upon crystallization temperature,  $\Delta T$ , impurities than pressure. The growth rate in this first experiment was 26.0 mils/day, Run No. 52. Although no subsequent run was made at exactly the same conditions at even higher pressures much lower growth rates were obtained. Scanning Table XI will reveal that lower rates were observed even when the variables other than pressure might be expected to produce higher rates.



Figure 39 - NaOH Etch Pattern on (0001) Surface

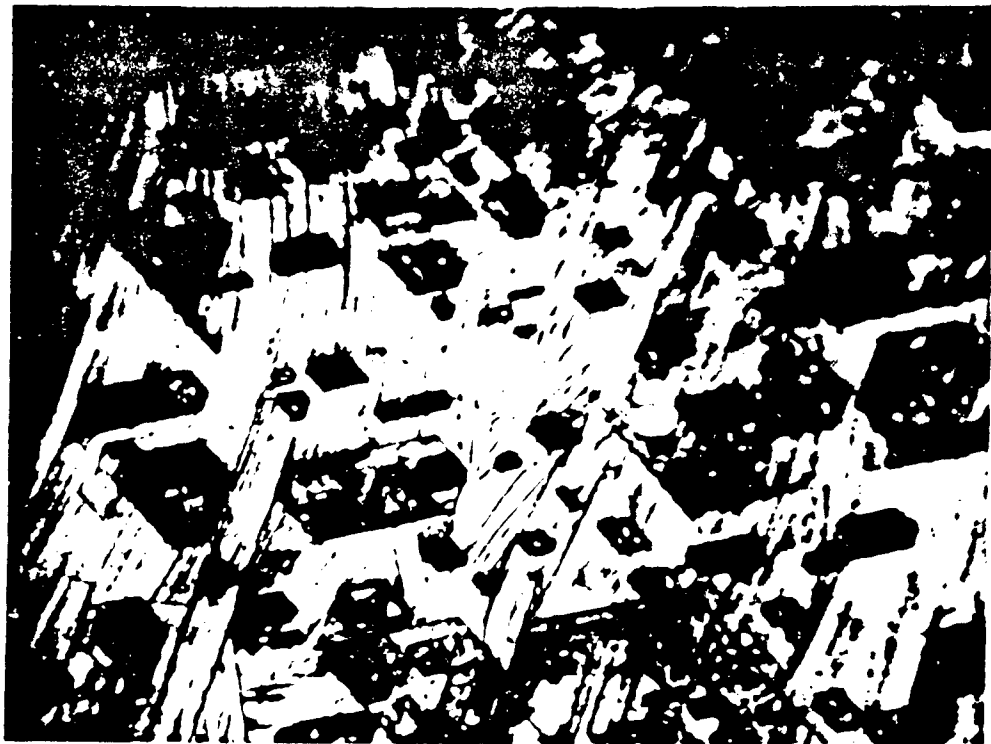


Figure 40 - NaOH Etch Pattern on (0001) Surface



Figure 41 - Photomicrograph of ZnO Electrical Twins After Etching

TABLE XI

## CRYSTAL GROWTH OPERATIONAL DATA

Run No.	$T_B$ ( $0^\circ$ )	$T_M$ ( $0^\circ$ )	$T_I$ ( $0^\circ$ )	$\Delta T$ ( $0^\circ$ )	Pressure (psi)	Lich Conc (M)	Operating Time (days)	Average Growth Rate (mils/day)	Remarks
65	335	316	316	19	9,700	1.0	38	7	
66	383	371	371	14	19,700	1.0	15	16	Best growth to date.
67	383	374	376	7	19,200	1.0	18	0.6	0.1 M In(OH) <sub>3</sub> added.
68	397	389	389	8	19,500	1.5	15	11	Crevice flawed growth.
69	337	318	321	16	9,100	1.0	31	6.8	Seed Development Run
70	395	388	389	6	19,800	1.0	16	9.4	
71	299	274	277	22	33,400	1.0	42	5.4	Metallic Zn added
72	310	282	286	24	23,300		18	10.0	Cu Doped Run
73	352	332	333	19	15,700		35	11.8	30.0 Ogm CuO added to nutrient
74	308	266	273	38	28,200	0	31	13.0	3.1 gm Zn metal added
75	350	332	332	18	16,300		34	15.0	20.1 gm CuO + 3 gm Cu metal added
76	308	270	274	36	24,500	1.0	46	7.8	2 gm Zn metal added
77	395	383	385	11	13,400		30	10.9	50 gm CuO, 3 gm Cu metal + 0.25 mg Zn added
78	310	270	274	38	26,000	1.0	60	10.9	3.0 gm Zn added - large crystal run

-Continued-

TABLE XI (Continued)

Run No.	$T_B$ ( $^{\circ}F$ )	$T_M$ ( $^{\circ}C$ )	$T_I$ ( $^{\circ}C$ )	$\Delta T$ ( $^{\circ}C$ )	Pressure (psi)	LICH Conc (M)	Operating Time (days)	Average Growth Rate ml/s/day	Remarks
79	310	270	274	38	26,000	1.0	60	10.9	2.0m Zn added - large crystal run
80									Vessel leaked
81	313	299	295	16	22,500	1.0	20	10.3	1.5 Inch vessel - doping run
82	312	270	274	40	25,500	1.0	56	7.1	2.0 gm Zn added - large crystal run
83	313	296	290	20	25,000	0.75	29	7.4	1.5 Inch vessel - doping run
84	312	298	294	16	22,400	0.40	29	6.6	1.5 Inch vessel - doping run
85	312	271	273	40	25,200	1.0	56	5.7	2.0 gm Zn added - large crystal run

Crystal Growth (Continued)

When the number of possible variables in the system are considered it is obvious that the total number of runs made throughout the course of the contract could not possibly examine each one thoroughly. Furthermore, even reducing the number to what are probably the principal ones i.e. crystallization temperature,  $\Delta T$ , and  $Li^+$  concentration, it is obvious that the number of exploratory runs could not possibly be expected to yield exact curves which could be used to interpret the crystal growth results. At best these few runs, summarized in Table XI, can only be interpreted as trends and compared to those of other more documented hydrothermal crystal growth systems. By approximately selecting the runs so that all but one of the other parameters are approximately the same in value, some comparison and conclusions can be extracted.

For instance the growth rates for Runs No. 62 and 71 are 31 mils/day and 5.4 mils/day, respectively. If the difference in  $Li^+$  content is neglected at the other variables except temperatures are nearly the same. As would be expected the rate increases as the temperature increased just as in quartz<sup>9</sup> and ruby<sup>13</sup>.

Similarly comparing the runs made for the growth of 150 gm crystals (the last five in the table) with Run No. 74 some indication of  $Li^+$  effect on growth rate can be seen. The large crystals were grown with 1.0M  $Li^+$  ion present in the growth fluid. In Run No. 74 the  $Li^+$  was inadvertently omitted from the run. The temperature pressure, and  $\Delta T$  conditions were nearly identical for all runs so that the almost double rate in the case of zero lithium must be due to the impurity effect.

If now runs No. 62, 66, 68, and 70 are considered and the difference in  $Li^+$  content is disregarded, one can see the effect of  $\Delta T$  on growth rate as with quartz and ruby. The increase in rate with  $\Delta T$  appears to be linear (Figure 42 ).

The last five runs listed in Table XII also demonstrate the reproducibility in the process. The difference in rates in these five runs is only 2 mils/day. As can be seen from the data in this table and also Table XIII the crystals were grown under very similar conditions and the growth rates from top to bottom of the chamber is quite uniform. The data prove that the system can be run in a production manner for the manufacturing of large zinc oxide crystals.

The growth parameters found most suitable for the growth of these large crystals are summarized below.

Nutrient Temperature-----	312°C
Crystallization Temperature-----	274°C
$\Delta T$ -----	38°C
Pressure-----	25,000 psi
Base Concentration-----	6 M KOH
Lithium Concentration-----	1.0 M LiOH

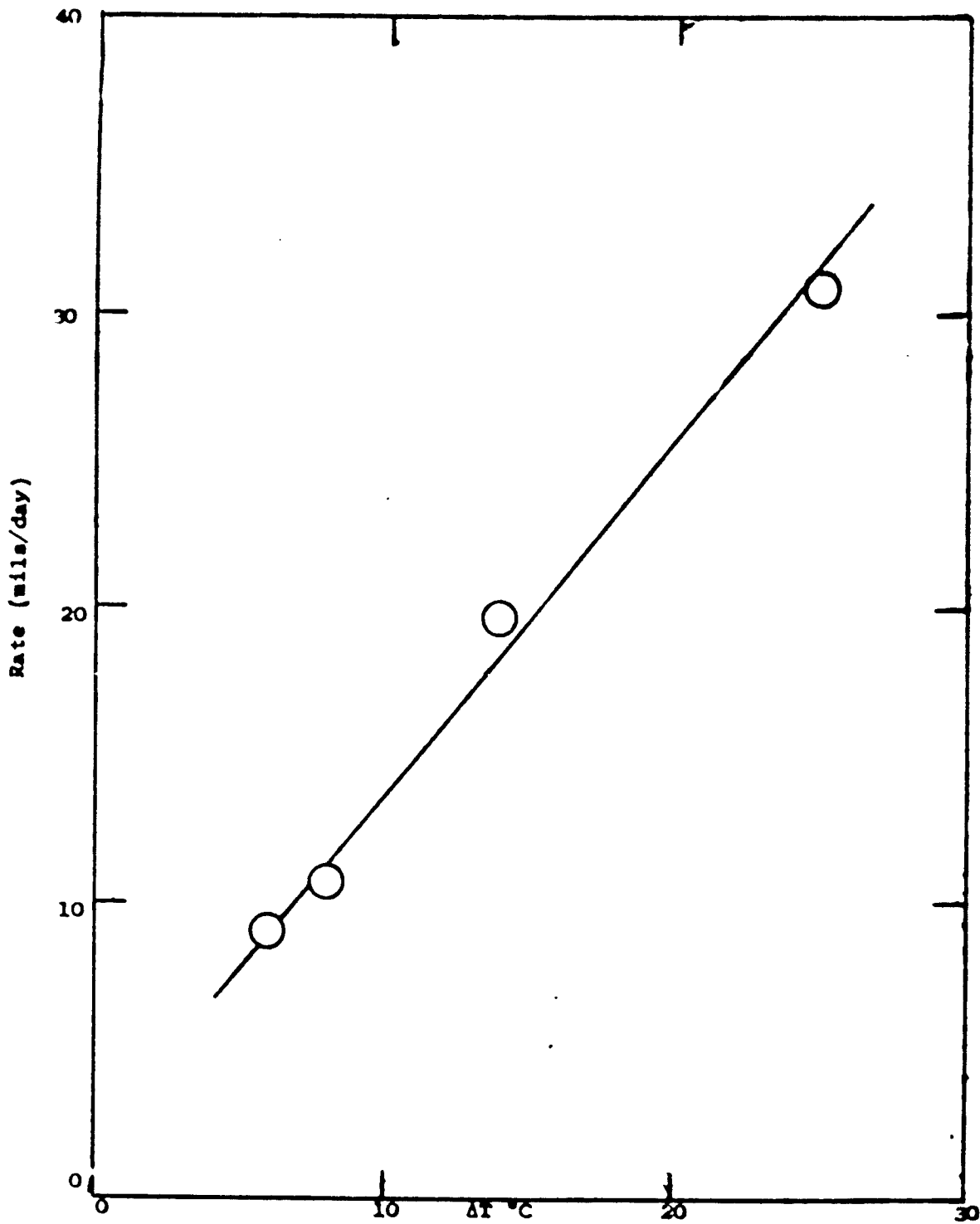


Figure 42 - Growth Rate vs  $\Delta T$  Neglecting  $\text{Li}^+$  Concentration Differences

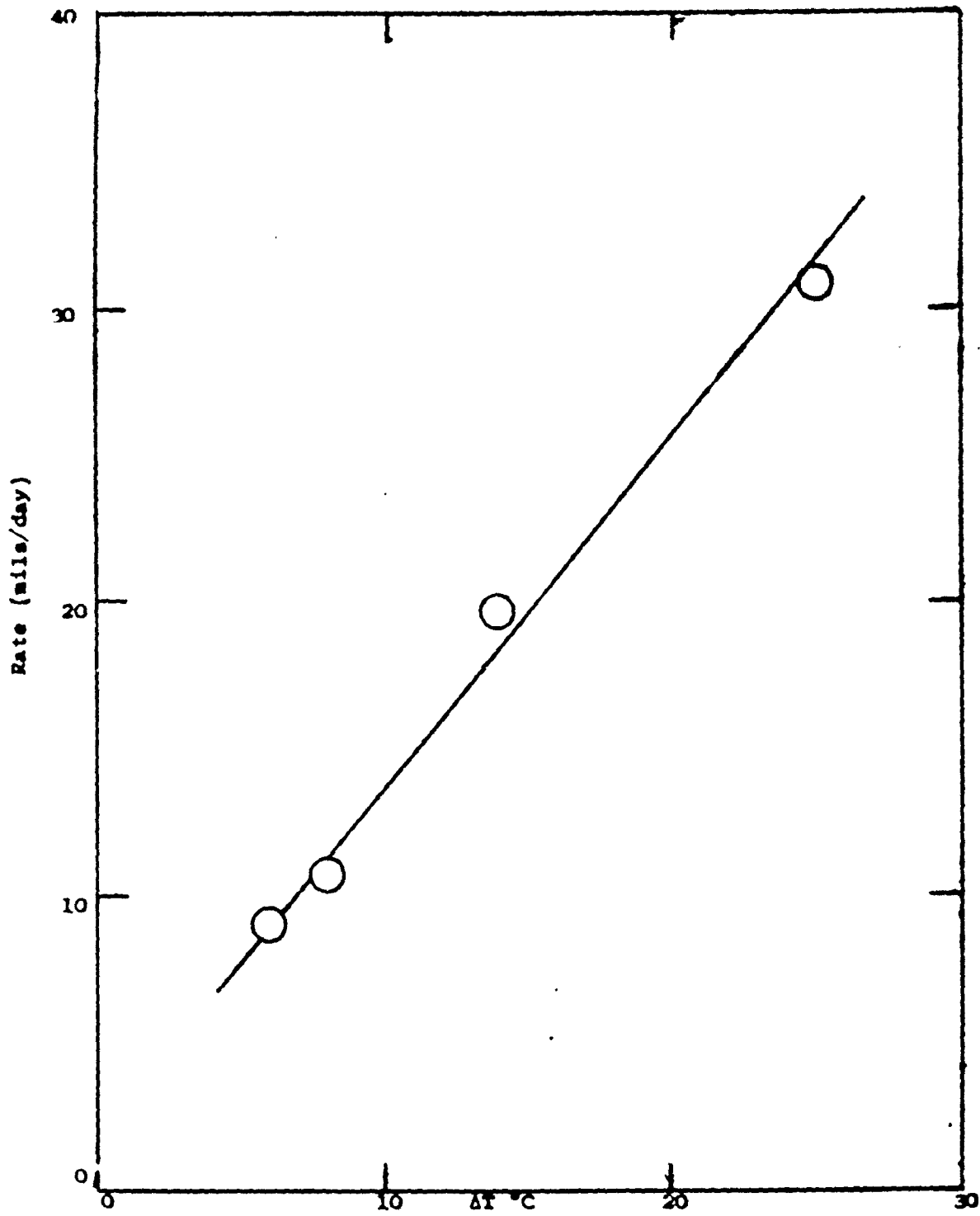


Figure 42 - Growth Rate vs  $\Delta T$  Neglecting  $\text{Li}^+$  Concentration Differences

TABLE XII

Summary of Selected High Pressure Crystal Growth Data

<u>Run No.</u>	<u>T cryst. (°C)</u>	<u>ΔT (°C)</u>	<u>P (psi)</u>	<u>Li<sup>+</sup> conc. (M)</u>	<u>&lt;0001&gt; Rate (mils/day)</u>
62	390	25	23000	0.2	31
64	388	12	19400	0.2	20
66	371	14	19700	1.0	16
68	369	8	19500	1.5	11
70	369	6	19800	1.0	9.4
71	277	22	33400	1.0	5.4
74	273	38	28200	0	12.0
81	295	16	22500	1.0	10.2
83	290	20	25000	0.75	7.4
84	294	16	22400	0.40	8.6
76	274	36	24500	1.0	7.8
78	274	30	26000	1.0	7.0
79	274	38	25500	1.0	6.3
82	274	40	25500	1.0	7.1
85	273	40	25200	1.0	5.7

TABLE XIII

SEED AND CRYSTAL DATA FOR RUN No. 58

<u>Crystal No.</u>	<u>Weight (grams)</u>		<u>Thickness (mils)</u>		<u>Growth Rate</u>	
	<u>Before</u>	<u>After</u>	<u>Before</u>	<u>After</u>	<u>(grams/day)</u>	<u>(mils/day)</u>
1A	13.2	25.1	90	137	.9	3
1B	2.2	3.0	--	---	.06	-
1C	25.7	38.7	148	213	.87	3
2A	10.1	19.3	76	119	.67	3
2B	26.2	37.1	174	226	.79	4
3A	5.1	12.3	42	77	.58	3
3B	18.6	29.8	107	155	.81	3
4A	10.6	13.3	329	430	.19	7
4B	18.3	28.3	104	148	.72	3
5A	18.7	31.1	73	123	.80	4
5B	6.2	12.8	49	82	.47	2
6A	20.0	28.2	135	171	.59	3
6B	7.2	14.0	55	80	.49	2

TABLE XIII (Continued)

SEED AND CRYSTAL DATA FOR RUN NO. 59

<u>Crystal No.</u>	<u>Weight (grams)</u>		<u>Thickness (mils)</u>		<u>Growth Rate</u>	
	<u>Before</u>	<u>After</u>	<u>Before</u>	<u>After</u>	<u>(grams/day)</u>	<u>(mils/day)</u>
1A	25.1	89.7	137	367	1.5	5
1B	3.0	10.7	---	---	---	-
1C	20.1	110.7	80	366	2.2	7
2A	12.3	61.5	77	366	1.2	7
2B	17.7	113.3	68	358	2.3	7
3A	29.8	102.8	155	465	1.7	7
3B	18.6	108.9	84	348	2.2	6
4A	28.3	97.2	148	391	1.6	6
4B	28.2	116.7	115	405	2.1	7
5A	13.3	33.0	430	787	1.0	
5B	16.9	98.4	62	342	1.9	7
6A	38.7	93.3	213	434	1.3	5
6B	17.4	84.0	82	297	1.6	5

SEED AND CRYSTAL DATA FOR RUN NO. 60

1	2.8	2.9	56	62	---	-
2	3.6	3.7	60	69	---	-
3	3.0	2.9	46	50	---	-
4	2.7	2.3	48	50	---	-

SEED AND CRYSTAL DATA FOR RUN NO. 62

1	1.6	19.7	40	383	---	31
2	2.8	14.0	88	347	---	24
3	1.0	5.5	48	182	---	12
4	1.4	2.9	56	140	---	8

TABLE XIII (Continued)

## SEED AND CRYSTAL DATA FOR RUN NO. 63

Crystal No.	Weight (grams)		Thickness (mils)		Growth Rate	
	Before	After	Before	After	(grams/day)	(mils/day)
1A	10.2	15.3	61	148	---	2.6
1B	5.4	27.5	74	110	---	2.3
2A	9.4	21.6	59	133	---	2.2
2B	2.9	5.7	62	126	---	1.9
2C	19.0	41.4	80	225	---	4.5
3A	11.5	23.8	75	153	---	2.3
3B	1.3	-----	--	---	---	---
3C	14.6	26.6	94	157	---	1.9
4A	16.0	34.1	79	164	---	2.7
4B	10.5	21.3	72	135	---	1.9
5A	11.1	21.4	67	134	---	2.0
5B	13.5	21.1	94	138	---	1.3
6A	12.9	22.8	77	127	---	1.5
6B	10.3	18.9	70	123	---	1.6

TABLE XIII (Continued)

## SEED AND CRYSTAL DATA FOR RUN NO. 64

Crystal No.	Weight (grams)		Thickness (mils)		Growth Rate	
	Before	After	Before	After	(grams/day)	(mils/day)
1A	17.7	3.1	65	452	----	22.8
1B	10.6	18.4	--	---	---	----
2A	13.7	64.3	81	409	---	18.8
2B	8.2	53.3	61	372	---	18.3
3A	2.8	11.0	63	191	---	7.5
3B	18.3	73.9	71	415	---	19.7
4A	11.2	56.2	64	301	---	19.9
4B	9.8	50.8	52	316	---	14.4
5A	7.7	48.9	44	258	---	12.6
5B	26.2	78.8	89	358	---	15.8
6A	12.5	43.7	79	278	---	11.7
6B	14.7	47.6	62	319	---	15.1

TABLE XIII (Continued)

SEED AND CRYSTAL DATA FOR ZIN NO. 65

<u>Crystal No.</u>	<u>Weight (grams)</u>		<u>Thickness (mils)</u>		<u>Growth Rate</u>	
	<u>Before</u>	<u>after</u>	<u>Before</u>	<u>After</u>	<u>(grams/day)</u>	<u>(mils/day)</u>
1A	21.4	90.1	131	472	1.81	9.0
1B	3.6	---	62	---	---	---
1C	15.2	60.1	106	336	1.18	6.1
2A	21.1	86.5	133	419	1.72	7.5
2B	5.6	24.7	130	360	0.50	6.1
3A	22.7	97.7	125	393	1.97	7.1
3B	21.3	70.3	133	336	1.29	5.3
4A	2.4	17.8	55	297	0.40	6.4
4B	18.7	78.5	122	428	1.57	8.1
4C	3.3	18.8	61	293	0.41	6.1
5A	11.3	62.7	81	343	1.35	6.9
5B	9.8	57.6	66	331	1.26	7.0
6A	4.6	30.1	57	275	0.67	5.7
6B	1.8	13.3	53	291	0.30	6.3
6C	7.7	46.4	68	332	1.02	7.0

TABLE XIII (Continued)

## SEED AND CRYSTAL DATA FOR RUN NO. 66

Crystal No.	Weight (grams)		Thickness (mils)		Growth Rate	
	Before	After	Before	After	(grams/day)	(mils/day)
1A	16.2	95.1	72	384	5.26	21.0
1B	17.7	32.5	--	---	0.99	----
1C	21.1	97.4	70	409	5.08	22.6
2A	14.4	74.9	68	326	4.04	17.2
2B	9.9	57.9	67	312	3.20	16.3
3A	9.0	61.5	58	296	3.50	15.9
3B	13.3	72.5	74	337	3.95	17.5
4A	11.0	29.1	191	362	1.21	11.4
4B	9.6	59.6	62	313	3.34	16.7
5A	7.6	48.1	44	236	2.70	12.8
5B	6.7	34.6	85	333	1.86	16.5
6A	5.4	27.1	84	284	1.45	13.3
6B	15.2	63.7	83	304	3.24	14.7

TABLE XIII (Continued)

SEED AND CRYSTAL DATA FOR RUN NO. 67

<u>Crystal No.</u>	<u>Weight (grams)</u>		<u>Thickness (mils)</u>		<u>Growth Rate</u>	
	<u>Before</u>	<u>After</u>	<u>Before</u>	<u>After</u>	<u>(grams/day)</u>	<u>(mils/day)</u>
1A	13.0	---	76	----	----	-
1B	2.4	---	60	----	----	-
1C	14.0	---	83	----	----	-
2A	12.6	26.1	73	93	0.750	1.11
2B	14.3	28.7	75	93	0.800	1.00
3A	14.9	30.9	63	79	0.889	0.89
3B	17.5	31.9	71	89	0.800	1.00
4A	10.1	17.8	65	75	0.428	0.56
4B	10.5	19.5	67	75	0.500	0.45
5A	6.0	11.2	69	76	0.288	0.39
5B	13.6	22.5	70	71	0.494	0.06
6	11.7	18.3	70	73	0.366	0.17

TABLE XIII (Continued)

SEED AND CRYSTAL DATA FOR RUN NO. 68

<u>Crystal No.</u>	<u>Weight (gms)</u>		<u>Thickness (mils)</u>		<u>Growth Rate</u>	
	<u>Before</u>	<u>After</u>	<u>Before</u>	<u>After</u>	<u>(grams/day)</u>	<u>(mils/day)</u>
1A	13.1	----	61	---	---	-
1B	2.2	5.0	137	229	0.19	6.1
1C	21.8	72.7	95	360	3.39	17.7
2A	11.2	----	59	---	---	-
2B	10.5	---	42	---	---	-
3A	19.8	70.3	73	305	3.36	15.5
3B	6.4	12.9	137	226	0.43	5.9
3C	14.7	61.6	68	259	3.12	12.7
4A	22.2	54.8	124	301	2.18	11.8
4B	24.1	59.6	112	271	2.37	10.6
5A	9.5	50.3	45	298	2.72	16.8
5B	5.1	12.1	92	173	0.47	5.4
5C	17.3	52.5	96	237	2.35	9.4
6	12.3	31.9	109	234	1.31	8.3

TABLE XIII (Continued)

SEED AND CRYSTAL DATA FOR RUN NO. 69

<u>Crystal No.</u>	<u>Weight (gms)</u>		<u>Thickness (mils)</u>		<u>Growth Rate</u>	
	<u>Before</u>	<u>After</u>	<u>Before</u>	<u>After</u>	<u>(grams/day)</u>	<u>(mils/day)</u>
1A	20.6	77.8	85	298	1.85	6.9
1B	18.9	82.9	84	297	2.06	6.9
2A	18.2	86.2	82	340	2.19	8.3
2B	9.0	26.3	111	293	0.56	5.9
3A	18.2	78.5	86	281	1.95	6.3
3B	19.0	81.4	79	295	2.01	7.0
4A	17.9	68.2	104	299	1.62	6.3
4B	24.4	76.6	123	348	1.69	7.3
5A	6.7	20.2	119	281	0.44	5.2
5B	16.5	73.9	73	282	1.85	6.7
6	9.9	37.1	89	260	0.88	5.5

TABLE XIII (Continued)

SEED AND CRYSTAL DATA FOR RUN NO. 77

<u>Crystal No.</u>	<u>Weight (grams)</u>		<u>Thickness (mils)</u>		<u>Growth Rate</u>	
	<u>Before</u>	<u>After</u>	<u>Before</u>	<u>After</u>	<u>(grams/day)</u>	<u>(mils/day)</u>
1A	4.3	12.4	65	185	0.51	7.5
1B	13.5	54.7	58	225	2.57	10.9
1C	3.8	10.9	63	170	0.44	6.7
2A	15.4	59.2	76	223	2.74	6.2
2B	17.1	81.5	52	250	4.02	12.5
2C	20.7	69.1	74	267	3.02	12.0
3A	14.0	51.5	59	223	2.34	10.2
3B	24.1	85.1	72	212	3.01	8.7
3C	2.1	5.5	54	131	2.12	4.8
4A	4.8	9.3	110	167	9.28	3.5
4B	19.3	61.3	68	178	2.62	6.8
4C	14.2	46.7	58	194	2.03	8.5
5A	22.3	55.3	93	240	2.06	9.2
5B	13.1	43.0	65	194	1.87	8.1
6	17.5	49.0	78	204	1.97	7.8

TABLE XIII (Continued)

SEED AND CRYSTAL DATA FOR RUN NO. 71

<u>Crystal No.</u>	<u>Weight (grams)</u>		<u>Thickness (mils)</u>		<u>Growth Rate</u>	
	<u>Before</u>	<u>After</u>	<u>Before</u>	<u>After</u>	<u>(grams/day)</u>	<u>(mils/day)</u>
1A	5.2	19.40	87	242	0.34	3.7
1B	19.9	91.58	113	347	1.71	5.6
2A	13.5	109.89	59	317	2.30	6.1
2B	18.4	87.10	74	329	1.63	6.1
3A	17.5	78.71	58	283	1.46	5.4
3B	15.7	71.61	76	297	1.33	5.3
4A	21.4	88.70	83	311	1.60	5.4
4B	20.3	89.31	72	242	1.64	4.1
5A	21.2	82.42	76	288	1.46	5.1
5B	13.6	65.37	69	284	1.23	5.1
6	4.0	12.00	83	187	0.19	2.5

TABLE XIII (Continued)

SEED AND CRYSTAL DATA FOR RUN NO. 72

<u>Crystal No.</u>	<u>Weight (gms)</u>		<u>Thickness (mils)</u>		<u>Growth Rate</u>	
	<u>Before</u>	<u>After</u>	<u>Before</u>	<u>After</u>	<u>(grams/day)</u>	<u>(mils/day)</u>
1A	12.9	51.70	45	215	2.16	11.3
1B	18.7	61.18	62	229	2.36	11.1
2A	0.6	0.58	71	79		
2B	4.8	16.50	50	205	0.65	9.7
2C	23.3	66.30	93	260	2.39	11.1
3A	14.6	46.10	72	215	1.75	9.5
3B	20.0	59.60	66	265	2.20	13.3
4A	10.2	26.75	80	214	0.92	8.9
4B	14.1	46.30	63	206	1.79	9.5
5A	14.7	40.53	73	199	1.38	8.4
5B	21.9	57.30	72	220	1.97	9.9
6	15.0	43.93	67	182	1.60	7.7

TABLE XIII (Continued)

SEED AND CRYSTAL DATA FOR RUN NO. 73

<u>Crystal No.</u>	<u>Weight (gms)</u>		<u>Thickness (mils)</u>		<u>Growth Rate</u>	
	<u>Before</u>	<u>After</u>	<u>Before</u>	<u>After</u>	<u>(gms/day)</u>	<u>(mils/day)</u>
1A	28.8	189.8	80	629	4.3	15.7
1B	12.6	137.1	63	576	3.6	14.7
2A	3.8	35.7	52	432	0.9	10.8
2B	20.2	149.0	95	512	3.7	11.9
2C	19.8	183.5	72	615	4.7	14.5
3A	22.0	135.5	85	492	3.2	11.6
3B	9.5	81.2	61	454	2.0	11.2
4A	11.2	75.8	86	440	1.8	10.1
4B	9.2	67.3	69	419	1.7	10.0
5A	26.2	109.3	95	395	2.4	8.6
5B	27.1	96.3	104	367	2.0	7.5

TABLE XIII (Continued)SEED AND CRYSTAL DATA FOR RUN NO. 74

<u>Crystal NO.</u>	<u>Weight (gms)</u>		<u>Weight (mils)</u>		<u>Growth Rate</u>	
	<u>Before</u>	<u>After</u>	<u>Before</u>	<u>After</u>	<u>(gas/day)</u>	<u>(mils/day)</u>
1A	10.4	112.9	27	435	3.3	12.8
1B	16.2	129.0	59	465	3.6	13.1
2A	20.2	133.8	67	477	3.7	13.2
2B	16.9	128.5	62	420	3.6	11.5
3A	15.6	90.8	78	435	2.4	11.5
3B	1.1	4.6	67	139		
3C	8.1	66.2	47	356	1.9	10.0
4A	15.4	105.4	58	483	2.9	13.7
4B	16.3	125.6	60	462	3.5	13.0
5A	13.5	102.2	61	410	2.9	11.2
5B	19.0	122.6	72	455	3.3	12.4
6	13.4	73.1	7	380	1.9	9.7

SEED AND CRYSTAL DATA FOR RUN NO. 75

Crystal No.	Weight (gms)		Thickness (mils)		Growth Rate	
	Before	After	Before	After	(gms/day)	(mils/day)
1A	9.8	98.0	71	635	2.6	16.6
1B	9.8	76.2	89	619	1.9	15.6
2A	13.8	134.6	72	712	3.6	18.8
2B	11.2	109.4	71	613	2.9	15.9
3A	11.8	95.6	91	702	2.5	18.0
3B	20.6	160.2	80	661	4.1	17.1
4A	6.4	53.1	70	593	1.4	15.4
4B	13.6	96.8	84	542	2.4	13.5
5A	9.2	60.0	90	572	2.1	14.2
5B	12.5	75.7	80	526	1.8	13.1
6A	9.6	52.2	88	435	1.3	10.2
6B	16.9	73.0	129	537	1.7	12.0

SEED AND CRYSTAL DATA FOR RUN NO. 76

1	29.5	152.7	107	456	2.7	7.6
2	26.0	151.8	96	455	2.7	7.8
3	27.8	148.9	98	448	2.6	7.6
4	14.3	128.3	50	451	2.5	8.7
5	13.0	106.3	63	419	2.0	7.7
6	15.8	117.1	68	390	2.2	7.7

APPENDIX II (Continued)

SEED AND CRYSTAL DATA FOR RUN NO. 77

Crystal No.	Weight (gms)		Thickness (mils)		Growth Rate	
	Before	After	Before	After	(gms/day)	(mils/day)
1A	7.2	95.5	67	581	2.94	17.1
1B	9.8	102.4	62	518	3.01	15.2
2A	9.6	105.0	59	535	3.18	15.9
2B	17.2	124.2	83	494	3.57	13.7
3A	17.3	106.4	110	501	2.97	12.9
3B	16.2	98.9	80	463	2.75	12.8
4A	11.5	56.4	87	378	1.50	9.7
4B	20.5	98.5	90	371	2.60	9.4
5A	9.0	41.4	66	272	1.08	6.9
5B	9.3	55.0	48	256	1.52	6.9
6A	15.9	37.3	96	243	0.71	4.9
6B	14.3	46.6	77	235	1.08	5.3

SEED AND CRYSTAL DATA FOR RUN NO. 78

1	24.8	195.9	75	498	2.85	7.0
2	29.1	210.5	101	547	3.14	7.4
3	17.6	198.2	54	539	3.01	8.1
4	21.8	180.0	70	466	2.64	6.6
5	25.6	175.4	75	460	2.50	6.4
6	16.4	161.3	53	448	2.42	6.6

SEED AND CRYSTAL DATA FOR RUN NO. 79

Crystal No.	Weight (gms)		Thickness (mils)		Growth Rate	
	Before	After	Before	After	(gms/day)	(mils/day)
1	22.8	197	57	409	2.64	6.5
2	29.1	194	97	546	2.50	6.8
3	32.9	215	91	549	2.76	6.9
4	19.2	185	60	489	2.52	6.5
5	23.3	180	79	458	2.38	5.7
6	16.6	161	55	426	2.18	5.6

SEED AND CRYSTAL DATA FOR RUN NO. 81

1	8.0	43.4	86	361	1.77	13.8
2	5.0	22.1	79	273	0.86	9.7
3	1.9	19.4	28	218	0.88	9.5
4	6.6	24.5	83	258	0.90	8.8
5	5.0	24.6	75	269	0.98	9.7

SEED AND CRYSTAL DATA FOR RUN NO. 82

1	11.2	130.8	45	447	2.14	7.2
2	12.6	121.0	56	432	1.94	6.7
3	20.5	144.1	82	492	2.21	7.3
4	21.3	196.9	57	520	3.14	8.0
5	25.3	199.7	72	450	3.11	6.8
6	20.8	167.0	61	429	2.61	6.6

TABLE III (continued)

SEED AND CRYSTAL DATA FOR RUN NO. 81

Crystal No.	Weight (gms)		Thickness (mils)		Growth Rate	
	Before	After	Before	After	(gms/day)	(mils/day)
1	6.6	34.3	90	320	.96	7.9
2	4.5	36.7	54	314	1.11	9.0
3	3.1	27.7	45	293	.85	8.0
4	3.7	24.2	44	239	.71	6.7
5	2.6	15.9	37	183	.46	5.0

SEED AND CRYSTAL DATA FOR RUN NO. 84

1	4.9	38.3	68	342	1.15	9.5
2	3.7	24.8	67	343	.73	9.5
3	4.3	31.7	66	370	.94	10.5
4	3.2	19.8	43	241	.57	6.8
5	3.1	14.2	69	263	.38	6.7

SEED AND CRYSTAL DATA FOR RUN NO. 85

1	19.6	159.6	56	392	2.50	6.0
2	42.1	192.1	128	452	2.68	5.8
3	31.8	159.9	95	397	2.29	5.4
4	16.6	164.2	52	400	2.64	6.2
5	23.7	158.9	76	406	2.40	5.9
6	28.1	151.0	77	340	2.19	4.7

### Crystal Growth Conditions

Aluminum added to prevent Ag corrosion-----	2.0 gm
Weight of Nutrient-----	1700 gm
Capacity of Silver Can-----	3.353 liter
Baffle Area-----	7.5%
Internal Fill-----	93%
External Fill-----	85%
Seeds-----	Highest quality hydrothermal plates available

Figure 43 shows the crystals grown in Run No. 76. The crystals shown here are typical of the size and quality of crystals grown using the conditions given above. The cracks and other defects visible in the photograph are at the interface of the grown crystal and the seed. When cut along the interface large slabs of crack-free material is obtained.

### 3.2.4 Silver Corrosion

From the very beginning of the hydrothermal crystal growth program the problem of silver corrosion appeared. Corrosion of the cans was a serious problem not only because of possible autoclave damage but also because the silver was chemically transported and subsequently deposited as crystalline silver. These silver crystals appeared on the can top, seed rack and were even included in the crystals. In addition to this, spectrographic analysis of clear crystals revealed the presence of silver in the crystal as an impurity, Table XIV. The effect of such silver on the electrical or acoustical properties of the crystals is not certain.

The approaches to reducing or eliminating this corrosion were undertaken until the solution was finally found. Landse and Koib<sup>14</sup> at Bell Telephone Laboratories working with essentially the same system and conditions for the growth of ZnO crystals had never encountered this silver corrosion problem. The only outstanding difference between the two systems was that the Bell Telephone Laboratories autoclaves have a permanent silver liner. The liner is fabricated from "vacuum melted oxygen-free silver," hereafter referred to as VMOF silver. The silver used for the can, baffle, etc. at Airtron was high purity silver.

VMOF silver was purchased and in the first run in which it was used there was little or no silver attack (Run No. 63.) In this run, however, it was quite clear that the  $\Delta T$  was low as seen from the (in growth rate of 1.2 mils/day). In the following runs where a higher  $\Delta T$  was employed the extent of silver corrosion with VMOF silver was as great as it had been with the fine silver.



Figure 43 - High Quality Crystals from Run No. 76

TABLE XIV

SPECTROGRAPHIC ANALYSIS FOR HYDROTHERMALLY GROWN ZnO

Ledoux & Co. Analysis No. 844547

	<u>Crystal from Run No. 55</u> <u>(Regular Can)</u>	<u>Crystal from Run No. 59</u> <u>(Gold Plated Can)</u>
Silver	0.03%	0.003%
Aluminum	0.005%	0.005%
Gold	ND < 0.01%	ND < 0.01 %
Zinc	High	High

Other elements not detected.

High - indicates 10 - 100 %

ND < - not detected less than.

Crystal Growth (Continued)

The second approach to eliminating the silver corrosion was to replace silver with another noble metal. Since platinum or gold would be excessive in cost an alternate approach of gold plating the internal surfaces of the cans was used. Nu-Line Industries Inc. + electrochemically gold plated the can, baffle and seed rack with approximately 0.2 mils thick gold. This can was used in Run No. 59.

The crystals grown on the better seeds in this run were very high quality crystals showing little or no flawing and were completely transparent. The outstanding feature of the crystals was the color of the crystal in the  $\langle 0001 \rangle$  direction. Instead of the normal buff color, this part of the crystal was emerald green and as a result the whole crystal appeared to be that color. The  $\langle 0001 \rangle$  side of the crystal was the usual pale green.

Examination of the ladder, baffle and walls of the can revealed that almost all the gold plating on the baffle and ladder had been dissolved away, but that the walls had not been attacked to any extent. The nature or cause of this dissolution of gold is not known. Why the dissolution was limited to the ladder and baffle is also unknown. There was no evidence of gold deposits anywhere as had happened in the case of the silver corrosion. There was also no evidence of silver attack.

Considering the gold dissolution and appearance of a new green color to the crystal, it seemed obvious that the two were related. However, x-ray fluorescence and spectrographic analyses were performed on a sample of this material, and also a crystal from Run No. 59 for comparison, and neither technique revealed the presence of gold in either sample. The limits of detection were about 1,000 ppm for the x-ray fluorescence and 100 ppm for the spectrographic analysis. The data from the spectrographic analysis are presented in Table XIV. Aside from not detecting any gold, the effectiveness of the gold plating is shown in order of magnitude decreases in the silver content.

The cause and solution to the problem was indicated from several observations:

1. Increases the size of the system, increases the extent of the silver attack
2. The larger the  $\Delta T$ , the greater the reaction
3. Use of oxidizing agents in other hydrothermal systems ~~temporarily~~ increased the silver attack

+ Nu-Line Industries Inc., 1015 South Sixth Street, Minneapolis, Minnesota 55415

Considering the above facts it was clear that a reducing agent should be tried. Zinc metal was chosen since it should be more reactive toward oxidizing agents than silver and when oxidized would form  $Zn^{2+}$  ions which are already present in the solution. Run No. 71 was the first run in which a small piece ( $\sim 2-3$  gm) of zinc metal was sealed in the nutrient section of the can. There was no trace of silver deposit or corrosion anywhere in the system. In every run after that to which zinc metal was added there was no corrosion.

The mechanism by which the silver corrosion appears is as follows. The initial attack on silver is caused by oxygen dissolved in the KOH solution and in the air entrapped in the silver can during its closure. In the nutrient zone, the hottest part of the can, a soluble silver complex is formed which is convectively transported to the cooler regions of the can. Because of thermal disturbance of the equilibrium a disproportionation reaction occurs which yields metallic silver and a silver complex of higher oxidation number.

Similar thermally dependent disproportionation reactions are popularly used for the vapor phase growth of III-V compounds. The lack of thermodynamic data for the possible silver species at the elevated pressures and temperatures makes it impossible to assign definite oxidation states to the silver in the transporting complex ions. In this system the silver was principally deposited in the two regions where the temperature drops are greatest, at the baffle plate (its purpose is to divide the fluid into two temperature regions), and the top of the can where the heat loss to the ambient is greatest.

This proposed mechanism explains the initial silver attack, its continued transport during the course of a run, and the observations which lead to using a reducing agent.

The added zinc metal is effective since it probably reacts with the enclosed oxygen and water to form zinc (II) ions and hydroxide ions, both of which are already present in the solution. Any zinc metal in excess of the amount that is not oxidized by the oxygen reacts with the fluid to form hydrogen.

The solving of silver corrosion in this system is important since it also provides a possible solution to noble metal corrosion in other systems. For example although the silver attack in the hydrothermal ruby system is not as extensive, the addition of metallic aluminum completely eliminates any trace of silver deposits.<sup>15</sup> Yttrium metal should also eliminate the silver attack in the hydrothermal growth of  $Y_3Fe_5O_{12}$ .

4.1 Resistivity Measurement Technique

The apparatus used to measure electrical resistivity was similar to that used by Kolb and Laudise,<sup>16</sup> using the V-I technique. In this technique a measured d.c. current is made to pass through the sample and the voltage drop is measured, the sample resistivity is calculated from the voltage, current, and dimensions of the sample.

The circuit diagram of the set-up is shown in Figure 44. The jig for holding the sample was enclosed in a metal box to provide electrical and light shielding of the sample during measurement. The jig for holding the sample was FF-91 formica and the sample contacts were a brass pin and gold foil. The direct current source was provided by four 7 v batteries connected in series. The current and voltage were measured by means of two meters: 1) Keithley Model 150A Microvolt Ammeter for small currents and voltages; and 2) a Triplet Model 800 multipurpose meter for the large currents and voltages. By appropriate interchanges of the meters, the entire range of resistivities ( $10^{-3}$  -  $10^{12}$  ohm cm) could be measured.

The sample was prepared by machining a parallelepiped typically about 7mm x 2.5mm x 1mm. The ends were then abraded and two opposing sides coated with a Hg-In alloy for contacts.

The resistivity measurements are presented in Tables XV and XVI. In some cases a large photo effect has been noticed. In all cases where this has appeared the reported measurement was not made until after photo effects had decayed (usually more than 24 hours). This photo effect is not new. It is interesting that in some crystals a large effect is noted; whereas, in others there is little or no effect.

4.2 Doping

4.2.1 Lithium

As already pointed out it is fortunate that the  $Li^+$  ion in ZnO acts both as an impurity improving crystal quality and to generate an acceptor center so that compensation may be attained. The majority of runs made during the lifetime of the contract all employed lithium as dopant with the exception of an indium doped run and several copper doped runs.

Having obtained good sound crystals of reasonable size, resistivity samples of both the  $c^+$  side and  $c^-$  side were cut from a crystal of each run. In general the crystals from the  $c^+$  side were of high resistivity i.e.  $>10^4 \Omega \text{cm}$ . On the other hand the  $c^-$  side was of low resistivity  $<10 \Omega \text{cm}$ . The difference is obvious due to the way in which the  $Li^+$  and zinc are incorporated just as the anisotropy in growth rate, etc. Spectroscopic analysis for lithium on both sides of the crystal, however, did not reveal sufficiently large difference in concentration to account for the orders of magnitude differences in resistivity.

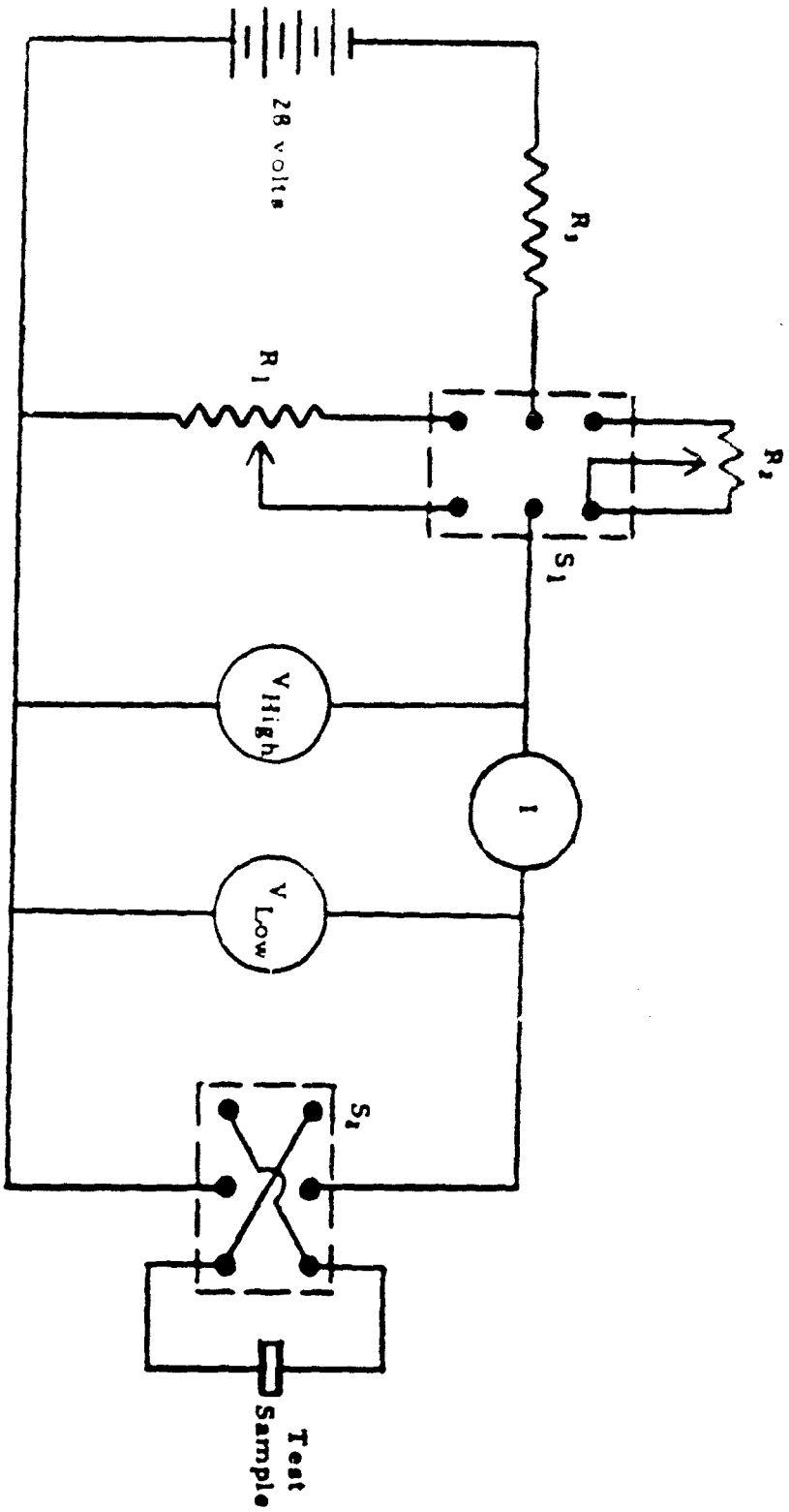


Figure 44 - Resistivity Measurement Circuit Diagram

TABLE XV  
RESISTIVITY MEASUREMENTS

<u>Crystal</u>	<u>Side</u>	<u>Shape</u>	<u><math>\rho(\Omega\text{-cm})</math></u>
39	c <sup>+</sup>	Cylindrical	$8.6 \times 10^7$
39	c <sup>+</sup>	Cylindrical	$7.9 \times 10^9$ *
39	c <sup>-</sup>	Rectangular	$4.4 \times 10^{-2}$
39	c <sup>-</sup>	Rectangular	$4.2 \times 10^{-4}$ *
41	c <sup>+</sup>	Rectangular	$1.4 \times 10^8$
41	c <sup>+</sup>	Cylindrical	$2.4 \times 10^8$
41	c <sup>+</sup>	Rectangular	$9.6 \times 10^6$ * *
41	c <sup>-</sup>	Rectangular	$1.9 \times 10^{-1}$
45	c <sup>+</sup>	Rectangular	$2.6 \times 10^7$
45-4	c <sup>+</sup>	Rectangular	$4.3 \times 10^7$
45-4	c <sup>+</sup>	Rectangular	$6.7 \times 10^9$ *
45-2	c <sup>-</sup>	Rectangular	$6.4 \times 10^{-1}$
48-1	c <sup>+</sup>	Rectangular	$2.6 \times 10^4$
48-1	c <sup>-</sup>	Rectangular	$2.1 \times 10^{-1}$
50-6	c <sup>+</sup>	Rectangular	$2.0 \times 10^6$
50-6	c <sup>+</sup>	Rectangular	$8.2 \times 10^6$
51-5	c <sup>+</sup>	Rectangular	$3 \times 10^8$

\* After heat treating in air at 600°C for 50 hours.  
\* \* Measured perpendicular to c-axis.

TABLE XVI

## RESISTIVITY MEASUREMENTS

Crystal No.	Crystal Orientation	Pressure (psi)	T <sub>cryst</sub> (°C)	Growth Rate (mil./day)	LiOH Conc. (M)	Resistivity (ohm cm)		AVT (ohm cm)	Photo Effects
						Before Heat Treat	After Heat Treat		
59-3B	c <sup>+</sup>	9,000	313	6.0	1.0	$1.05 \times 10^4$	$1.45 \times 10^6$	$1.4 \times 10^2$	Low
59-4B	c <sup>-</sup>	9,000	313	6.0	1.0	$4.6 \times 10^{-2}$	$2.0 \times 10^3$	$4.4 \times 10^1$	Low
62-2A	c <sup>+</sup>	23,000	390	24.0	0.2	$1.9 \times 10^5$	$3.45 \times 10^5$	$1.8 \times 10^0$	Low
62-3	c <sup>-</sup>	23,000	390	24.0	0.2	$1.3 \times 10^{-1}$	$5.2 \times 10^1$	$4.1 \times 10^2$	None
63-4A	c <sup>+</sup>	9,000	317	2.7	1.0	$1 \times 10^3$	$3 \times 10^5$	$3 \times 10^2$	Low
64-5A	c <sup>+</sup>	19,400	388	12.6	0.2	$2.5 \times 10^7$	$2.1 \times 10^5$	$8 \times 10^{-3}$	High
64-2B	c <sup>-</sup>	19,400	388	12.6	0.2	$4.9 \times 10^{-1}$	$1.6 \times 10^1$	$3.3 \times 10^1$	Low
65-4B	c <sup>+</sup>	9,700	316	8.1	1.0	$7.5 \times 10^8$	$2.5 \times 10^3$	$3 \times 10^{-4}$	High
65-4B	c <sup>-</sup>	9,700	316	8.1	1.0	$9.6 \times 10^{-1}$	$1.2 \times 10^0$	$1.3 \times 10^0$	None
66-5B	c <sup>+</sup>	19,700	371	16.5	1.0	$1.6 \times 10^{10}$	$1.7 \times 10^3$	$1 \times 10^{-5}$	High
66-5B	c <sup>+</sup>	19,700	371	16.5	1.0	$9.2 \times 10^{-4}$	$4.8 \times 10^0$	$5.25 \times 10^3$	None
67-5A	-	19,500	389	-----	1.0	$4.4 \times 10^1$	$7.2 \times 10^2$	$1.6 \times 10^1$	None
68-6	c <sup>+</sup>	19,500	390	8.3	1.5	$1.8 \times 10^4$	$9.8 \times 10^3$	$5.4 \times 10^1$	Low
68	c <sup>-</sup>	19,500	390	8.3	1.5	$6.1 \times 10^{-2}$	$6.3 \times 10^4$	$1.0 \times 10^4$	None

No. 0.1 M In(OH)<sub>3</sub> added to solvent

TABLE XVI (Continued)

Crystal No.	Crystal Orientation	Pressure (psi)	T <sub>cryst</sub> (°C)	<0001> Growth Rate (mils/day)	LiOH Conc. (M)	Before Heat Treat (ohm cm)	After Heat Treat (ohm cm)	AHT/BHT	Photo Effects
69-3A	c <sup>+</sup>	9100	320	1.0	6.3	5 x 10 <sup>8</sup>	1.24 x 10 <sup>5</sup>	2.48 x 10 <sup>-3</sup>	Very high
69-2A	c <sup>-</sup>	9100	320	1.0	8.3	4.6 x 10 <sup>-2</sup>	4.87 x 10 <sup>0</sup>	1.06 x 10 <sup>2</sup>	None
70-4C	c <sup>+</sup>	19800	389	1.0	8.5	4.2 x 10 <sup>7</sup>	1.33 x 10 <sup>8</sup>	3.7 x 10 <sup>3</sup>	High
70-2C	c <sup>-</sup>	19800	389	1.0	12.0	4.2 x 10 <sup>-2</sup>	7.84 x 10 <sup>0</sup>	1.86 x 10 <sup>2</sup>	None
Zn { 71-3A	c <sup>+</sup>	33400	275	1.0	5.4	9.84 x 10 <sup>-1</sup>	3.24 x 10 <sup>1</sup>	3.3 x 10 <sup>4</sup>	Low
	c <sup>-</sup>	33400	275	1.0	5.4	3.6 x 10 <sup>-1</sup>	1.06 x 10 <sup>6</sup>	2.8 x 10 <sup>6</sup>	None
72-2B	c <sup>+</sup>	21300	284	Cu	9.7	9.3 x 10 <sup>1</sup>	9.3 x 10 <sup>2</sup>	1 x 10 <sup>1</sup>	None
72-2B	c <sup>-</sup>	23300	284	Cu	9.7	1.44 x 10 <sup>-1</sup>	2.99 x 10 <sup>0</sup>	2.08 x 10 <sup>1</sup>	None
73-3A	c <sup>+</sup>	15700	333	Cu	11.3	4.46 x 10 <sup>3</sup>	2.63 x 10 <sup>3</sup>	3.89 x 10 <sup>-1</sup>	Slight
73-3A	c <sup>-</sup>	15700	333	Cu	11.9	1.01 x 10 <sup>0</sup>	3.34 x 10 <sup>0</sup>	3.31 x 10 <sup>0</sup>	None
74-3A	c <sup>-</sup>	28200	270	0	12.0	1.83 x 10 <sup>-1</sup>	2.61 x 10 <sup>-1</sup>	1.423 x 10 <sup>0</sup>	None
74-6	c <sup>+</sup>	28200	270	0	12.0	4.6 x 10 <sup>0</sup>	1.37 x 10 <sup>1</sup>	3.4 x 10 <sup>0</sup>	None
75-3A	c <sup>+</sup>	16900	332	Cu	15.0	1.9 x 10 <sup>3</sup>	1.06 x 10 <sup>3</sup>	5.6 x 10 <sup>-1</sup>	None
75-3A	c <sup>-</sup>	16900	332	Cu	15.0	1.04 x 10 <sup>1</sup>	2.77 x 10 <sup>1</sup>	2.66 x 10 <sup>0</sup>	None
76-3	c <sup>+</sup>	24500	272	1.0	7.8	5.58 x 10 <sup>9</sup>	1.68 x 10 <sup>4</sup>	3.01 x 10 <sup>-6</sup>	None
76-3	c <sup>-</sup>	24500	272	1.0	7.8	1.46 x 10 <sup>-1</sup>	2.10 x 10 <sup>3</sup>	1.44 x 10 <sup>4</sup>	None
77-6	c	13400	384	Cu	10.9	3.9 x 10	Sample Decapitated	-----	None

TABLE XVI (Continued)

Crystal No.	Crystal Orientation	Pressure (Psi)	Cryst Temp (°C)	<0001> Growth Rate (mils/day)	LiOH Conc (M)	Before Heat Treat (ohm cm)	After Heat Treat (ohm cm)	$\rho_{MIT}$	Photo Effects
77-6	c <sup>-</sup>	13400	384	Cu	10.9	$4.1 \times 10^1$	$7.47 \times 10^1$	$1.82 \times 10^0$	None
81-9	c <sup>+</sup>	22500	297	1.0	10.2	$1.5 \times 10^5$			Low
83-2	c <sup>+</sup>	25000	293	0.75	7.4	$6.3 \times 10^3$	$2.7 \times 10^5$	$4.28 \times 10^1$	Low
83-2	c <sup>-</sup>	25000	293	0.75	7.4	$5.1 \times 10^{-2}$	$9.44 \times 10^0$	$1.86 \times 10^2$	None
84-2	c <sup>+</sup>	22400	296	0.4	8.6	$2.7 \times 10^8$	$6.0 \times 10^4$	$2.2 \times 10^{-4}$	1 *
84-2	c <sup>-</sup>	22400	296	0.4	8.6	$2.2 \times 10^{-2}$	$2.4 \times 10^1$	$1.1 \times 10^{-3}$	None

Doping and Electrical Properties (Continued)

As the contract proceeded and the measurement was refined, heat treatment of the resistivity samples was also carried out. The purpose of the heat treatment was to diffuse out or to locate on lattice sites the residual interstitial zinc or lithium. In any case In-Hg amalgam was removed from the sample which was then placed on inert substrate. The sample was then heated in air for 50 hours at 800°C. After this time the resistivity was remeasured.

Until the silver corrosion problem was solved the samples would exhibit very large photo conductivity effects on the  $c^+$  side. Analysis of the crystals has shown that these crystals contained significant amounts of silver and the photo conductivity has been attributed to the presence of such silver. Once the corrosion was eliminated very little or no photo effects were noted. Also of interest is that the  $c^+$  side of crystals grown during the silver corrosion period were buff colored while those which were silver free were colorless. The  $c^-$  side in all cases was pale green.

Throughout the course of the work attempts were made to relate the resistivity of the crystal to any and all of the growth parameters. Since Laudise and Kolb<sup>16,17</sup> had shown a relationship of resistivity after heat treatment to lithium content this same attempt was made to crystals grown during this work. No relationship was established. Only in the case where lithium was omitted from the fluid (Run No. 74) was a significant difference in resistivity noted. Otherwise there is no apparent relationship of resistivity to lithium content. As stated previously the growth conditions for most runs varied quite significantly making it difficult to compare results. Work performed at the end of the contract and since that time may help shed some light on the reasons for being unable to relate and interpret the resistivity results.

Dr. Hickernell of Motorola, Electronics Division, Scottsdale, Arizona was in receipt of several samples of ZnO. Among these were one lithium doped sample (76-5) and two copper doped samples (73 and 75-4B). Dr. Hickernell measured the resistivity of this sample (76-5) and found it to be  $0.5-2 \times 10^6 \Omega \cdot \text{cm}$  which is about two orders of magnitude greater than an Airtron measurement on crystal 76-2. While somewhat disturbing, the difference is not surprising as will be discussed in section 4.3. Dr. Hickernell also attempted to measure the mobility of this sample but its resistivity was too high for a good measurement. Acoustic velocity measurements were also made on these samples and are summarized in Table XVII.

#### 4.2.2 Copper Doping

Copper, like lithium, serves to produce acceptor centers which can increase the crystal resistivity. The objective in attempting copper doping in the ZnO crystal growth was to produce crystals in the  $10^3 - 10^5 \Omega \cdot \text{cm}$  region.

TABLE XVII

ACOUSTIC VELOCITY MEASUREMENTS  
OF COPPER DOPED ZINC-OXIDE

Sample Designation	Propagation Mode	Propagation Direction	Particle Displacement	Velocity Value ( $\times 10^5$ cm/sec)
73	Shear	// C	IC	2.747 $\pm$ .002
	Shear	// C	IC	2.733 $\pm$ .005
75-48	Shear	IC	IC	2.794 $\pm$ .005
	Shear	// C	IC	2.797 $\pm$ .005
	Shear	I	IC	2.802 $\pm$ .002
76-5	Shear	IC	// C	2.835 $\pm$ .002

### Doping and Electrical Properties (Continued)

The first run, No. 72, was successful in producing lower resistivity material. In this run 24 grams of CuO were added to the nutrient. The complete operating conditions for all the copper doped runs are presented in Table XI. The growth temperature in this run was 284°C with a  $\Delta T$  of 24°. After the runs there was evidence of CuO crystals in the growth chamber indicating that the solution had been saturated, thus limiting the amount of copper ions available for incorporation into the ZnO crystals. The resulting crystals were fairly high quality, with the  $c^+$  side having a pale brown color and the  $c^-$  side being dark green.

The resistivity of the  $c^+$  side was 100- $\Omega$ -cm and on heat treatment increased to 1000- $\Omega$ -cm.

In order to increase the amount of copper in the next run, the crystallization temperature was increased from 284°C to 333°C. Two such runs (Nos. 73 and 75) were made in which 30.0 grams of CuO (No. 73) and 26.1 grams of CuO and 3 grams of copper metal (No. 75) were added to the nutrient. The crystals were high quality and had resistivities of about 1000- $\Omega$ -cm which did not increase substantially on heat treatment.

The crystallization temperature in Run No. 77 was increased to 384°C trying to raise the resistivity to  $10^4$ - $\Omega$ -cm or greater. In the run, the crystal quality deteriorated to the point where it was difficult to find a section sufficiently large to fabricate a resistivity sample. A piece measured  $4 \times 10^3$ - $\Omega$ -cm which on heat treatment completely decrepitated. Thus it appeared that further increasing of the crystallization temperature would not increase the degree of compensation and the crystal quality would probably continue to degenerate.

Dr. Hickernell measured the resistivities in the low  $10^3$ - $\Omega$ -cm range for the crystals from runs Nos. 73 and 75 which were in agreement with the Airtron measurements. Dr. Hickernell also measured the mobility of these two samples and obtained values of 161  $\text{cm}^2/\text{volt sec}$  and 136  $\text{cm}^2/\text{volt sec}$  for Nos. 73 and 75 respectively. Airtron's mobility measurement on the heat treated sample from run No. 72 was 152  $\text{cm}^2/\text{volt sec}$ . Dr. Hickernell determined the electromechanical coupling factor,  $K_{15}$ , for crystals 75-6 and obtained a value of 0.26 which he compared with values of 0.24 - 0.28 which we had measured on lithium doped crystals.

#### 4.2.3 Indium Doping

In Run No. 67.0 gm In(OH)<sub>3</sub> was added in an effort to lower the resistivity, hopefully to  $10^3$   $\Omega$ -cm or less... Indium has been shown by Kolb and Laudise<sup>16</sup> to be a donor type impurity in ZnO. A lowering of resistivity was produced in two runs at Bell Telephone Laboratories by adding In(OH)<sub>3</sub> to normal growth solution. The results of Run No. 67 were quite surprising. Little or no growth occurred in

### Doping and Electrical Properties (Continued)

the  $\langle 0001 \rangle$  direction, however, lateral growth in the  $\langle 10\bar{1}0 \rangle$  and  $\langle 11\bar{2}0 \rangle$  direction was very extensive. In addition to the lack of a growth in the  $\langle 0001 \rangle$  direction both sides of the seed were covered with spontaneously nucleated crystals. The spontaneously nucleated crystals were peculiar for two reasons. The usual habit or form of spontaneously nucleated crystal in the hydrothermal system is a heximorphic nugget with nearly equal width and height. In this run, however, the crystals were much like those obtained from molten salt crystallization which have the plate like habit with  $\langle 0001 \rangle$  faces forming the major surfaces. This habit was undoubtedly also another manifestation of impurities changing crystal growth rates.

The second peculiarity of the spontaneous nucleation was that the crystals occurred principally over the original seed crystals and were not over any of the new lateral growth, Figure 45. Figure 46 shows another crystal from this same run but with the spontaneously nucleated crystals scrapped away from the surface. The extent of lateral growth and lack of  $\langle 0001 \rangle$  growth is clearly shown. The lateral growth appeared to be of quite high quality and was a pale blue-green color. The spontaneously nucleated plates were also of the same color.

In addition to the spontaneous nucleation on the seeds, the walls of the can, ladder parts and top were blanketed by a deposit of the ZnO plates.

#### 4.3 Run Uniformity and Crystal Uniformity

Considering the scatter of resistivity results from run to run the question arose as to the uniformity of the doping of crystals within a run and this uniformity within a single crystal.

Resistivity samples from four of five crystals of run Nos. 83 and 84 were cut and the resistivity measured. All samples were heat treated, and measured. Some of these have undergone three heat treatments. The results are presented in Table XVIII.

As can be seen from the data the virgin crystals show a wide range of resistivity of  $10^4 \Omega \text{ cm}$  or greater. Upon heat treatment, however, this spread is reduced to one order of magnitude. Subsequent heat treatment up to three show less and less change in resistivity with each heat treatment cycle.

It appears that the initial resistivity cannot be reasonably controlled by growth conditions. Each subsequent heat treatment, either by diffusion or by site incorporation of impurities,  $\text{Li}^+$ , and zinc tends to bring the sample to a final or "equilibrium" <sup>17</sup> resistivity.

Similarly a crystal, No. 84-3, was made into 12 samples to construct a resistivity map of the crystal. Figure 47 shows the map and values. As with the individual crystals there is a large spread

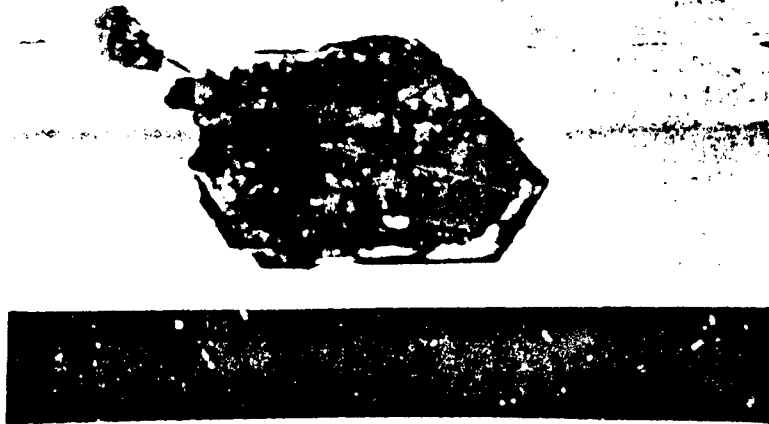


Figure 45 - Crystal from Run No. 67 Showing Spontaneous Nucleation and Lateral Growth

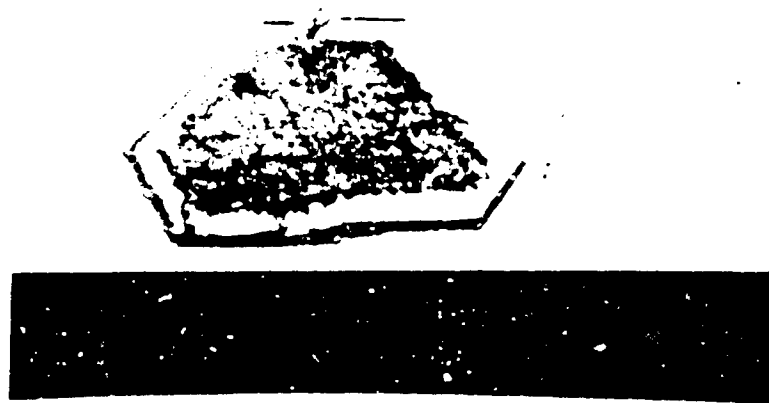


Figure 46 - Crystal from Run No. 67 with Spontaneous Nucleation Removed

TABLE XVII

Resistivity Change on Subsequent Heat Treatments

<u>Crystal No.</u>	<u>Virgin</u>	<u>H.T. No. 1</u>	<u>H.T. No. 2</u>	<u>H.T. No. 3</u>
83-2 c <sup>+</sup>	$4.9 \times 10^3$	$4.5 \times 10^3$	$5.3 \times 10^3$	$2.9 \times 10^3$
83-3 c <sup>+</sup>	$3.9 \times 10^2$	$3.8 \times 10^4$		
83-4 c <sup>+</sup>	$3.8 \times 10^4$	$6.1 \times 10^4$		
83-5 c <sup>+</sup>	$9.1 \times 10^5$	$3.0 \times 10^4$	$4.4 \times 10^3$	$1.9 \times 10^3$
84-2 c <sup>+</sup>	$2.7 \times 10^8$	$6.0 \times 10^4$	$2.6 \times 10^4$	$1.3 \times 10^4$
84-3 c <sup>+</sup>		$3.2 \times 10^5$		
84-4 c <sup>+</sup>	$6.5 \times 10^4$	$8.9 \times 10^4$		
84-5 c <sup>+</sup>	$7.2 \times 10^4$	$1.8 \times 10^4$	$5.4 \times 10^3$	$2.8 \times 10^3$

84-3 c<sup>+</sup>  
Resistivity ( $\Omega$ cm)

	<u>Virgin</u>	<u>First H.T.</u>
A	$\infty$	$3.2 \times 10^5$
B	$3.8 \times 10^4$	$1.7 \times 10^5$
C	$2.8 \times 10^4$	$1.2 \times 10^5$
D	$3.9 \times 10^7$	$1.5 \times 10^5$
E	$1.3 \times 10^4$	$4.5 \times 10^4$
F	$4.6 \times 10^5$	$1.3 \times 10^5$
G	$5.3 \times 10^5$	$1.2 \times 10^5$
H	$1.6 \times 10^5$	$5.8 \times 10^4$
I	$4.6 \times 10^4$	$1.5 \times 10^5$
J	$4.0 \times 10^4$	$2.1 \times 10^5$
K	$2.5 \times 10^5$	$8.4 \times 10^4$
L	$6.7 \times 10^4$	$1.6 \times 10^4$

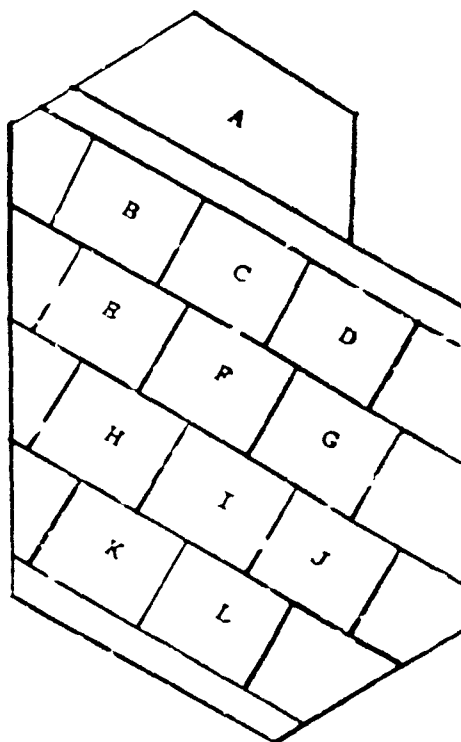


Figure 47 - Resistivity Map Crystal No. 84-3

Doping and Electrical Properties (Continued)

in resistivity for the virgin crystal. On heat treating the spread was reduced to about one order of magnitude.

The final run made under the contract was No. 85 which was a large crystal growth run. Zinc oxide for nutrient preparation had been from the same lot throughout the contract up to this run in which a new lot was used. The crystals grown using this new lot were green in color compared to the previous colorless material.

An analysis of both lots was obtained but no detectable differences were noted. Table XIX. Even though the ZnO is of high purity close examination of this material showed that it contained many fine foreign particles and several large pieces of metallic chips.

It appears that commercially available zinc oxide powder cannot form the basis of a process where the addition of small amounts of impurities can radically affect the electrical properties of the crystal. It also appears that no data on virgin crystals is reliable because of the large variation noted from crystal to crystal and within a crystal. Encouraging though is the fact that on heat treatment the resistivity does appear to reach an "equilibrium" value.

TABLE XIX

Results of Spectrographic Analysis of ZnO

	<u>Lot No. 1</u>	<u>Lot No. 2</u>
Silver	ND<0.001%	ND<0.001%
Aluminum	ND<0.001%	ND<0.001%
Arsenic	ND<0.05%	ND<0.05%
Gold	ND<0.05%	ND<0.05%
Boron	ND<0.005%	ND<0.005%
Barium	ND<0.001%	ND<0.001%
Beryllium	ND<0.001%	ND<0.001%
Bismuth	ND<0.001%	ND<0.001%
Calcium	ND<0.005%	ND<0.005%
Cadmium	ND<0.05%	ND<0.05%
Cobalt	ND<0.001%	ND<0.001%
Chromium	ND<0.001%	ND<0.001%
Copper	ND<0.001%	ND<0.001%
Iron	ND<0.001%	ND<0.001%
Gallium	ND<0.001%	ND<0.001%
Germanium	ND<0.005%	ND<0.005%
Hafnium	ND<0.05%	ND<0.05%
Lithium	ND<0.001%	ND<0.001%
Indium	ND<0.001%	ND<0.001%
Iridium	ND<0.05%	ND<0.05%
Magnesium	0.005%	0.005%
Manganese	ND<0.001%	ND<0.001%
Molybdenum	ND<0.001%	ND<0.001%
Sodium	ND<0.001%	ND<0.001%
Columbium	ND<0.005%	ND<0.005%
Nickel	ND<0.001%	ND<0.001%
Osmium	ND<0.05%	ND<0.05%
Lead	ND<0.003%	ND<0.003%
Palladium	ND<0.001%	ND<0.001%
Platinum	ND<0.005%	ND<0.005%
Rhodium	ND<0.005%	ND<0.005%
Ruthenium	ND<0.05%	ND<0.05%
Antimony	ND<0.05%	ND<0.05%
Silicon	ND<0.001%	ND<0.001%
Strontium	ND<0.001%	ND<0.001%
Tantalum	ND<0.05%	ND<0.05%
Tellurium	ND<0.1%	ND<0.1%
Thallium	ND<0.01%	ND<0.01%
Titanium	ND<0.001%	ND<0.001%
Vanadium	ND<0.001%	ND<0.001%
Tungsten	ND<0.05%	ND<0.05%
Zinc	High	High
Zirconium	ND<0.001%	ND<0.001%
Tin	ND<0.001%	ND<0.001%

ND< - Not Detected Less Than

## 5.0 CONCLUSIONS

This report contains the description of the manufacturing technology required to produce large high quality crystals of zinc oxide. It is a peculiar situation that with all that is known concerning ZnO and all of the interest in it as a material no device requirements for large amounts of material yet exist. It is a case where the crystal growth technology has preceded the corresponding device development. Part of the reason for this may be that before this contract only small vapor grown crystals were available which were not suited for device fabrication.

The work performed in the molten salt area, though not completely successful, did provide sufficient seed material for the hydrothermal process at that time.

The hydrothermal portion of the program was quite successful in that it was demonstrated that very large crystals of high quality could be grown by this process. Although crystals doped at all resistivity levels cannot be grown as reproducibly as desired, crystals can be grown in the  $10^2 - 10^5$  range. This is the range required for acoustic amplifier devices. Furthermore crystals have been grown with very high resistivities and it may be that this area may be brought under better control.

Prior to this contract the only large crystal hydrothermally grown was quartz. The hydrothermal technique for crystal production has thus been extended and concomitantly new techniques had to be developed. In order to grow large ZnO crystals, the large silver can technique was perfected and a positive sealing procedure for the can was developed.

As opposed to quartz where acmite is generated to insure the sealing of the autoclave, only water is present in the external fill and the sealing pieces of the autoclave must be perfect if the seal is to close effectively. In order to accomplish such sealing on a routine but guaranteed basis, certain tools and techniques were evolved during the course of the program.

In addition to the new tools to be used with the autoclaves, the autoclave design itself was improved so that the manufacturer has included these modifications in this standard vessel.

Several unexpected problems were encountered during the work: one of these was silver corrosion under hydrothermal conditions. This form of corrosion had not been reported until this time. Considering the serious consequences of the corrosion it was imperative to solve the problem. The solution was achieved and similar techniques have been applied to other hydrothermal systems ( $Al_2O_3$ , YIG, BeO) to eliminate the corrosion in those systems.

Another problem which arose was the discovery that the phenomenon of electrical twinning occurs in hydrothermal ZnO. The formation of the twin during crystal growth could not be eliminated but twinned material

Conclusions (Continued)

was removed mechanically after growth.

Copper doping in the hydrothermal was first attempted and success achieved in producing high quality crystals in the intermediate resistivity range. The largest zinc oxide crystals ever grown (15 crystals all weighing in excess of 150 grams were produced and delivered to the Air Force Materials Laboratories.

In addition to growing and delivering the required large crystals it should be noted that throughout the course of the contract large numbers of crystals have been made available and delivered to many researchers. These include government, industrial and educational laboratories whose interest varied from the measurement of fundamental properties of ZnO to device fabrication. It is hoped that material from this program will shed new light on the fundamental properties and yield a device for which crystal material is readily available.

## 6.0 RECOMMENDATIONS FOR FUTURE WORK

Although the requirements as set forth to develop the manufacturing process, techniques and equipment for the hydrothermal growth of large ZnO crystals has been accomplished it is clear that many facets of growth of this crystal should be investigated in greater depth.

- 1) A fundamental study should be carried out to investigate in detail the dependence of growth rate on pressure, temperature,  $\Delta T$ , solute concentration and impurity ion effects.
- 2) From such a study a set of conditions might be observed which could be developed to yield a process wherein higher growth rates and higher quality crystals could be obtained.
- 3) A program is required to develop a process which could yield purer starting ZnO powder and also purer KOH for solvent preparation.
- 4) Further improvements are required in the ability to dope at more levels and in a more reproducible uniform manner.
- 5) A study should be carried out to dope ZnO with ions other than lithium, copper and indium to see if the objectives of No. 4 above could be more easily accomplished and/or yield a crystal with other interesting properties.
- 6) Finally a program must be carried out to develop the growth whereby crystals are produced whose major dimension lies in the  $\langle 0001 \rangle$  axis.

7.0 REFERENCES

1. A. R. Hutson, Phys. Rev. Letters, 4, 305 (1960).
2. A. R. Hutson, J. H. McFee, and D. L. White, Phys. Rev. Letters, 7, 237 (1961).
3. J. H. McFee, J. Appl. Phys., 34, 1548 (1963).
4. A. R. Hutson, Bell Telephone Laboratories, Private Communication.
5. J. J. Lander, J. Phys. Chem Solids, 15, 136 (1960).
6. J. J. Charlton, USARL, Ft. Monmouth, Private Communication.
7. J. W. Nielsen and E. P. Dearborn, J. Phys. Chem., 64, 1763 (1960).
8. R. A. Laudise, E. D. Kolb, and A. J. Caporaso, J. Am. Ceram. Soc., 47, 9 (1964).
9. R. A. Laudise and J. W. Nielsen, "Hydrothermal Crystal Growth", Solid State Physics, 12, Academic Press, New York, 1961.
10. R. A. Laudise, "Hydrothermal Synthesis of Single Crystals", Progress in Inorganic Chemistry, 3, Interscience Publishers, New York (1962).
11. R. A. Laudise, Bell Telephone Laboratories, Private Communication.
12. A. N. Mariano and R. E. Hanneman, J. Appl. Phys., 34, 384 (1963).
13. R. R. Monchamp, R. C. Puttback, and J. W. Nielsen, Final Report AF Contract AF33(657)-10508, October, 1965.
14. R. A. Laudise and E. D. Kolb, Bell Telephone Laboratories, Private Communication.
15. R. R. Monchamp, R. C. Puttback and J. W. Nielsen. J. Electrochem. Soc., 113, 1233 (1966).
16. E. D. Kolb and R. A. Laudise, J. Am. Ceram. Soc., 49, 302, (1966).
17. E. D. Kolb and R. A. Laudise, J. Am. Ceram. Soc., 48, 342 (1965).

UNCLASSIFIED

Security Classification

DOCUMENT CONTROL DATA - R&D		
<small>Remarks: Classification of title, body of abstract and indexing annotation must be entered when the overall report is classified.</small>		
1. ORIGINATING ACTIVITY (Corporate suffix)		14. REPORT SECURITY CLASSIFICATION
Airtron Division Litton Precision Products, Inc. 200 E. Hanover Ave., Morris Plains, New Jersey		UNCLASSIFIED
		15. GROUP
2. REPORT TITLE		
Hydrothermal Growth of Zinc Oxide Crystals AFML-TR-67-144		
4. DESCRIPTIVE NOTES (Type of report and inclusive dates)		
Final Report - 1 June 1962 to 31 December 1966		
3. AUTHOR(S) (Last name, first name, initial)		
Monohamp, Booh R. Nielsen, J. W. Putzbach, Richard C.		
6. REPORT DATE	7a. TOTAL NO. OF PAGES	7b. NO. OF REFS
June 1967	175	17
8a. CONTRACT OR GRANT NO.		8b. ORIGINATOR'S REPORT NUMBER(S)
AF33(657)-8795 & AF33(615)-2228		R11-534
a. PROJECT NO.		8c. OTHER REPORT NO(S) (Any other numbers that may be assigned this report)
7-988		
10. AVAILABILITY/LIMITATION NOTES This document* is subject to special export controls and each transmittal to foreign governments or foreign nationals may be made only with prior approval of the Manufacturing Technology Division, AFML, W-PAFB, Ohio 45433.		
11. SUPPLEMENTARY NOTES		12. SPONSORING MILITARY ACTIVITY
		AF Materials Laboratory Manufacturing Technology Division (MATE) Wright-Patterson AFB, Ohio 45433
13. ABSTRACT		
<p>A pilot line for the production of large high quality ZnO single crystals was established and many large crystals were produced. The pilot line can be divided into two units, 1) a molten salt line for the production of seed plates to be used in 2) the hydrothermal crystal growth pilot line. The design and construction of both lines were successfully completed and functioned as planned. The molten salt crystal growth effort was not as successful as had been anticipated. Large area, high quality crystals could not be made reproducibly by this technique. The most apparent reasons for the failure to do so rests in thermal gradient control during the growth cycle and/or the presence or absence of impurities. Although these problems were not completely resolved the molten salt pilot line did yield sufficient plates for the initial portion of the hydrothermal crystal growth program. Once growth conditions and procedures were established in the hydrothermal pilot line, the hydrothermally grown crystals were sectioned and used as seeds for subsequent runs. The area of the crystals were increased by continued growth until large high quality crystals weighing more than 150 grams could be grown on such seeds within reasonable operating times. One problem arose which had not been encountered in previous hydrothermal systems. It was found that the silver liner or can was corrosively attacked during the course of the growth cycle. The silver which was dissolved in the fluid in the fluid in the nutrient chamber would also be deposited in the crystals in the growth chamber. This problem was solved by adding a reducing agent (metallic zinc) to the reactants. The cause of the corrosion apparently is due to the presence of oxygen dissolved in the solvent and as air entrapped in closure of the can. The reason this phenomenon had not been observed in other small systems using noble metal liners is that no other similar system has been scaled-up to the ZnO size. The solution of this problem for the ZnO case will undoubtedly be of value to other large hydrothermal crystal growth systems.</p>		

DD FORM 1473  
1 JAN 64

UNCLASSIFIED

Security Classification

KEY WORDS	LINE A		LINE B		LINE C	
	ROLE	WT	ROLE	WT	ROLE	WT
Molten Salt Crystal Growth Hydrothermal Crystal Growth Zinc Oxide Crystals Doped Zinc Oxide						

**INSTRUCTIONS**

**1. ORIGINATING ACTIVITY:** Enter the name and address of the contractor, subcontractor, grantee, Department of Defense activity or other organization (*corporate author*) issuing the report.

**2A. REPORT SECURITY CLASSIFICATION:** Enter the overall security classification of the report. Indicate whether "Restricted Data" is included. Marking is to be in accordance with appropriate security regulations.

**2B. GROUP:** Automatic downgrading is specified in DoD Directive 5200.10 and Armed Forces Industrial Manual. Enter the group number. Also, when applicable, show that optional markings have been used for Group 3 and Group 4 as authorized.

**3. REPORT TITLE:** Enter the complete report title in all capital letters. Titles in all cases should be unclassified. If a meaningful title cannot be selected without classification, show title classification in all capitals in parentheses immediately following the title.

**4. DESCRIPTIVE NOTES:** If appropriate, enter the type of report, e.g., interim, progress, summary, annual, or final. Give the inclusive dates when a specific reporting period is covered.

**5. AUTHOR(S):** Enter the name(s) of author(s) as shown on or in the report. Enter last name, first name, middle initial. If military, show rank and branch of service. The name of the principal author is an absolute minimum requirement.

**6. REPORT DATE:** Enter the date of the report as day, month, year; or month, year. If more than one date appears on the report, use date of publication.

**7A. TOTAL NUMBER OF PAGES:** The total page count should follow normal pagination procedures, i.e., enter the number of pages containing information.

**7B. NUMBER OF REFERENCES:** Enter the total number of references cited in the report.

**8A. CONTRACT OR GRANT NUMBER:** If appropriate, enter the applicable number of the contract or grant under which the report was written.

**8B, 8C, & 8D. PROJECT NUMBER:** Enter the appropriate military department identification, such as project number, subject number, system numbers, task number, etc.

**9A. ORIGINATOR'S REPORT NUMBER(S):** Enter the official report number by which the document will be identified and controlled by the originating activity. This number must be unique to this report.

**9B. OTHER REPORT NUMBER(S):** If the report has been assigned any other report numbers (either by the originator or by the sponsor), also enter this number(s).

**10. AVAILABILITY/LIMITATION NOTICE:** Enter any limitations on further dissemination of the report, other than those

imposed by security classification, using standard statements such as:

- (1) "Qualified requesters may obtain copies of this report from DDC."
- (2) "Foreign announcement and dissemination of this report by DDC is not authorized."
- (3) "U. S. Government agencies may obtain copies of this report directly from DDC. Other qualified DDC users shall request through \_\_\_\_\_."
- (4) "U. S. military agencies may obtain copies of this report directly from DDC. Other qualified users shall request through \_\_\_\_\_."
- (5) "All distribution of this report is controlled. Qualified DDC users shall request through \_\_\_\_\_."

If the report has been furnished to the Office of Technical Services, Department of Commerce, for sale to the public, indicate this fact and enter the price, if known.

**11. SUPPLEMENTARY NOTES:** Use for additional explanatory notes.

**12. SPONSORING/MONITORING AGENCY NAME(S) AND ADDRESS(ES):** Enter the name of the departmental project office or laboratory sponsoring (paying for) the research and development. Include address.

**13. ABSTRACT:** Enter an abstract giving a brief and factual summary of the document indicative of the report, even though it may also appear elsewhere in the body of the technical report. If additional space is required, a continuation sheet shall be attached.

It is highly desirable that the abstract of classified reports be unclassified. Each paragraph of the abstract shall end with an indication of the military security classification of the information in the paragraph, represented as (TS), (S), (C), or (U).

There is no limitation on the length of the abstract. However, the suggested length is from 150 to 225 words.

**14. KEY WORDS:** Key words are technically meaningful terms or short phrases that characterize a report and may be used as index entries for cataloging the report. Key words must be selected so that no security classification is required. Identifiers, such as equipment model designation, trade name, military project code name, geographic location, may be used as key words but will be followed by an indication of technical context. The assignment of links, roles, and weights is optional.

DD Form 1473 Item No. 13. ABSTRACT - continued

In addition to the growth of the large crystals many smaller crystals were grown which were doped with copper to give resistivities in the  $10^2 - 10^4 \Omega$  cm range. This is the range most desirable for acoustical amplifier devices. Other doping studies indicate a wide variation of resistivities within the virgin crystal, and from crystal to crystal within a run. After heat treatment, however, the variation of resistivity is reduced to an order of magnitude or less. It was also observed that impurities not detected by spectrographic analysis may be as important in determining the resultant resistivity as deliberate doping additions and growth conditions. During the course of these contracts many samples of hydrothermally grown ZnO were given to scientists and engineers in government, industrial and university laboratories for measurement of the fundamental properties of ZnO and for device design and development.